

**Improved delivery of hydrophobic drugs by a  
self-microemulsifying drug delivery system and  
electrospun polymer fibers**

Kumulative Dissertation

zur Erlangung des  
Doktorgrades der Naturwissenschaften (Dr. rer. nat.)

der

Naturwissenschaftlichen Fakultät I  
– Biowissenschaften –  
der Martin-Luther-Universität Halle-Wittenberg,

vorgelegt von

Frau Johanna Zech  
geb. am 19.01.1989 in Göttingen

Gutachter:

1. Prof. Dr. Karsten Mäder
2. Prof. Dr. Eyal Zussman
3. PD Dr. Christian Schmelzer

Tag der öffentlichen Verteidigung: 09.11.2022 in Halle (Saale)



*If an expert says it can't be done, get another expert.*

David Ben-Gurion, First Prime Minister of Israel



# Table of content

ABBREVIATIONS .....	ii
LIST OF FIGURES .....	iv
LIST OF TABLES .....	v
1. PREFACE .....	2
2. INTRODUCTION .....	3
2.1 Poorly soluble drugs - classification and delivery strategies .....	3
2.2 Self-microemulsifying systems for drug delivery .....	8
2.3 Electrospun polymer fibers .....	12
2.4 Artemisone .....	16
2.5 Nimodipine .....	19
3. CUMULATIVE PART .....	21
3.1 Artemisone self-microemulsifying drug delivery system .....	23
3.2 Electrospun polymer fibers .....	25
4. RESULTS AND DISCUSSION .....	27
4.1 Artemisone self-microemulsifying drug delivery system .....	27
4.2 Electrospun polymer fibers .....	39
4.2.1 Electrospun Nimodipine-loaded polymer fiber mats .....	40
4.2.2 Polymer fiber sponges .....	44
5. SUMMARY AND FUTURE PERSPECTIVES .....	48
5.1 Artemisone self-microemulsifying drug delivery system .....	48
5.2 Electrospun polymer fibers .....	51
BIBLIOGRAPHY .....	54
APPENDIX .....	I

## Abbreviations

$\mu$ CT	Micro-computed tomography
$^1\text{H}$ NMR	Proton nuclear magnetic resonance
3D	Three-dimensional
AM	Anemic malaria
ART	Artemisone
AUC	Area under the curve
BCS	Biopharmaceutical Classification System
BSA	Bovine serum albumin
CM	Cerebral malaria
$C_{\text{max}}$	Maximum serum concentration
cryoEM	Cryogenic electron microscopy
Da	Dalton
DCS	Developability Classification System
DDS	Drug delivery system
DFG	Deutsche Forschungsgemeinschaft
DLS	Dynamic light scattering
DMEM	Dulbecco's Modified Eagle Medium
DMEM-F12	Dulbecco's Modified Eagle Medium: Nutrient Mixture F-12
DMSO	Dimethyl sulfoxide
DSC	Differential Scanning Calorimetry
dTempol	4-Hydroxy-Tempo-d17
$\text{ED}_{50}$	Effective dose for 50 % of a population
EMA	European Medicines Agency
EPF	Electrospun polymer fibers
EPR	Electron Paramagnetic Resonance
FDA	U.S. Food and Drug Association
GIT	Gastrointestinal tract
GRAS	Generally Recognized As Safe
HLB	Hydrophilic Lipophilic Balance
HPLC	High performance liquid chromatography
ICH	International Council for Harmonisation of Technical Requirements for Pharmaceuticals for Human Use

IF	Impact factor
i.p.	Intraperitoneally
LBF	Lipid-based formulation
LFCS	Lipid Formulation Classification System
LLQ	Lower limit of quantification
Log P	$\text{Log}_{10}$ (partition coefficient <sub>[organic]/[aqueous]</sub> )
MCT	Medium-chain triglycerides
ME	Microemulsion
MPC	Minimum parasitocidal concentration
MS	Mass spectrometry
$M_w$	Molecular weight
NIMO	Nimodipine
PBS	Phosphate buffered saline
PE	Parasitized erythrocytes
PEG	Polyethylene glycol
PFS	Polymer fiber sponge
$\text{pK}_a$	$-\text{Log}_{10}$ (acid dissociation constant)
PLA	Poly(D,L-lactide)
PLGA	Poly(D,L-lactide-co-glycolide)
PPX	Poly(p-xylylene)
REACH	Registration, Evaluation, Authorisation and Restriction of Chemicals
SEDDS	Self-emulsifying drug delivery system
SEM	Scanning electron microscopy
SMEDDS	Self-microemulsifying drug delivery system
$T_2$	Transverse magnetization relaxation
$T_g$	Glass transition temperature
$T_m$	Melting temperature
$t_{\text{max}}$	Time to maximum plasma concentration
WHO	World Health Organization
wt. %	Weight percent
$\phi_w$	Water volume fraction

## List of Figures

<b>Figure 1.</b> The Biopharmaceutical Classification System.....	3
<b>Figure 2.</b> The Developability Classification System.....	4
<b>Figure 3.</b> Optimized drug therapy through solubility enhancing formulations.....	7
<b>Figure 4.</b> Types of microemulsions .....	9
<b>Figure 5.</b> Schematic representation of an electrospinning setup .....	12
<b>Figure 6.</b> Electrospun non-wovens.....	13
<b>Figure 7.</b> Graphical abstract of publication I (Zech et al. <sup>130</sup> ). .....	24
<b>Figure 8.</b> Graphical abstract of publication V (Zech et al. <sup>157</sup> ). .....	26
<b>Figure 9.</b> pH-dependent stability and solubility of artemisone .....	28
<b>Figure 10.</b> Final formulation SMEDDS-100 .....	28
<b>Figure 11.</b> Physicochemical characterization of SMEDDS-100 and resulting ME.....	30
<b>Figure 12.</b> Cryo-electron microscopy of SMEDDS-50 and SMEDDS-20. ....	31
<b>Figure 13.</b> Stability of artemisone in SMEDDS-100, SMEDDS-50, and PBS pH 6.5 .....	32
<b>Figure 14.</b> Animal models used in the in vivo testing.....	33
<b>Figure 15.</b> Hematoxylin-eosin stained liver sections from <i>S. mansoni</i> infected mice .....	34
<b>Figure 16.</b> Parasitaemia in dose dependence study in murine cerebral malaria.....	35
<b>Figure 17.</b> Effect of ART-SMEDDS dosing intervals and route of application.....	37
<b>Figure 18.</b> Transdermal treatment with artemisone-SMEDDS.....	38
<b>Figure 19.</b> SEM images of 1 % and 10 % nimodipine fiber mats.....	40
<b>Figure 20.</b> DSC curves and x-ray powder diffractometry patterns of nimodipine fiber mats. ....	41
<b>Figure 21.</b> Nimodipine in vitro release.....	42
<b>Figure 22.</b> Changes in fiber morphology during release experiment .....	43
<b>Figure 23.</b> Preparation of PLA-PPX polymer fiber sponges.....	44
<b>Figure 24.</b> Characteristics of the PFS used in this study .....	44
<b>Figure 25.</b> $\mu$ CT scans of PFS liquid-uptake.....	46
<b>Figure 26.</b> <sup>1</sup> H NMR spectroscopy and release from free MCT and MCT-loaded PFS .....	47



## List of Tables

<b>Table 1.</b> Solubility enhancing formulation approaches and mechanisms.....	5
<b>Table 2.</b> The Lipid Formulation Classification System .....	8
<b>Table 3.</b> Examples of marketed SMEDDS.....	11
<b>Table 4.</b> Physicochemical characteristics of artemisone.....	17
<b>Table 5.</b> Physicochemical characteristics of the polymorphs of nimodipine .....	19
<b>Table 6:</b> Peer-reviewed scientific journals where the work of this thesis was published .....	21
<b>Table 7.</b> Declaration of contributions to the publications presented in this thesis.....	22
<b>Table 8.</b> SMEDDS-100-derived microemulsions SMEDDS-50 and SMEDDS-20: Composition and route of administration in the in vivo experiments .....	31
<b>Table 9.</b> Oral treatment of murine schistosomiasis.....	34
<b>Table 10.</b> ART serum concentrations .....	36
<b>Table 11.</b> Possible parameters controlling drug delivery mechanisms from the electrospun polymer fiber systems studied in Zech et al. 2020 <sup>74</sup> and Zech et al. 2020 <sup>157</sup> .....	39
<b>Table 12.</b> Sample holders used for sponge incubation and liquid-loading results. Duration of liquid uptake of different fluids in the nanofiber derived PPX-coated PLA sponges.....	45



# 1. Preface

## Aim of the work and research objectives

The work of this thesis was part of the DFG funded trilateral *German Israel Palestine* cooperative research project, an interdisciplinary research cooperation between the Hebrew University of Jerusalem, the Palestinian Al-Quds University, the Technion - Israel Institute of Technology, the University Bayreuth, and the Martin-Luther-University Halle-Wittenberg.

The aim of the project was the investigation of electrospun fibers as functional carriers for biological agents, including drugs, and specifically the antiprotozoal artemisone. The goal was to design, to manufacture and to evaluate suitable drug delivery systems and assess electrospun fiber-based structures of cooperation partners with regards to drug delivery.

The results of these profitable and rewarding cooperations have been made available in five peer-reviewed research articles that form the basis of this doctoral thesis. Due to the diversity of the cooperation partners and the resulting multifariousness of the explored subjects, the research objectives of this thesis cover two different areas of study that are presented separately:

### *Artemisone self-microemulsifying drug delivery system*

A self-emulsifying lipid-based formulation for artemisone, as an alternative to the electrospun delivery platforms, was developed for the research groups of Dr. Golenser and Prof. Jaffe of the Department of Microbiology and Molecular Genetics at the Hebrew University of Jerusalem. Artemisone delivery was then extensively tested in in vivo animal models by the author during two research visits to the Hebrew University.

### *Electrospun polymer fibers*

Parameters governing drug release from three-dimensional electrospun polymer fiber sponges produced by the research group of Prof. Greiner at the Macromolecular Chemistry Department of the University Bayreuth were studied via non-invasive characterization. Experiments were carried out by the author in cooperation with the Department of Nuclear Medicine at the University Hospital Halle (Saale).

To further explore electrospun fibers as functional carriers in drug delivery, a nimodipine releasing implant based on electrospun nonwovens was designed for intracranial local drug delivery. These fiber mats were then examined for their biological activity in in vitro brain cell cultures by the Department of Neurosurgery at the University Hospital Halle (Saale).

The main theme of the thesis can be found in the common goal these diverse systems are addressing: exploring novel ways of optimized delivery of small molecule drugs, particularly the challenges posed by poorly soluble compounds, such as artemisone and nimodipine.

Enhanced bioavailability through increased solubility remains a key issue in formulation design that has still only partly been addressed. Its great potential to improve therapy, taken together with the increasing number of poorly soluble compounds, makes it one of the most urgent and relevant fields of study in drug delivery today, to which the author hopes this thesis may contribute.

## 2. Introduction

### 2.1 Poorly soluble drugs - classification and delivery strategies

Solubility and permeability have long been identified as key factors for successful drug delivery, allowing for sufficient bioavailability and, consequently, therapeutic efficacy<sup>1,2</sup>. With few exceptions (e.g., nanoparticle formulations<sup>3</sup>), a compound must be in solution to permeate barriers like the intestinal epithelium, nasal mucosa, or the skin, to enter systemic circulation, travel to the relevant target sites, and exert the desired response. Sufficient lipophilicity as a prerequisite for high permeability often conflicts with the aqueous solubility required by various bodily fluids such as blood, tear film, and digestive fluids<sup>4</sup>. Depending on the drug's characteristics, either permeation or dissolution can act as the rate-limiting factor for absorption<sup>1,2,4</sup>.

For oral drug delivery via immediate-release formulations, the Biopharmaceutical Classification System [BCS] proposed by Amidon et al.<sup>1</sup> suggests a correlation of in vitro dissolution and in vivo bioavailability. By classing a molecule according to its aqueous solubility and intestinal permeability, the BCS allows to predict which factor is mainly controlling drug uptake (**Figure 1**)<sup>5</sup>.

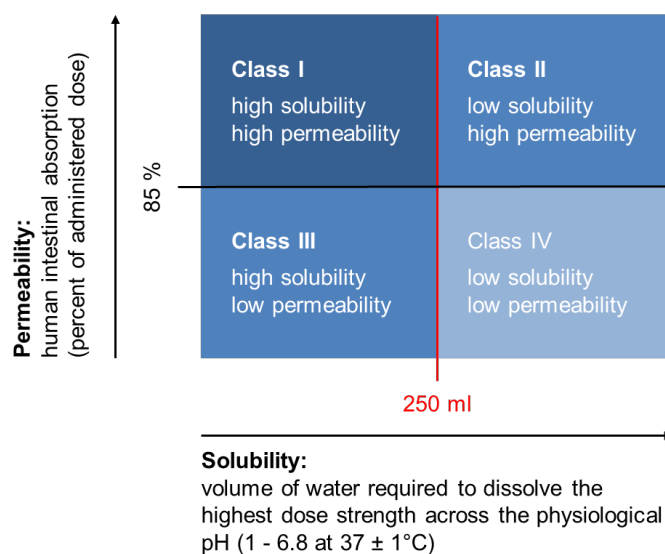


**Figure 1.** The Biopharmaceutical Classification System as described by Amidon et al. in 1995<sup>1</sup>. Modified from Dahan et al.<sup>6</sup> according to U.S. Food and Drug Administration [FDA] Guidelines<sup>5</sup>. The permeability is to be ascertained via a mass balance determination or in comparison to an intravenous reference dose. For regulatory purposes, the BCS is only applied to immediate oral release systems.

It goes without saying that solubility, dissolution rate, and permeability also affect the non-oral routes of drug delivery. E.g., poor solubility can hinder the infusion of drugs if the needed volume for dissolution exceeds the amount that could be safely administered. Similarly, intranasal or ocular delivery is often only possible if a compound can be dissolved in the small amount of fluid that can be applied via those routes<sup>7</sup>. Sufficient permeation is also the key to transdermal therapeutic systems that deliver the drug via an area of only a few cm<sup>2</sup>.

However, until now, no widely accepted, comprehensive classification system has been established for parenteral or slow-release oral dosage forms. The categorization of a drug within the BCS thus still provides valuable information on its in vivo performance via these forms of delivery systems.

Over the last decades, combinatorial chemistry and computational drug design, combined with high-throughput screening and the focus on lipophilic targets, has led to more and more compounds of poor aqueous solubility entering the first discovery phase as potential drug candidates <sup>4,8,9</sup>. It is estimated that up to 90 % of new pharmaceutical entities are poorly soluble according to their BCS classification, with 60 – 70 % of them belonging to the BCS class II <sup>8</sup>. Insufficient solubility significantly raises the cost of drug development and the likelihood of ultimate failure of a drug candidate. Therefore, in recent years, the pharmaceutical industry has started to pay more attention to solubility issues, including solubility prediction and screening methods early on in the drug discovery process <sup>9,10</sup>.

For BCS class I compounds, sufficient absorption can be expected. To achieve adequate bioavailability for classes III and IV, Pouton recommends changes to the molecular structure during lead optimization <sup>11</sup>. For class II compounds, the appropriate formulation approach can ensure good absorption because these molecules possess inherent good permeability. Consequently, formulation scientists are essential for the development of these drugs.

To better assess the actual developability of new molecules, a variation of the BCS system has been introduced, categorizing drugs according to factors limiting their oral absorption: the Developability Classification System [DCS] <sup>2</sup>. It is more closely oriented on the specific conditions in the small intestine as the main area for drug absorption, allowing better prediction of the crucial factors for the in vivo performance. The DCS also makes a more differentiated assessment of the considerably large class of BSC II compounds (**Figure 2**).

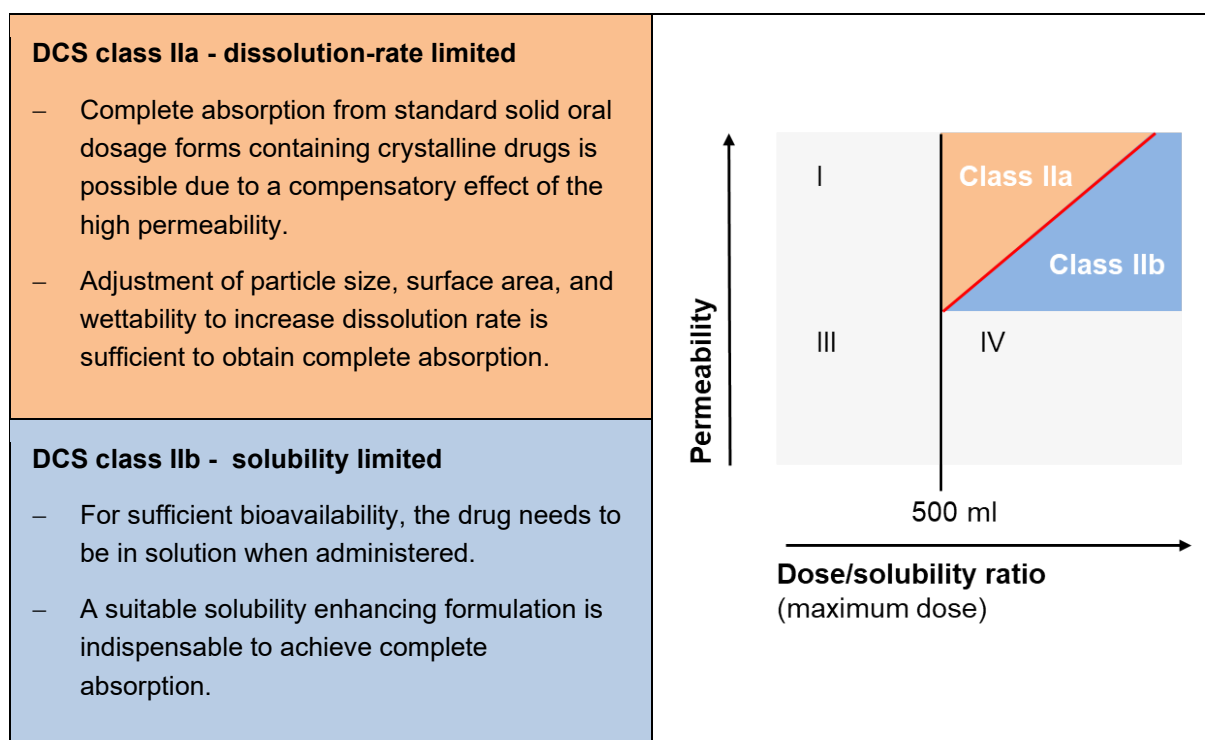


**Figure 2.** The Developability Classification System, modified from <sup>2</sup>.

For DCS class IIa drugs, a target drug particle size can be calculated. Below that, the dissolution rate is high enough to allow the administration of the solubility limited absorbable dose as crystalline drug in simple, immediate release oral drug delivery systems [DDS].

Contrarily, the DCS class IIb provides the formulation scientist with the greatest challenge, requiring appropriate formulation design to ensure drug solubility and consequent bioavailability. Ideally, so-called enabling formulations (formulations that make poorly soluble drugs bio-available)<sup>12</sup> are developed alongside the drug molecule<sup>8,10</sup>. But the design of such delivery systems also offers significant potential to improve therapy with already established and marketed compounds.

The main formulation-based approaches, containing the drug in solution or the amorphous form, are summarized in **Table 1** (not including nanocrystals and liposomes). These approaches too are also relevant not only for oral but also for parenteral application and controlled release oral formulations.

**Table 1.** Solubility enhancing formulation approaches and mechanisms with examples of marketed products<sup>8,10,12-14</sup>.

Formulation principle	Mechanisms	Marketed DDS	
<b>Non-aqueous pharmaceutical solvents</b>	Increased solubility in non-aqueous solvent	<i>Nymalize</i> <sup>®</sup>	15
<b>Co-solvency and solubilization with surfactants</b>	Solubilization/micellization	<i>Taxol</i> <sup>®</sup>	16
<b>Lipid-based DDS</b>			
• Liquid or solid solutions	Solution in lipid excipients;	<i>Avodart</i> <sup>®</sup>	17
• (Micro/Nano-)Emulsions	Solubilization after lipid digestion;	<i>Diprivan</i> <sup>®</sup>	18
• Self-emulsifying DDS [SEDDS]	SEDDS: formation of (micro/nano)emulsion upon mixing with bodily fluids	<i>Neoral</i> <sup>®</sup>	19
• Solid lipid nanoparticles			
<b>Solid solution/amorphous solid dispersions</b>			
• Spray drying	Molecularly dispersed or amorphous drug in a (polymer) matrix;	<i>Intelence</i> <sup>®</sup>	20
• Hot-melt extrusion	Increased Gibbs free energy results in enhanced apparent solubility and supersaturation	<i>Kaletra</i> <sup>®</sup>	21
• Electrospinning			
• Polymeric micro/nanoparticles			
<b>Cyclodextrin complexation</b>	Solubilization of drug as inclusion complex in lipophilic cavity of cyclodextrin	<i>Sporanox</i> <sup>®</sup>	22
<b>Mesoporous silica carriers</b>	Molecularly dispersed or amorphous drug within the mesoporous silica carrier network	Not available yet	

The suitability of a specific formulation technique is greatly determined by the drug's physicochemical properties (Log P,  $T_m$ ,  $pK_a$ , salt formation) and stability<sup>10</sup>. As discussed in depth by Ditzinger et al.<sup>13</sup>, both hydrophobicity ( $T_m$ , crystal lattice energy) and lipophilicity (Log P) of the compound need to be considered for a complete understanding of its solubility characteristics. Only then can the rational design of a suitable carrier for the individual drug be successful.

However, solubility enhancing formulations can also come with a range of specific challenges that need to be addressed in the formulation design approach:

- An uncontrolled increase in dissolution rate will affect  $t_{max}$  and  $c_{max}$ . As a result, toxic peak serum concentrations through fast and more complete absorption are possible<sup>11</sup>. For controlled release formulations, a careful balancing of enhanced drug availability and prevention of an excessive burst release will be necessary to achieve the desired release profile and avoid toxicity.
- Monitoring drug stability is crucial as degradation, hydrolysis, and oxidation are more likely to occur if a compound is already in solution. This is particularly common for aqueous systems or lipid-based DDS that contain unsaturated fatty acids and polyethylene glycol [PEG] moieties. Stability must be assured over a reasonable temperature range to guarantee acceptable storage conditions, simple distribution, and global use in different climatic stability zones.
- For solid dispersions and metastable amorphous materials, the recrystallization of the components during the product's shelf-life needs to be ruled out as resulting changes in the release profile will have major implications on patient safety<sup>11</sup>.
- Excellent solubility in the carrier can lead to incomplete drug release due to partitioning effects. Solubilization in carrier structures might reduce drug permeation compared to free molecularly dissolved drug<sup>12</sup>.
- Supersaturation of the drug solution after administration through increased apparent solubility is prone to instability and uncontrolled recrystallization.
- Dissolution and absorption processes are always more complex and unpredictable in vivo than in any in vitro assay. Depending on the DDS, it can be determined by a complex interplay of factors such as residence time (e.g., gastric emptying, mucociliary clearance), supersaturation/recrystallization tendency, food effects (digestion, solubilization in bile salt micelles and lymphatic transport), and biodegradability of excipients. Even if a successful formulation can bring the solubility of a BSC class II or IV drug up to that of a class I compound, the bio-fate of the drug molecule is still determined by its physicochemical properties.

If the requirements of limited solubility compounds are appropriately addressed through careful formulation development, the patient benefits greatly from safer, more effective drug therapy (**Figure 3**). Further research on the formulation of such delivery systems is necessary to make new drug candidates accessible but also facilitate the use and expand the range of application of already known compounds.

The reformulation and repurposing of already marketed drugs also hold several attractions for the pharmaceutical companies. Besides the considerably lower development costs

compared to de novo drug development, patent life-cycle extension can also be granted for novel solubility and bioavailability enhancing DDS<sup>23</sup>. That driving force for drug delivery research and development is thus in the interest of both the patient and the industries.

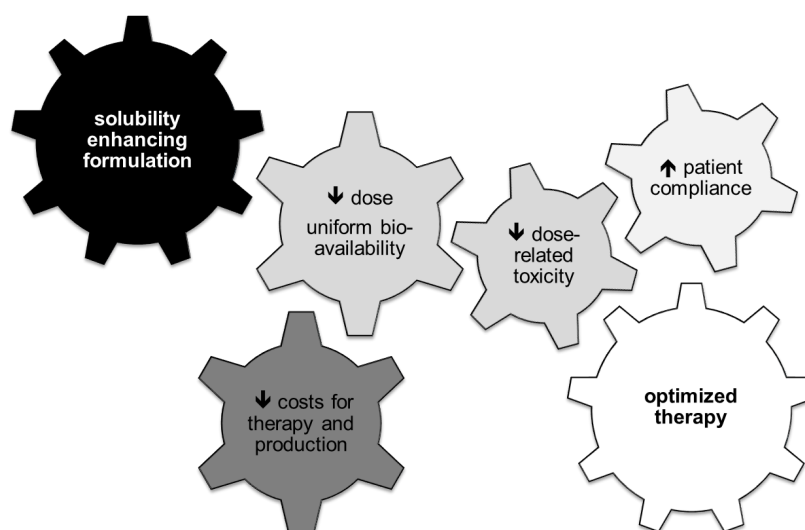


**Figure 3.** Optimized drug therapy through solubility enhancing formulations. Arrows indicate an increase (↑) or decrease (↓) of a parameter.

This work explores two different formulation approaches for the BCS class II drugs nimodipine and artemisone that both pose the additional challenge of poor stability. The two molecules possess untouched potential for their repurposing beyond the initial indication, for which additional suitable DDS, optimizing delivery and stability, are needed.

For artemisone, a lipid-based self-microemulsifying delivery system is developed to increase oral drug availability. Electrospraying is examined for local intracranial delivery of nimodipine. As a combination of electrospraying and lipid DDS, electrospun fiber sponges are assessed for their in vitro performance and drug loading with oily drug solutions.

A short introduction to the applied formulation techniques and relevant properties of the corresponding drugs is given in the following sections.



## 2.2 Self-microemulsifying systems for drug delivery

### Lipid-based formulations and the Lipid Formulation Classification System

Self-microemulsifying drug delivery systems [SMEDDS] belong to the class of lipid-based formulations [LBF].

The LBF' essential principle as solubility enhancing formulations is their ability to keep poorly soluble drugs in solution or solubilized after administration <sup>24</sup>. The main excipients in those DDS are triglycerides or partial glycerides, lipophilic or hydrophilic surfactants, co-surfactants, and water-soluble co-solvents <sup>24</sup>. Most of these excipients are food substances - categorized as Generally Recognized As Safe [GRAS] by the FDA - or derived from those, minimizing the potential toxicity of the LBF and generally ensuring good tolerability.

Lipid-based formulation principles range from simple oily solutions and coarse emulsions to complex, ordered liquid crystalline structures. LBF come in a variety of very different dosage forms, including creams and ointments, fixed-dose oral DDS like lipid matrix tablets and liquid-filled gelatine capsules as well as solid lipid nanoparticles.

A Lipid Formulation Classification System [LFCS] was established by Pouton in 1999 (**Table 2**) <sup>25</sup> to help predict lipid DDS' performance based on their composition. The ability to self-emulsify, the potential loss of components through dissolution in water after administration, and their digestibility by lipases are the main classification criteria <sup>25</sup>.

**Table 2.** The Lipid Formulation Classification System as suggested by Pouton. Modified from <sup>11,25</sup>. \*[HLB] hydrophilic lipophilic balance

Excipients in formulation	Increasing hydrophilic content →				
	Type I	Type II	Type IIIA	Type IIIB	Type IV
	<i>Oil</i>	<i>SEDDS</i>	<i>SEDDS/SMEDDS</i>	<i>SMEDDS</i>	<i>Lipid-free</i>
Oils: Triglycerides or mixed mono/diglycerides	100	40-80	40-80	<20	-
Water-insoluble surfactants (HLB* <12)	-	20-60	-	-	0-20
Water-soluble surfactants (HLB >12)	-	-	20-40	20-50	30-80
Hydrophilic co-solvents	-	-	0-40	20-50	0-50
Typical particle size of dispersion (nm)	Coarse	250-2000	100-250	100-50	Micelles (7-20)

If taken orally, tri- and partial glycerides can be digested by the pancreatic lipases in the human gastrointestinal tract [GIT], leading to the inclusion of the resulting fatty acids and monoglycerides - and possibly solubilization of the drug - in the bile salt mixed micelles. Therefore, the consequent increase in drug uptake is highly food-dependent <sup>11,24</sup>.

While drugs with a Log P > 4 are often more likely to be soluble in LFCS Type I DDS, the increasing hydrophilic content in LFCS Type III formulations is more suitable for compounds with a Log P between 2 and 4 <sup>24</sup>. Less lipophilic hydrophobic drugs can be best solubilized in

LFCS Type IV systems. Savla et al.<sup>26</sup> found that in 2017 55 % of 27 FDA-approved LBF were carriers for DCS class IIb compounds, underlining their importance as solubility enhancing DDS. In any case, sufficient interactions of the drug with lipid excipients are a prerequisite to develop lipid-based DDS.

Due to a large number of excipients of often varying composition (e.g., differences in the amount of saturation, degree of esterification and chain length of PEG and fatty acid moieties between batches and suppliers), and the countless different structures that can be formed by lipid systems, formulation of LBF is in large parts still based on an empirical approach.

### SMEDDS and microemulsions

SMEDDS are lipid mixtures usually comprised of oil, surfactants, co-surfactants, and co-solvents. Upon contact with aqueous media, the SMEDDS spontaneously disperse into structures in the range of several 10 to a few 100 nm. The resulting microemulsions [ME] are optically isotropic, clear or translucent, and thermodynamically stable liquids of varying viscosity. Though they possess distinct lipophilic and aqueous structures, they are usually referred to as single-phase systems or “critical solutions”<sup>27</sup>.

Driving force behind the spontaneous self-microemulsification and thermodynamic stability of ME are the significant increase in entropy  $\Delta S$  through dispersion, accompanied by very low surface energy  $\gamma$ . This leads to negative free energy  $\Delta G_s$  of formation, outweighing the dramatic increase in surface area  $\Delta A$  (**Equation 1**,  $T$  = temperature).

$$\Delta G_s = \gamma \Delta A - T \Delta S \quad (\text{Equation 1.})$$

The use of a mix of surfactants with co-surfactant and/or co-solvent contributes to increased entropy and reduced surface energy, increasing the surfactant layer at the lipid-aqueous phase interface.

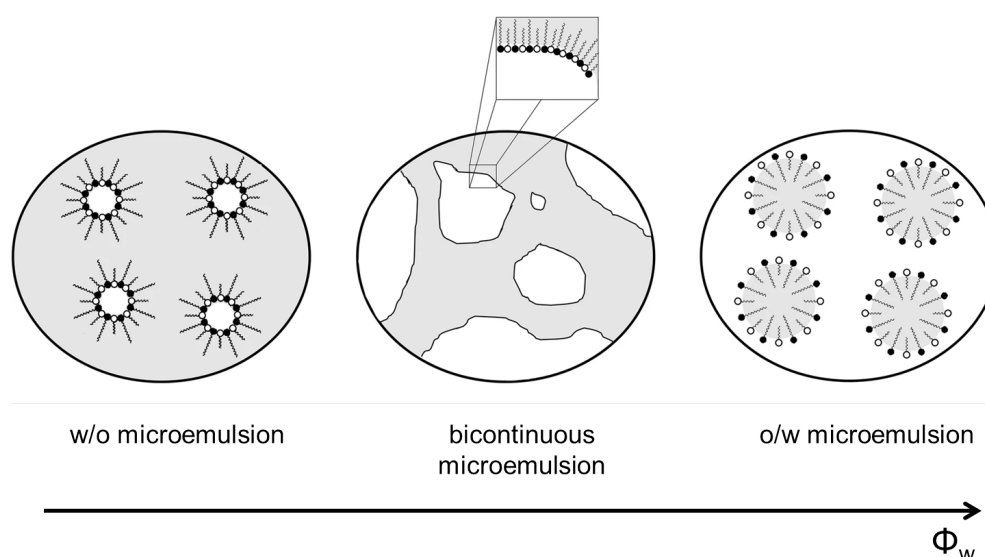


**Figure 4.** Types of microemulsions depending on the water volume fraction  $\phi_w$ . Oil in water (o/w) and water in oil (w/o) ME can be seen as swollen micellar systems formed from oil or water-loaded micelles/reverse micelles of varying shapes. In bicontinuous ME, lipid and aqueous phases (both continuous) are stabilized by a surfactant-packed interface of zero net curvature<sup>28</sup>. Gray: oil; white: water. Modified from<sup>29</sup>.

Depending on the composition and water volume fraction  $\phi_w$ , microemulsions are comprised of densely packed swollen micelles/reverse micelles (or microemulsion droplets, depending on the preferred terminology) or a bicontinuous structure with no distinct inner or outer phase (**Figure 4**)<sup>28</sup>. Though this categorization is obviously a simplification due to the large number of different structures that can be formed in these complex mixtures, it is generally applied and has overall proven to be useful. In addition, ME have to be understood as highly dynamic systems.

In drug delivery, SMEDDS are the water-free pre-formulations of ME. For oral SMEDDS, the aqueous dispersion media involved in the formation of the ME are usually gastrointestinal fluids, while gastrointestinal motion accelerates the self-microemulsification process.

### **SMEDDS as drug delivery systems**

SMEDDS can facilitate drug bioavailability based on their good solvent capacity for a wide variety of compounds. For lipid/surfactant mixtures, the solubility of a drug is the weighted average of the solubility values in the individual components<sup>30,31</sup>. Thus, the good solubility of lipophilic molecules in SMEDDS depends on their good solubility in lipid excipients. However, for ME, solubility can additionally be increased by interfacial/surface properties which can create additional domains for drug solubilisation<sup>31</sup> that may contribute to drug dissolution upon ME formation from SMEDDS. But drug solubility can also be reduced upon dispersion due to the water solubility of the majority of the excipients<sup>11</sup>. Therefore, attention must be paid to the continued dissolution of the drug upon administration, possible metastable supersaturation, and consequent uncontrolled crystallization<sup>11</sup>.

For oral administration, drug absorption from SMEDDS is much less dependent on digestion than from other LBF<sup>25</sup>, resulting in a more uniform bioavailability. The most prominent example of this are the DDS for Cyclosporine A. While a distinct food effect was observed for the coarse emulsion formed from the mainly oil based Sandimmune®, lipid digestion is not necessary to absorb the drug from the SMEDDS Neoral®<sup>32,33</sup>.

ME are thought to protect drugs from possible enzymatic degradation<sup>34,35</sup>. Similarly, for compounds with poor aqueous or pH-dependent stability, the inclusion of drugs in the lipid domains of the forming ME might also increase stability in the GIT<sup>36</sup>.

Besides solubility enhancement, SMEDDS and ME can also increase drug absorption by enhanced penetration, especially for topically applied systems. The flexible surfactant film at the lipid/aqueous interface can facilitate drug diffusion into the tissue. Additionally, many of the excipients used in ME can affect the skin barrier and are inherent permeation enhancers, as comprehensively reviewed in<sup>37</sup>.

As water-free systems, SMEDDS provide good storage stability and consequent self-life. Manufacturing is comparatively easy, mostly only requiring simple mixing of the components. Most excipients have long been established and possess excellent tolerability, simplifying regulatory concerns. However, to date, only a very limited number of SMEDDS are available for several prescription drugs, marketed in the form of liquid-filled capsules or oral solutions. Examples are given in **Table 3**.

**Table 3.** Examples of marketed SMEDDS.

Trade name	Drug	BSC/DCS	Dosage forms	Excipients for SMEDDS-formation	
<b>Neoral®</b> (Pfizer)	Cyclosporine A	II / IIb	Oral solution / Liquid filled soft gelatine capsule	Corn oil mono/diglycerides Polyoxyl 40 hydrogenated castor oil Ethanol PEG	19
<b>Norvir®</b> (Abbvie)	Ritonavir	IV/ IIb	Liquid filled soft gelatine capsule	Oleic acid Polyoxyl 35 castor oil Ethanol	38
<b>Aptivus®</b> (Boehringer)	Ritonavir	IV/ IIb	Liquid filled soft gelatine capsule	Mono/diglycerides of caprylic/capric acid Polyoxyl 35 castor oil Ethanol PEG	39

Considering their good tolerability, versatility, and their potential as enabling formulation for the increasing number of poorly soluble drug candidates, the introduction of more SMEDDS for a range of different compounds can be expected in the future.

### 2.3 Electrospun polymer fibers

Electrospinning is a simple, cost-effective, and easily adaptable approach for the fabrication of continuous ultrafine fibers from a wide variety of different polymer materials. In 1887 Boys first reported a form of melt electrospinning <sup>a</sup>, the formation of “*perfectly uniform cylindrical thread*” and a “*delicate [...] shade produced by innumerable fibres separately almost invisible*” with the help of an electrical field <sup>40</sup>. The actual term “electrospinning” was first introduced by Doshi and Renecker in 1993 <sup>41</sup>. Since then, the method has gained increasing interest in various fields of academic research, with publications rising from 3 in 1995 to around 2,420 in 2020 <sup>b</sup> <sup>42</sup>.

#### The electrospinning process

During electrospinning, an electrical field is applied to a polymer fluid - a melt, solution, or dispersion - between the outlet of the polymer fluid reservoir and a grounded collector (**Figure 5**). The charges thereby induced on the surface of the fluid increase with the electrical field until repulsion forces overcome surface tension. The fluid then forms a conical shape, known as a Taylor cone, and as the applied high voltage reaches a critical value, a jet is ejected from the fluid cone <sup>43-45</sup>. On its way towards the collector, jet instabilities lead to a drastic reduction in diameter through bending, whipping, stretching, and sometimes splaying of the jet with cooling/evaporation of the solvent taking place simultaneously <sup>46,47</sup>. As a result, hardened/dry fibers with a diameter in the range of nm to several  $\mu\text{m}$ , conventionally termed nanofibers, are deposited on the collector. If collected after random fiber deposition, the resulting fleece mats and structures are referred to as electrospun non-wovens (**Figure 6**).

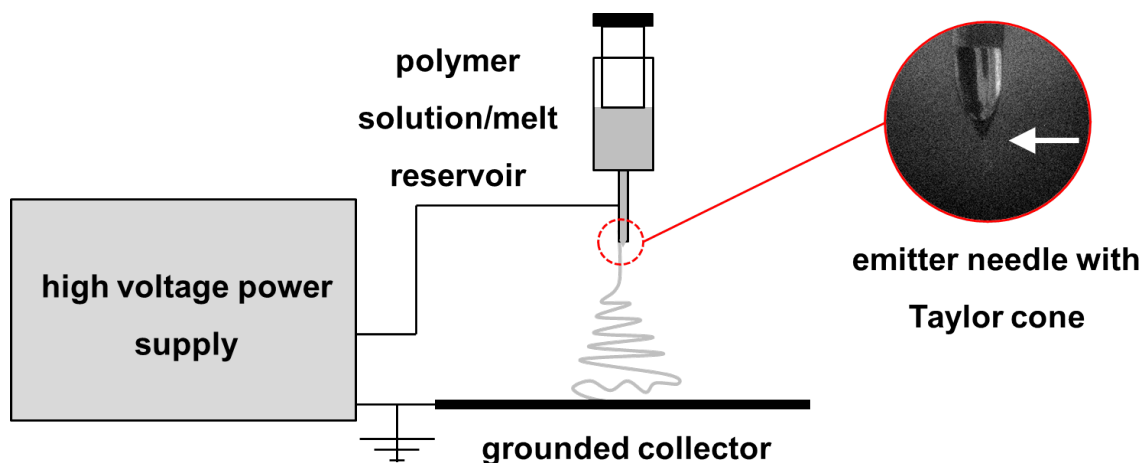


**Figure 5.** Schematic representation of an electrospinning setup. This basic principle is realized in various electrospinning apparatuses, small laboratory setups as used in this work, and industrial large-scale needleless spinnerets <sup>48</sup>. The arrow indicates the polymer solution jet ejecting from the Taylor cone.

<sup>a</sup> Though he referred to it as “*old, but now apparently little-known experiment of electrical spinning*” <sup>40</sup>.

<sup>b</sup> Google scholar, Sept. 23 2021: electrospinning OR electrospun OR “electro spinning” in the title of the document, no patents or citations included

For further adjustment of the nanofiber mats' properties and functions, various additional treatments such as crosslinking on the molecular level<sup>49,50</sup> or coating<sup>51</sup> may be applied. Most electrospun structures are fabricated via simple blend electrospinning, i.e., from a single solution/melt of a polymer or a polymer blend with active compounds dissolved in the spinning solution. Through a coaxial/multi-axial set-up or emulsion electrospinning the formation of core-shell fibers can be achieved, permitting the incorporation of liquids<sup>52</sup> and un-spinnable or sensitive material, such as enzymes or cells<sup>53–57</sup>, inside a protective outer layer. Core-shell fibers are not part of this work and are, therefore, not further considered in the following text.

On the molecular level, the formation of fibers in electrospinning is dependent on the presence of a deformable, long-range polymer network. This prevents the break-up of the jet into droplets due to Raleigh instability and shear stress during stretching and thinning of the developing fiber. Sufficient polymer molecular weight [ $M_w$ ] or chain length, concentration as well as solvent properties are crucial for a sufficient chain entanglement and thus the development of such a stable network<sup>58</sup>. The relationship between other relevant process parameters (polymer characteristics, ambient conditions, equipment, physicochemical properties of the spinning fluid) and the properties of the obtained fiber mats is less distinct and straightforward due to their large number and complex interdependence<sup>59–63</sup>. Therefore, process development and optimization in electrospinning are still based mainly on an empirical approach.

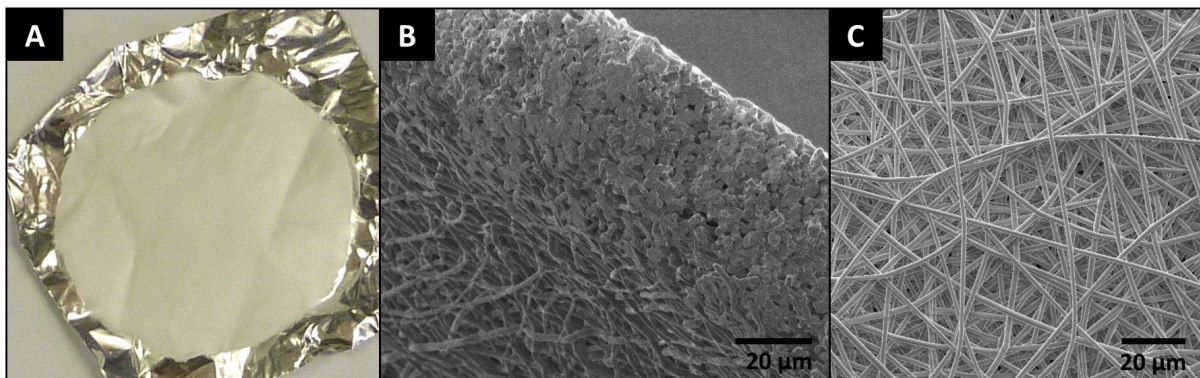


**Figure 6.** Electrospun non-wovens; (A) fiber mat; (B) and (C) scanning electron microscopic [SEM] images of electrospun polymer fiber mat.

### Non-woven polymer fibers as drug delivery systems

For drug delivery, electrospun fibers combine the advantages of micro- and nanosized materials with the easy handling of monolithic systems. They provide structures in the nm to  $\mu\text{m}$  range with an extremely high surface-area to volume ratio (estimates in the range of several  $\text{m}^2$  per g or  $\text{cm}^3$  <sup>64,65</sup>) without the need to address aggregation, sufficient dispersion, and suspension media, key challenges for disperse systems such as nano- and microparticles. Additionally, excellent drug encapsulation efficiency can be achieved through electrospinning, thus minimizing the wastage of valuable drug substances.

One of the most significant challenges for the use of electrospun materials in drug delivery remains the control of the drug release profile, as extensively reviewed in <sup>66</sup>.

The main parameters controlling drug release from electrospun non-wovens can - in a fairly simplified categorization - be attributed to:

#### (a) Fiber geometry and dimensions

Large surface area and small fiber diameters can increase dissolution rate compared to monolithic systems like solvent cast films <sup>67,68</sup>. The large polymer/fluid interface of the fiber scaffolds accelerates liquid penetration, polymer dissolution or swelling, and pore formation, thereby increasing the dissolution rate and drug release <sup>67,69,70</sup>. If drug crystallization occurs, the formed crystals are usually only in the range of several nm to  $\mu\text{m}$  due to the rapid drying/cooling of the spinning solution and the restriction through the small fiber diameter.

#### (b) State of drug and polymer matrix.

In blend electrospinning, drug solubility and concentration, drug/polymer compatibility, and solvent polarity and evaporation rate are key parameters. They each greatly influence drug distribution throughout the fibers, the formation of amorphous solid dispersions or crystallization of the drug/polymer components during fiber formation, and the consequent dissolution rate and apparent solubility of the electrospun drug <sup>68,69,71,72</sup>. In most settings, the rapid drying or cooling process during electrospinning favors the “freezing” of the electrospun fluid in the state of an amorphous solid dispersion <sup>73</sup>. Still, crystallization of compound inside or on the fiber surface is also possible <sup>71,72</sup>.

For BCS class II and IV compounds, the formation of a solid solution or amorphous dispersions in the polymer can be employed as a dissolution rate and solubility enhancing formulation approach. But overly increased dissolution rate and solubility may also inadvertently lead to burst release, the immediate, unintentional and uncontrolled, almost complete drug liberation. Usually caused by drug-polymer incompatibility, burst release is a major drawback of electrospun DDS <sup>71,72,74</sup>. Carefully controlling the interplay of poor drug solubility and high affinity to the fiber material can be employed to obtain a more sustained release from electrospun fibers, despite their very small diameter and short diffusion length <sup>75</sup>.

However, in many cases, the fiber dimensions seem to be the all-dominant release governing factor, leading to a fast drug liberation, independent of the EPF composition <sup>75</sup>. Consequently, constant drug release over several weeks from electrospun fibers manufactured via simple blend electrospinning has rarely been accomplished. Some reports in literature claim release over several weeks to month <sup>76-79</sup>. But no detailed investigations of

the controlling parameters are given, and in some cases, sufficient drugs solubility in the release medium seems not to have been appropriately considered.

Most electrospun materials are collected as highly porous, flexible fleece mats and are consequently mainly suitable for DDS in the form of patches, small flat disks, or drug-loaded wound dressings. Due to their low density and weight, they are best suited for delivering drugs with high potency and consequently low required doses. Local drug delivery, either to a particular tissue or compartment where comparatively small amounts of drug are needed, can be more easily achieved than systemic treatment.

To overcome the limits of the sheet-like geometry of the electrospun non-wovens, three-dimensional electrospun systems have been explored. While most of these scaffolds are designed for tissue engineering applications<sup>80</sup>, Duan et al. proposed macroporous electrospun polymer fiber sponges as drug carriers<sup>81,82</sup>. A prolonged release was observed for sponges with higher density, suggesting that 3D electrospun structures present an additional way to control drug release from nanofiber-based systems, possibly through the rate of liquid penetration into the pores of the carrier scaffold and impeded diffusion.

As an enabling formulation approach, electrospinning can be seen as akin to spray drying and hot-melt extrusion - thought, for solvent electrospinning, without the high temperatures often imposed during those techniques. Similar, amorphous solid dispersions can be attained. For various possible applications, electrospun nonwovens, unlike extrudates and spray-dried powders, do not need extensive further processing.

Drug stabilization and increase in dissolution and solubility via electrospinning are effective, simple, and have shown to scale up for industrial production<sup>83,84</sup>. Electrospinning, therefore, provides another valuable approach to the fabrication of solubility-increasing drug delivery systems. A multitude of proposed electrospun DDS for local and systemic delivery successful in in vivo animal models can be found in literature<sup>85-90</sup>.

But the extensive translation from research settings to commercially marketed electrospun products is still in the early stages. Over the last two decades, suppliers of electrospinning equipment started offering large-scale spinnerets with an output of up to 5 kg per day or 20 million m<sup>2</sup> per year<sup>83,91,92</sup>. Today, small to medium-sized electrospinning companies offer process development and contract manufacturing for research and commercial applications<sup>93-95</sup>. However, drug delivery systems based on electrospun fibers are still missing from among the marketed therapeutic systems.



## 2.4 Artemisone

### Artemisinin drugs – areas of application and relevance

Artemisone [ART] (**Structure 1**) is a comparatively recent second-generation derivative of artemisinin, belonging to the most effective and fast-acting class of antimalarial drugs currently available. The artemisinins are crucial in the global fight against malaria, a protozoan disease caused by *Plasmodium* species. In 2020 alone, malaria led to over 200 million infections and 409,000 deaths (mainly in young children under the age of five)<sup>96</sup>. Malaria is also responsible for economic losses of over 12 billion US \$ each year, primarily affecting some of the poorest countries in the world<sup>97</sup>. Artemisinin, the parent compound of the artemisinins, is a sesquiterpene lactone initially found in *Artemisia annua* L, a type of wormwood used in traditional Chinese medicine. Its commercially available derivatives - artesunate, artemether, and dihydroartemisinin - are recommended by the World Health Organization [WHO] as the first-line treatment of malaria and are included in the WHO list of essential medicines<sup>98,99</sup>

However, only intravenous or intramuscular artesunate and artemether are available in the case of the fast-progressing, often fatal severe and cerebral malaria. Stable, easy-to-administer dosage forms (e.g., for oral, intranasal, transdermal delivery) for immediate treatment could bring much-needed therapy to large parts of the afflicted population in underdeveloped rural areas where professional health care is not immediately available. Moreover, with growing resistance to the currently marketed artemisinins reported for *Plasmodium* strains in Southeast Asia<sup>100-102</sup>, new and more effective artemisinin derivatives and dosing regimens, to which the plasmodia are still susceptible, are fast becoming indispensable.

Their redox-driven effect also makes artemisinins a potential drug class for treating a variety of very different diseases other than malaria<sup>103-105</sup>. The artemisinins and artemisone in particular are also being investigated for their use in cancer therapy - especially melanoma<sup>106,107</sup>, against different forms of leishmaniasis<sup>108</sup>, cutaneous tuberculosis<sup>109</sup>, protozoal bovine diseases<sup>110,111</sup>, and the human cytomegalovirus<sup>112</sup>.

It was speculated that artemisinins are also active in schistosomes, like in plasmodia, by the heme-initiated formation of free radicals<sup>113-115</sup>. Therefore, various artemisinin derivatives have been suggested as an alternative to praziquantel for the treatment of schistosomiasis, a disease caused by parasites of the genus *Schistosoma*<sup>114</sup>.

Schistosomiasis is responsible for poor health and long-term disability in some of the least developed areas of the world<sup>116</sup>. Affecting an estimated 200 million people, schistosomiasis is second only to malaria as the world's most common parasitic disease, but its debilitating effects on individuals and whole communities are often overlooked<sup>116-118</sup>. Preventive chemotherapy and treatment with praziquantel are currently the only strategies implemented by the WHO. With the repurposing of the artemisinins as antischistosomal drugs, an additional treatment option could be made available<sup>114</sup>.

For these vastly different targets, a better understanding of how to stabilize and formulate ART and specifically tailored DDS both for systemic and local delivery will be needed to unlock the drug's full potential in the future.

### Current status in development

Artemisone was introduced by Haynes et al. in 2006<sup>119</sup> as a promising development candidate due to its increased antimalarial activity, favorable toxicity profile, and superior physicochemical properties compared to other artemisinin derivatives. The superiority of artemisone over artesunate (WHO-recommended first-line treatment for severe and cerebral malaria<sup>98</sup>) has since been demonstrated in both in vitro and animal in vivo studies<sup>119,120</sup>.

A first phase I study showed that multiple doses of up to 80 mg ART in immediate release oral tablets were well tolerated in healthy human subjects<sup>121</sup>. Artemis Therapeutics, Inc., a company dedicated to the research of ART, has received Orphan Drug Designation from the FDA for ART for the treatment of malaria<sup>122</sup>. The company claims to have completed phase II trials against malaria with 95 individuals. Preliminary results were already presented at the XVIth International Congress for Tropical Medicine<sup>123</sup>. But as they do not provide access to the actual data, little is known about the studies' success, the employed route of administration, and especially the DDS<sup>124,125</sup>.

Recent investigations by Gibhard et al. showed that artemisone is, in fact, a metabolite of the artemisinin derivative artemiside<sup>126</sup>.

### Physicochemical characteristics and formulation approaches

Due to its physicochemical properties, ART is generally considered a small molecule BCS class II drug (**Table 4**). With an aqueous solubility of only 89 mg/L, ART is poorly soluble according to the BCS threshold.

**Structure 1.** Artemisone

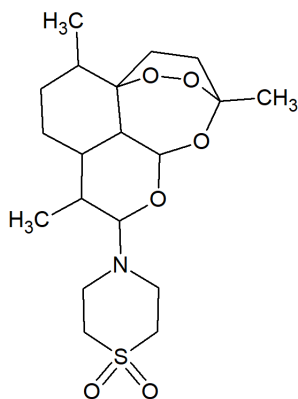


**Table 4.** Physicochemical characteristics of artemisone.

$M_w$ <sup>127</sup>	$T_m$ <sup>III</sup>	Log P <sup>I, 119</sup>	Aqueous solubility <sup>II, 119</sup>
401.5 Da	160 °C	2.49	89 mg/L

<sup>I</sup> Log P determined at pH 7.4. <sup>II</sup> Aqueous solubility at pH 7.2. No temperature was given for solubility and Log P data. <sup>III</sup> Obtained via Differential Scanning Calorimetry [DSC] by the author.

However, determination of the permeability via the FDA-mandated mass balance determination or in comparison to an intravenous reference dose in humans has not been published for ART. Only a comparative assessment is, therefore, possible. Following Lipinsky's "rule of five"<sup>128</sup>, a widely recognized rule of thumb to estimate a compound's bioavailability, artemisone would be classed as possessing good absorption and permeation. The molecule has less than 5 hydrogen bond donors (none) and 10 acceptors (7), a  $M_w < 500$ , and a  $\text{Log P} < 5$ .

Results of an in vitro assessment of drug permeability in a Caco-2 cell monolayer model predict a complete drug absorption for ART<sup>129</sup>, placing it above the required 85 % for good permeability according to the BCS. An estimation of the permeability of ART via a Caco-2

cell monolayer model was also published by Heyns et al., concluding that artemisone cannot be classed as poorly permeable <sup>130</sup>.

ART is a highly crystalline compound that does not exhibit polymorphism and possesses good thermal stability as a solid <sup>121</sup>. But its poor, pH-dependent aqueous stability remains one of the major difficulties in the development of ART DDS. A limited shelf-life, the uncontrolled formation of unknown, potentially toxic degradation products, and cost-intensive, demanding distribution and storage conditions are all associated with poor drug stability, significantly hampering further drug development.

A variety of formulation attempts have been made to address both ART's poor solubility and stability, as reviewed in <sup>131</sup> and <sup>132</sup>. However, of these proposed DDS, none was carried further than first in vivo animal studies, and none meets the criteria for simple manufacturing and administration combined with adequate drug stability.

Polymer implants showed good performance in mice, but for oral and topical application, lipid and surfactant-based systems were most successful. This observation is supported by theoretical considerations on lipid solubility of compounds based on their Log P and  $T_m$  °. Alskä et al. found that reasonable solubility in glycerides was indicated by a  $T_m$  of < 150 °C and suggests that drugs with higher melting points could be solubilized in lipid formulations containing high quantities of co-solvents and surfactants <sup>133</sup>. Accordingly, ART is considered a borderline substance with only intermediate solubility in triglyceride excipients that can be better formulated in partial glycerides or surfactants. Additionally, Pouton theorized that sufficient solubility in triglycerides can be expected for compounds with a Log P > 4, while also recommending that "*solvent capacity for less hydrophobic drugs [like ART] can be improved by blending triglycerides with other oily excipients which include mixed monoglycerides and diglycerides*" <sup>24</sup>. This is in good accordance with the observation that the author made in preliminary solubility studies for ART in lipid excipients. A generally higher solubility for ART in more polar lipids compared to triglycerides was found <sup>134</sup>. These observations and considerations served as the starting point for formulation development for artemisone in this work, focusing on solubility enhancing lipid-based DDS systems that can provide reasonable drug stability and cater to different routes of application.

---

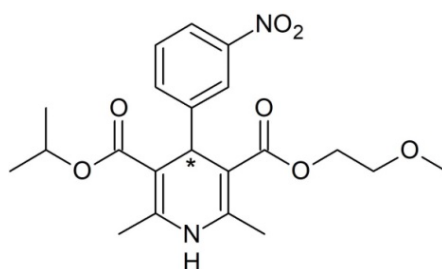
° Simplified predictions with only one of these denominators, should however, be treated with great care, as discussed in detail by Ditzinger et al. <sup>13</sup>.

## 2.5 Nimodipine

Nimodipine [NIMO] belongs to the class of dihydropyridine calcium channel blockers. NIMO possesses a selective vasodilatory effect, acting on cerebral arteries more than those in the systemic circulation, and is thus mainly used for the treatment of cerebrovascular disorders<sup>135</sup>. The FDA and European Medicines Agency [EMA] have both granted NIMO DDS orphan drug status for the therapy of aneurysmal subarachnoid hemorrhage where the drug can reduce incidence and severity of ischemic deficits<sup>136,137</sup>. Additionally, the administration of NIMO was successful for hearing preservation after vestibular schwannoma surgery. It has also been shown to accelerate peripheral facial nerve regeneration and prevent delayed ischemic deficits due to cerebral vasospasm after surgically-caused brain trauma<sup>138–142</sup>. However, the protective mechanism of action of NIMO is still under debate<sup>143</sup>.

### Physicochemical characteristics and stability concerns

Nimodipine (**Structure 2**) is a BCS class II drug with almost complete absorption from GIT but poor aqueous solubility (**Table 5**)<sup>144</sup>.



**Structure 2.** Nimodipine

**Table 5.** Physicochemical characteristics of the polymorphs of nimodipine.

Modification <sup>145</sup>	M <sub>w</sub>	T <sub>m</sub> <sup>I, 145</sup>	Log P <sup>II, 146</sup>	Aqueous solubility <sup>III, 145</sup>
	418.4 Da		3.05	
I (racemic, yellow, metastable)		124 °C		0.86 mg/L
II (conglomerate, white, stable)		116 °C		0.44 mg/L

<sup>I</sup> DSC onset temperature. <sup>II</sup> Log P (temperature not given). <sup>III</sup> Aqueous solubility at 37 °C in water.

NIMO exists in two polymorphic forms<sup>d</sup>. Through both possess activity, polymorphism presents the potential risk of alterations in processing properties, shelf-life, and most importantly, bioavailability of NIMO from a DDS through transformation into the more stable modification II with particularly poor aqueous solubility<sup>145,147</sup>. Furthermore, like other compounds of its dihydropyridine calcium antagonist class, NIMO also undergoes

<sup>d</sup> Note that the classification as polymorphism applied to a racemic mixture and the corresponding conglomerate as in the case of nimodipine is not universally agreed upon<sup>145</sup>.

photodecomposition, resulting in the oxidation to its pyridine analogue<sup>148,149</sup>. Therefore, extra care must be taken to address these instabilities in the design of a novel nimodipine DDS.

### **Available dosage forms and intracranial delivery**

Currently, NIMO is available in several immediate-release formulations - oral capsule or tablet (Nimotop®<sup>150,151</sup>) and an oral solution (Nymalize®<sup>15</sup>) as well as a concentrated intravenous infusion solution that can also be instilled intracisternally<sup>151</sup>. To address dissolution rate and low solubility nimodipine is available in a non-aqueous pharmaceutical solvent<sup>15,150,151</sup> or in the form of a solid amorphous dispersion of the drug in PEG 4000 obtained through spray drying<sup>151,152</sup>. In addition to their enabling characteristic, these systems also circumvent the issue of the drug's two polymorphic forms.

Despite its good absorption, NIMO has a low oral bioavailability of only 13 % due to the extensive hepatic metabolism. Rapid elimination requires frequent dosing every 4 hours<sup>135</sup>. NIMO can cross the blood-brain barrier, but the concentration is lower in the central nervous systems than in the periphery where it can cause hypotension as the most common dose-limiting side effect<sup>135</sup>. Contrasting drug pharmacokinetics and available DDS, the need for sustained-release formulations and specific brain targeting is thus immanent. Development of such systems has been attempted by several research groups, as reviewed in<sup>75</sup>, but no sustained release formulations are currently available.

For aneurysmal subarachnoid hemorrhage, phase I-III clinical trials with single-dose, intraventricular sustained-release NIMO poly-(D,L-lactide-co-glycolide) [PLGA] microparticles (EG-1962, Edge Therapeutics) have recently been done<sup>153-155</sup>. At similar peripheral serum concentrations, the authors could achieve cerebrospinal fluid concentrations two orders of magnitude higher than for oral NIMO, with a considerable, steady drug release over 21 days<sup>155</sup>. Unfortunately, this did not increase overall favorable outcomes compared to oral NIMO<sup>153</sup>. Additionally, the microparticles were designed to be administered via a mandatory extraventricular drain and the drain to be closed - if cerebral pressure and perfusion permitted this - for the particles to circulate into the basal cisterns<sup>154</sup>. Thus, specific deposition of the microparticles at the hemorrhage site was not achieved. Due to the dependence on adequate cerebral pressure, the method allows for inter-patient variations. Also, serum concentrations in the periphery were still considerable and could again be dose-limiting.

Higher local NIMO concentration only in the immediate proximity of the site of cerebral damage, through a well-placed implant, might provide a better option, particularly for patients already undergoing neurosurgical procedures. This is especially true for the off-label use during neurosurgery, where local NIMO treatment is still limited to the very imprecise method of soaking the surgical field with drug solution or insertion of NIMO loaded biodegradable swabs<sup>142</sup>. More work towards the development of suitable drug delivery platforms, therefore, has the potential to greatly improve and alter the way NIMO can be provided for the therapy of the brain.

### 3. Cumulative part

The work presented in this thesis was published in five full research articles in scientific peer-reviewed journals. An overview is given in **Table 6**.

All applied methods and results are described in detail in these articles and the corresponding supplementary material. While this thesis presents the main findings in chapter 4. *Results and discussions*, more in-depth discussions can be found in the individual publications (see *Appendix*).

**Table 6.** Peer-reviewed scientific journals where the work of this thesis was published and corresponding impact factor [IF].

Publication	Journal	IF*	Publisher
I <i>Oral administration of artemisone for the treatment of schistosomiasis: Formulation challenges and in vivo efficacy</i> <sup>131</sup>	Pharmaceutics	6.32	MDPI
II <i>Efficient treatment of experimental cerebral malaria by an artemisone-SMEDDS system: impact of application route and dosing frequency</i> <sup>132</sup>	Antimicrobial agents and chemotherapy	5.19	American Society for Microbiology
III <i>Transdermal delivery of artemisinin for treatment of pre-clinical cerebral malaria</i> <sup>156</sup>	International Journal for Parasitology: Drugs and Drug Resistance	4.08	Elsevier
IV <i>Electrospun Nimodipine-loaded fibers for nerve regeneration: Development and in vitro performance</i> <sup>75</sup>	European Journal of Pharmaceutics and Biopharmaceutics	5.57	Elsevier
V <i>Noninvasive characterization (EPR, <math>\mu</math>CT, NMR) of 3D PLA electrospun fiber sponges for controlled drug delivery</i> <sup>157</sup>	International Journal of Pharmaceutics: X	n.a.	Elsevier

\*The impact factor was published by Clarivate Analytics as  
 IF 2021 = (citations 2020 + citations 2019) / (papers published 2020 + papers published 2019) <sup>158</sup>

A declaration of the author's contribution of this doctoral thesis to the experimental part and the writing of the manuscript of each article is given in **Table 7**.

**Table 7.** Declaration of the author's contributions to the publications presented in this thesis.  
A: Planning, execution, data analysis, and evaluation of the experiments  
B: Preparation of the manuscript

Publication	A	B
<b>I</b> Zech J, Gold D, Salaymeh N, Sasson NC, Rabinowitch I, Golenser J, <i>et al.</i> Oral administration of artemisone for the treatment of schistosomiasis: Formulation challenges and in vivo efficacy. <i>Pharmaceutics</i> 2020; <b>12</b> .	<b>75 %</b>	<b>70 %</b>
<b>II</b> Zech J, Salaymeh N, Hunt NH, Mäder K, Golenser J. Efficient treatment of experimental cerebral malaria by an artemisone-SMEDDS system: Impact of application route and dosing frequency. <i>Antimicrob Agents Chemother</i> 2021; <b>65</b> .	<b>70 %</b>	<b>85 %</b>
<b>III</b> Zech J, Dzikowski R, Simantov K, Golenser J, Mäder K. Transdermal delivery of artemisinins for treatment of pre-clinical cerebral malaria. <i>Int J Parasitol Drugs Drug Resist</i> 2021; <b>16</b> : 148–54.	<b>30 %</b>	<b>50 %</b>
<b>IV</b> Zech J, Leisz S, Göttel B, Syrowatka F, Greiner A, Strauss C, <i>et al.</i> Electrospun Nimodipine-loaded fibers for nerve regeneration: Development and in vitro performance. <i>Eur J Pharm Biopharm</i> 2020; <b>151</b> :116–26.	<b>80 %</b>	<b>80 %</b>
<b>V</b> Zech J, Mader M, Gündel D, Metz H, Odparlik A, Agarwal S, <i>et al.</i> Noninvasive characterization (EPR, $\mu$ CT, NMR) of 3D PLA electrospun fiber sponges for controlled drug delivery. <i>Int J Pharm X</i> 2020; <b>2</b> .	<b>75 %</b>	<b>50 %</b>

### 3.1 Artemisone self-microemulsifying drug delivery system

#### Publication I

Zech J, Gold D, Salaymeh N, Sasson NC, Rabinowitch I, Golenser J, *et al.* Oral administration of artemisone for the treatment of schistosomiasis: Formulation challenges and in vivo efficacy. *Pharmaceutics* 2020; **12**.

<https://www.mdpi.com/1999-4923/12/6/509/htm>

Supplementary material:

<https://www.mdpi.com/1999-4923/12/6/509#supplementary>

#### Publication II

Zech J, Salaymeh N, Hunt NH, Mäder K, Golenser J. Efficient treatment of experimental cerebral malaria by an artemisone-SMEDDS system: Impact of application route and dosing frequency. *Antimicrob Agents Chemother* 2021; **65**.

<https://doi.org/10.1128/AAC.02106-20>

#### Publication III

Zech J, Dzikowski R, Simantov K, Golenser J, Mäder K. Transdermal delivery of artemisinins for treatment of pre-clinical cerebral malaria. *Int J Parasitol Drugs Drug Resist* 2021; **16**: 148–54.

<https://doi.org/10.1016/j.ijpddr.2021.05.008>

**Publication I – III** describe the successful development of a SMEDDS system for the administration of the antimalarial drug artemisone.

Formulation development and physicochemical characterization are laid out in **publication I**<sup>131</sup>. As ART is poorly soluble in water and also possesses poor aqueous stability, special attention was paid to drug solubility and stability in the formulation. Variation of microstructure upon dilution and self-emulsifying properties were also assessed to discern the behavior of the system after administration. The SMEDDS was then tested in vitro against the human malaria parasite *Plasmodium falciparum*.

To examine the applicability of the carrier as a solubility enhancing formulation for ART, the efficacy of oral treatment with the drug-loaded SMEDDS against a murine model of infections with *Schistosoma mansoni* was investigated. Parasite worm and egg burden and histology of liver sections clearly demonstrate the superiority of the treatment over placebo (**Figure 7**).

Pharmacokinetics of ART delivery via the SMEDDS system were focused on in **publication II**<sup>132</sup>, using cerebral malaria in mice caused by *Plasmodium berghei* infections as in vivo model. Drug serum concentrations after oral administration were analyzed via high performance liquid chromatography-mass spectrometry [HPLC-MS], and clear dose-dependence was established for the ART DDS.



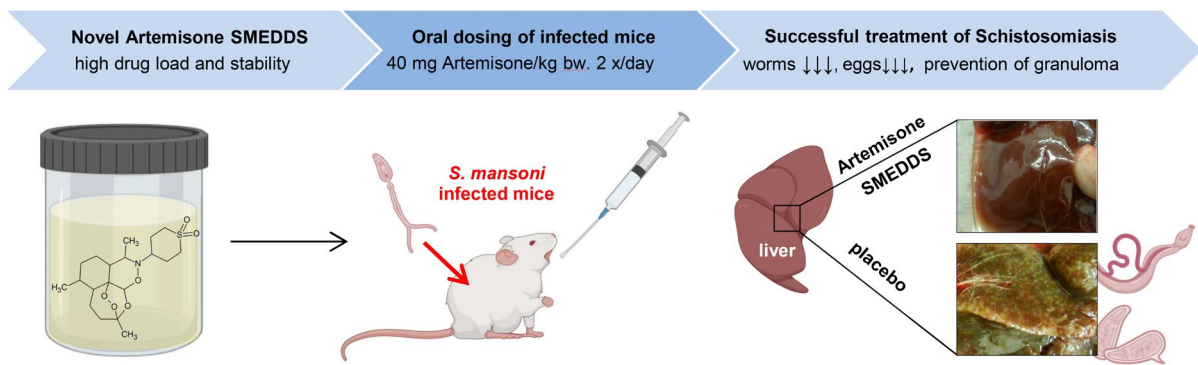


**Figure 7.** Graphical abstract of **publication I** (from <sup>131</sup>).

Evaluation of the effect of dosing frequency revealed the clear advantage of a split daily dose compared to once-daily administration for the same daily ART dose. The effectivity of different routes of administration was also examined, comparing intranasal (most successful), oral, and intraperitoneal delivery (least successful). The results again confirmed the suitability of the carrier as enabling formulation for ART.

**Publication III** <sup>156</sup> examined the formulation as a transdermal delivery system for ART, also employing the murine cerebral malaria model. Drug availability via that route was estimated based on cultured *P. falciparum* as a bioassay for ART mouse serum concentrations. The efficacy of ART in the SMEDDS system was compared to artesunate, which was also delivered transcutaneously. Different doses and dosing schemes were tested and showed a good efficacy of transdermal ART delivery.

## 3.2 Electrospun polymer fibers

### Publication IV

Zech J, Leisz S, Göttel B, Syrowatka F, Greiner A, Strauss C, et al. Electrospun Nimodipine-loaded fibers for nerve regeneration: Development and in vitro performance. *Eur J Pharm Biopharm* 2020; **151**:116–26.

<https://doi.org/10.1016/j.ejpb.2020.03.021>

### Publication V

Zech J, Mader M, Gündel D, Metz H, Odparlik A, Agarwal S, et al. Noninvasive characterization (EPR,  $\mu$ CT, NMR) of 3D PLA electrospun fiber sponges for controlled drug delivery. *Int J Pharm X* 2020; **2**.

<https://doi.org/10.1016/j.ijpx.2020.100055>

Supplementary material:

<https://www.sciencedirect.com/science/article/pii/S2590156720300177#s0135>

Different aspects controlling the drug release from electrospun polymer fibers [EPF] and fiber-based polymer sponges were examined in **publications IV** and **V**.

Nimodipine-releasing polymer fiber mats as possible intracranial implants are described in **publication IV**<sup>75</sup>. A stable blend-electrospinning process for PLGA fiber mats was established to prepare biodegradable non-wovens with 1 and 10 % drug and fiber diameters between 1 and 4  $\mu$ m. DSC and x-ray diffractometry analysis confirmed the successful encapsulation of the drug and the amorphous state of NIMO within the fiber matrix. Drug-loaded fibers remained stable for at least six months.

Drug release assayed in two different media showed their decided impact on the drug release profile:

In 1 % Tween 80, a burst release was observed, and the complete amount of drug was liberated within 6-8 days. In addition, a loss of fiber geometry over a 14 day incubation period was observed that potentially also affected the release profile.

In contrast, linear drug release was achieved in cell culture media with only 35 – 55 % NIMO released after 4 days.

The NIMO EPF showed no toxicity towards different brain-relevant cell lines but instead had cytoprotective activity in differently stressed cells in vitro.

Polymer fiber sponges [PFS], ultralight, highly porous, and hydrophobic scaffolds formed from short EPF, were studied in **publication V**<sup>157</sup>. To assess their suitability as DDS, PFS-specific traits governing drug delivery were analysed (**Figure 8**).

Slow water penetration might sustain drug release from these scaffolds. Non-invasive characterization via micro-computed tomography [ $\mu$ CT] and electron paramagnetic resonance [EPR] imaging was applied to follow and quantify the uptake of aqueous liquids

into the sponge. Incubation in a surface-active protein solution, as a model bodily fluid, and prevention of air entrapment within the samples were identified as influential governing parameters and reduced water penetration time from 45 to just 4 weeks.

Loading of the lipophilic sponges with oily drug solutions was explored as a different delivery option. Oil uptake, mechanical stability, and oil holding capacity were assessed as prerequisites for this form of application. Restricted diffusion within the sponge and interaction of the fiber scaffold with the oil on a molecular level was demonstrated through proton nuclear magnetic resonance [ $^1\text{H}$  NMR] measurements of transverse magnetization relaxation and the diffusion coefficient  $D$ . However, the oil-loaded PFS did not significantly alter drug release when compared to simple oily drug solution.

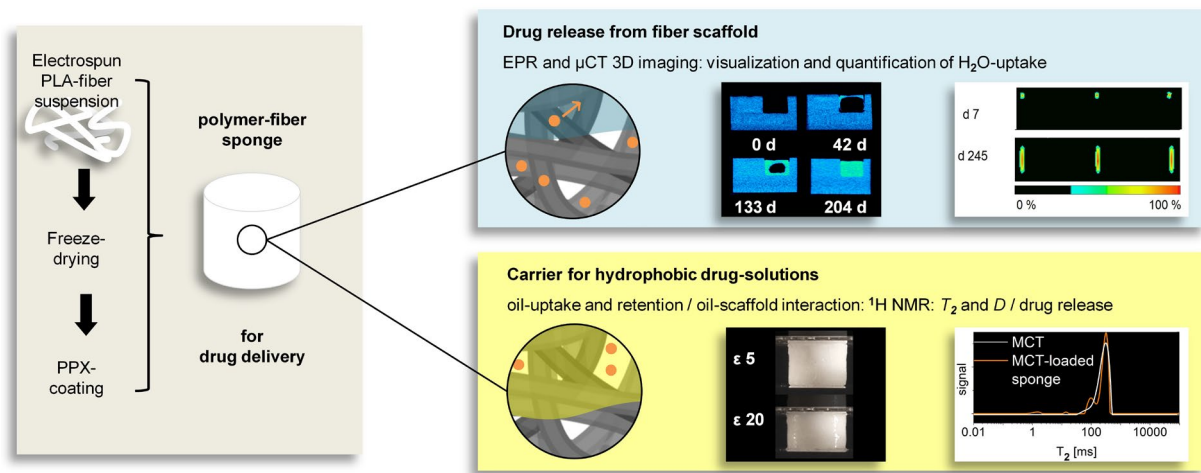


**Figure 8.** Graphical abstract of **publication V** (from <sup>157</sup>).

## 4. RESULTS AND DISCUSSION

### 4.1 Artemisone self-microemulsifying drug delivery system

The objective of this part of the work - presented in publication I-III - was the formulation development, in vitro and in vivo testing of a solubility enhancing DDS for the artemisinin derivative artemisone. Based on the properties of ART laid out in the introduction, a SMEDDS was selected as formulation principle.

Particular emphasis was placed on evaluating the in vivo performance of the DDS in mouse models of severe malaria and schistosomiasis as a tool to get a profound understanding of the release kinetics for the different routes of administration (oral, i.p., intranasal, and transdermal). Drug liberation from SMEDDS and microemulsions is difficult to test reliably in vitro, mainly because the formulation is usually completely dispersed into micelles in the aqueous release medium at sink conditions. Similarly, no standardized in vitro model for intranasal drug uptake has yet been proposed. This makes the animal models invaluable for correctly assessing successful solubility enhancement and drug absorption. Results from the treatment of mice also allow a first general estimation of possible dosing regimens and treatment frequency and the most suitable route of administration for the later possible use in humans.

#### Formulation development

Though ART was introduced in 2006<sup>119</sup> and the development of several DDS has since been attempted, no systematic screening of the drug's molecular properties with relation to formulation design has been published. A methodical analysis of solubility in different excipients and stability studies were thus the starting point in the formulation development.

Poor aqueous stability has been reported for various artemisinin derivatives<sup>159-161</sup>. To predict ART's possible degradation, drug recovery in aqueous solutions was monitored. The degradation rate is pH-dependent, but degradation occurs over a broad pH range (**Figure 9A**). Results confirm that storage stability can best be achieved in a water-free formulation. The exposure of the drug to gastrointestinal fluids might be a cause for poor bioavailability due to drug degradation.

Most of the proposed first attempts at formulations for ART found in literature are lipid-based<sup>132</sup>, and in preliminary solubility studies the author also found a particularly good solubility of ART in lipid excipients<sup>134</sup>. More systematic solubility testing further specified that solubility was generally higher in more polar lipids (**Figure 9B**), which is in accordance with the theoretical considerations on lipid solubility of ART based on Log P and  $T_m$  (see 2.4 *Artemisone*).

As the solubility of a drug in a mixed lipid-based formulation is mainly achieved through its good solubility in the individual components<sup>30,31</sup>, the excipients with the best solubility for ART were selected as potential ingredients for the SMEDDS. In addition to well-known, routinely-used substances, the REACH compound Polysorb ID 46 was included as new excipient. The C8-C10 isosorbide diester proved to be a good solvent for artemisone (55 mg/g) and is used here in formulation design for the first time. Results seem to confirm its suitability as an exciting novel pharmaceutical excipient.

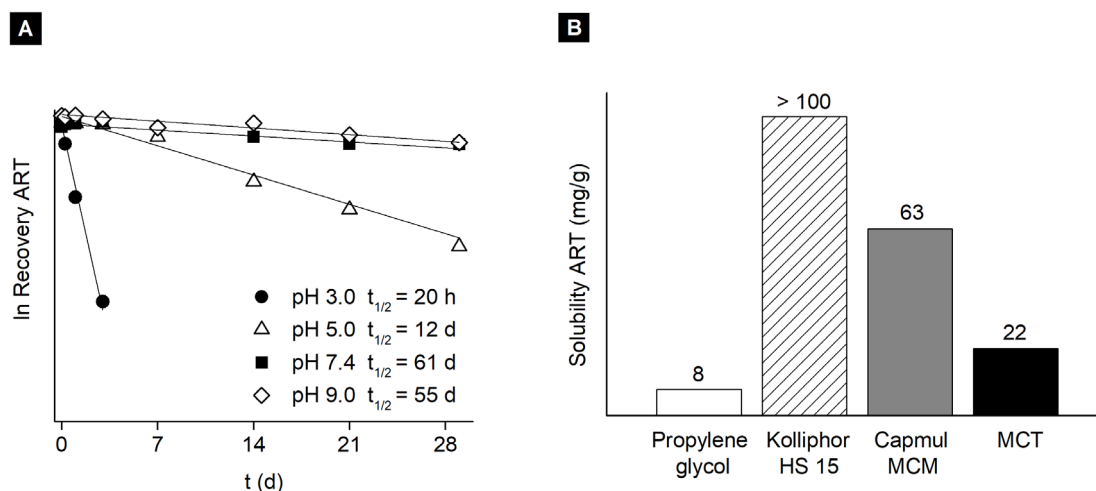


**Figure 9.** (A) pH-dependent stability of ART in phosphate buffer solutions measured via HPLC (modified from <sup>131</sup>, data fitted according to first-order kinetics,  $R^2 > 0.9$ ). (B) Solubility of ART in different excipients of decreasing polarity (left to right, based on data from <sup>131</sup>). Co-surfactant/co-solvent propylene glycol; surfactant Kolliphor HS 15 (polyoxyl (15) hydroxyl-stearate, HLB 15); partial glycerides Capmul® MCM (glycerol monocaprylocaprate); medium-chain triglycerides [MCT] (glycerol tricaprylocaprate).

The composition of the final optimized SMEDDS formulation [SMEDDS-100] was chosen based on its excellent dilution/self-emulsification behavior and resulting large isotropic area. The composition and corresponding ternary phase diagram are given in **Figure 10**.

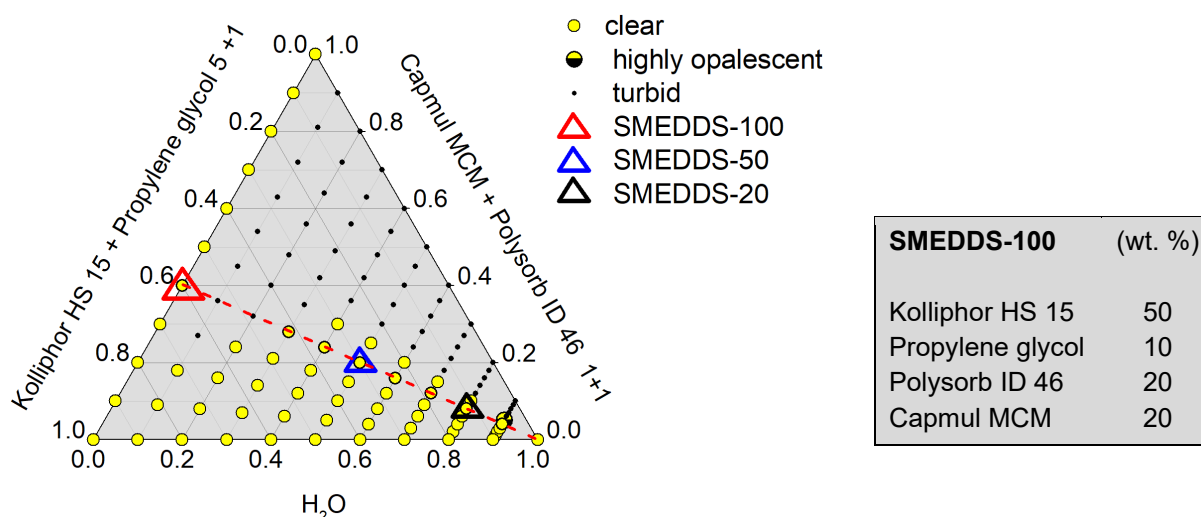


**Figure 10.** Final formulation SMEDDS-100: Ternary phase diagram of the pseudo-ternary mixtures (w/w) of distilled water, surfactant/co-solvent (Kolliphor HS 15 and propylene glycol), and lipid excipient (Capmul MCM and Polysorb ID 46). Note that the partial glyceride Capmul MCM also acts as co-surfactant. Any formulations that did not appear completely clear were classed as turbid. Open triangles mark the water-free SMEDDS-100 and resulting ME SMEDDS-50 and SMEDDS-20 selected as possible DDS. The dotted line indicates the dilution pathway of SMEDDS-100. Modified from <sup>131</sup>  
**Inserted table:** Composition of SMEDDS-100.

According to Pouton's Lipid Formulation Classification System<sup>24,25</sup>, SMEDDS-100 can be classified as a Type III lipid formulation. The high amount of surfactant suggests a Type IIIB, but the 40 % mix of partial glyceride and Polysorb ID 46 and only 10 % co-solvent propylene glycol instead indicate a Type IIIA system.

The transformation of a SMEDDS when brought into contact with aqueous fluids can give some information on the fate of the formulation after administration, upon increasing dilution, e.g., in the GIT. Complete self-emulsification could be reached through gentle shaking of SMEDDS-100 overlaid with phosphate buffered saline [PBS], indicating that GI motion would be sufficient to form a ME after oral administration.

Typically, a transition from a SMEDDS to a w/o ME is observed after adding moderate amounts of water to the system. Further increasing the water volume fraction  $\phi_w$  will lead to a bicontinuous structure and eventually result in an o/w ME. To better understand the changes in the microstructure of self-emulsifying formulation, a series of dilutions of the SMEDDS-100 in steps of 10 % (w/w), from  $\phi_w$  0.1 to 0.9, was studied. The physicochemical properties and the possible microstructures of the resulting ME were investigated by applying a variety of analytical methods, including:

- Conductivity measurements – changes in conductivity as an indicator for a percolating aqueous or lipid phase.
- Optical determination of cloud point – sensitivity to temperature changes.
- Polarized light microscopy – observation of the formation of liquid crystalline structures at the SMEDDS-100/water interface.
- Solubilization assay – solubility of Sudan Red (lipophilic dye) to visualize the existence of lipid-rich domains in the ME microstructure.
- Rheology – changes in dynamic viscosity (capillary viscometer) and shear viscosity (rotational rheometer).
- Cryogenic electron microscopy [cryoEM] – imaging of the microstructure of the ME
- Dynamic light scattering [DLS] - changes in apparent particle size as an indication of the rearrangement in microstructure<sup>e</sup>.

Exemplary results are given in **Figure 11**, while more detailed findings are included in the supplementary material<sup>162</sup> of publication I<sup>131</sup>.

---

<sup>e</sup> Dynamic light scattering/photon correlation spectroscopy is frequently used to study ME but correct quantitative particle size distributions are difficult to obtain, due to multiple scattering effects and the interaction of the analyzed structures. Additionally, the structures are mostly of unknown shape or even bicontinuous, so shape correction could not be performed and the diameter distributions are calculated based on spherical particles. In addition, ME are highly dynamic systems and therefore, the rapid change of the light scattering intensity could be caused by different processes.

Consequently DLS was only employed to trace changes in the detected microstructures and to discover possible trends. Resulting hydrodynamic diameters were not considered as correct dimensions of the structures present in the samples.

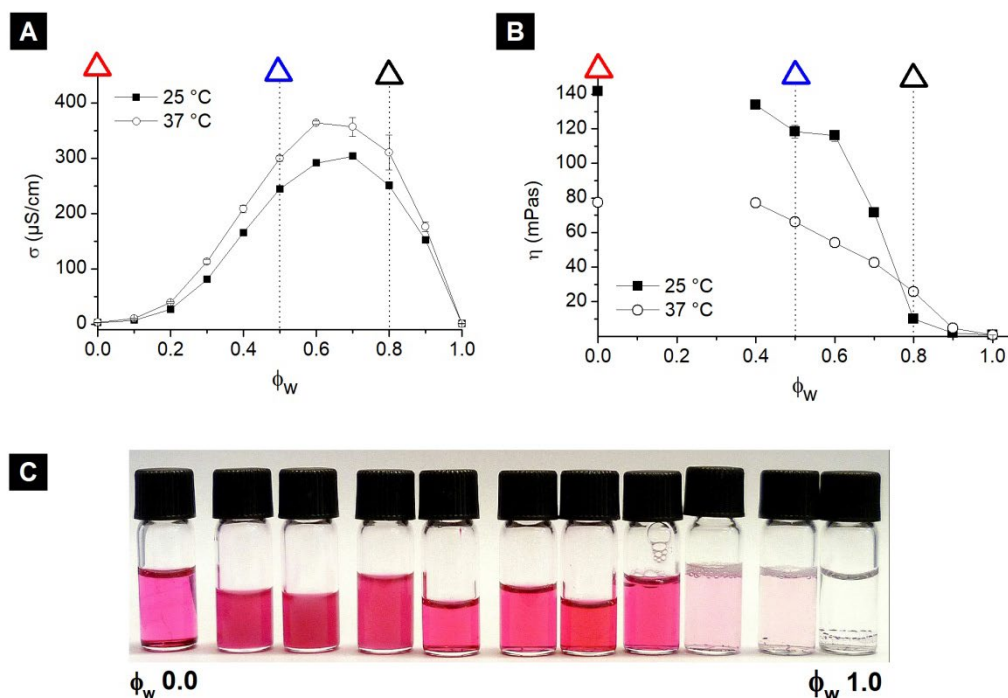


**Figure 11.** Physicochemical characterization of SMEDDS-100 and resulting ME regarding the water volume fraction  $\phi_w$ . The triangles indicate SMEDSS-100  $\blacktriangle$ , SMEDDS-50  $\triangle$ , and SMEDDS-20  $\blacktriangle$ . **(A)** Conductivity of dilutions of SMEDDS-100 with distilled water. **(B)** Dynamic viscosity measured with a capillary viscometer. **(C)** Sudan Red solubilization assay: the same amount of Sudan Red powder was added to dilutions of SMEDDS-100 with distilled water (steps of 10 %). Incomplete dilution was observed for  $\phi_w$  of 0.8 and higher. **(B)** and **(C)** modified from <sup>162</sup>.

Examining the data which were obtained with this broad spectrum of different methods and comparing it to similar observations for other ME found in literature <sup>163–171</sup>, it was hypothesized that:

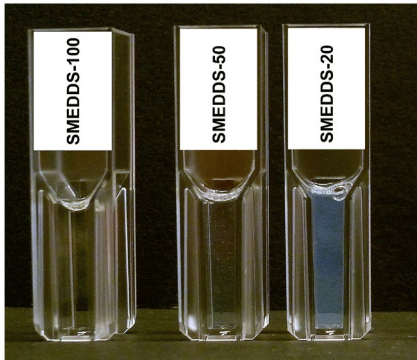
- At  $\phi_w$  0.1 to 0.3, a coarse w/o emulsion is present as indicated by the cloudy appearance and phase separation together with low conductivity.
- Between  $\phi_w$  0.3 and 0.5 a w/o ME is formed with increasing clustering and percolation of the water phase, resulting in linear growth in conductivity of the optically isotropic mixtures.
- A bicontinuous system is suspected to be present at  $\phi_w$  0.5 and possibly 0.6 (shear thinning and little change in viscosity and conductivity) before the formulation is transformed to an o/w ME (rapid decrease in viscosity at 25 °C but increased conductivity for  $\phi_w$  0.7; still good solubility of Sudan Red).
- Micelles make up the formulations at  $\phi_w$  0.8 and 0.9 (very low viscosity due to water as dispersion medium of micelles; poor solubility of Sudan Red, strong blue opalescence, structures < 100 nm in DLS.  $\phi_w$  0.8 exhibited thixotropic behavior, suggesting a three-dimensional clustered network of micelles).

Based on these observations, two of the ME, containing 50 % SMEDDS [SMEDDS-50] ( $\phi_w$  0.5) and 20 % SMEDDS [SMEDDS-20] ( $\phi_w$  0.8), were identified as possible additional DDS in vivo studies respectively (**Table 8**).



**Table 8.** SMEDDS-100-derived microemulsions SMEDDS-50 and SMEDDS-20: Composition and route of administration in the in vivo experiments. **Inserted image:** Observed transparency of the formulations. SMEDDS-20 exhibits a strong blue opalescence. Image from <sup>132</sup>.

	SMEDDS-50	SMEDDS-20
<b>Composition (wt. %)</b>		
SMEDDS-100	50	20
PBS pH 7.4 or H <sub>2</sub> O	50	80
<b>Route of administration</b>	Intranasal	Oral, i.p. transdermal



Cryogenic electron microscopy further verified the findings for these two ME (**Figure 12**). All results considered together strongly indicate that SMEDDS-50 is a bicontinuous system while SMEDDS-20 is formed from a clustered network of cylindrical micelles.

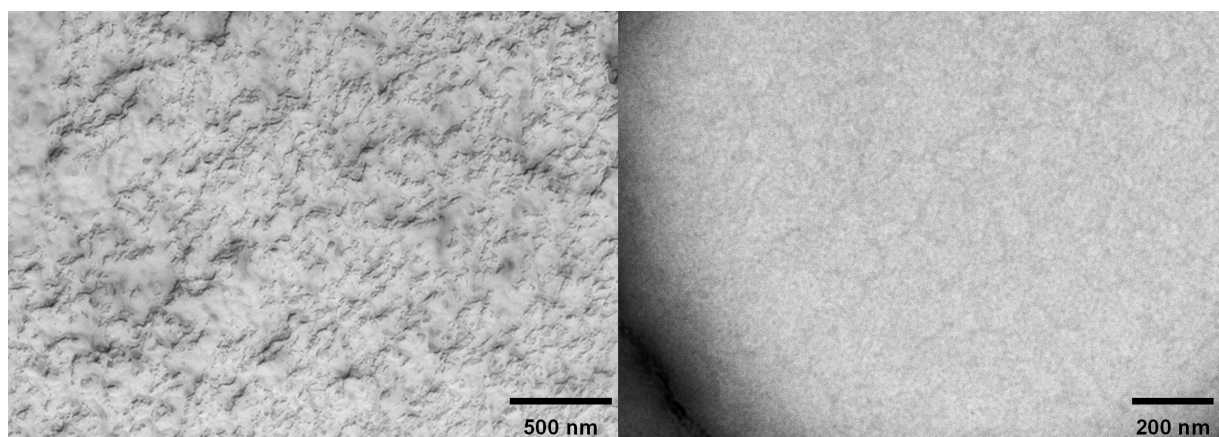


**Figure 12.** Freezing fracture micrographs of SMEDDS-50 (**left**) and cryogenic transmission electron microscopy image of SMEDDS-20 (**right**). The pictures suggest a bicontinuous structure for SMEDDS-50 and cylindrical micelles for SMEDDS-20. Modified from <sup>162</sup>.

Physicochemical experiments all had to be carried out with drug-free SMEDDS because ART is too scarce and expensive to be used in the large quantities that would have been necessary. But DLS showed slight to no changes in apparent particle size if ART was added to the formulation. That suggests that the physicochemical characteristics are the same for SMEDDS and ME with and without drug.



SMEDDS-100 proved to be excellent at increasing ART solubility. The saturation solubility was 59 mg/g at room temperature, a 660 fold increase in solubility compared to PBS. Drug-loaded ME were usually prepared by adding water or PBS to the drug-containing SMEDDS-100. To rule out the severe loss of solvent capacity upon dilution, common for LFCS class III systems<sup>11</sup>, SMEDDS-100 with 5 wt. % ART, the resulting SMEDDS-50, SMEDDS-20, and a 1:20 dilution (w/w) of the drug-containing SMEDDS-100 with distilled water, were monitored via light microscopy. No drug precipitation was observed over 24 h, suggesting that drug uptake would not be hindered by possible recrystallization due to the dilution of the formulation.

ART's chemical stability in SMEDDS-100, SMEDDS-50, and SMEDDS-20 at 30 °C was studied via HPLC analysis and compared to the drug's aqueous stability at the pH found for SMEDDS-50 and SMEDDS-20 (**Figure 13**). ART showed unexpectedly high stability, even in the presence of 50 % water, with less than 2 % drug degradation over three months. The incorporation of ART in water-free lipid domains within the bicontinuous SMEDDS-50 could protect ART from water-mediated degradation<sup>34–36</sup>. The micelle-based SMEDDS-20 did not provide such structures and possessed poor storage stability. ART was stable in SMEDDS-20 for 24 hours, long enough for oral drug uptake, but the drug-loaded formulation exhibited precipitation after 7 days. Fast decomposition of ART dissolved in 1 % sodium lauryl sulfate was observed by Bagheri<sup>172</sup>, also suggesting that solubilization in simple micelles does not protect ART from degradation in an aqueous environment. The developed SMEDDS-50 as a lipid-rich, bicontinuous system showed superior performance.

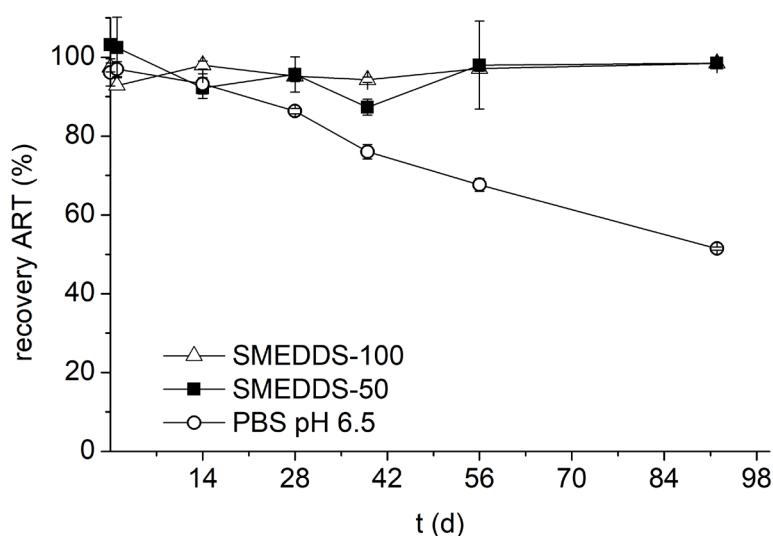


**Figure 13.** Stability of ART in SMEDDS-100, SMEDDS-50, and PBS pH 6.5 (pH equivalent to that of SMEDDS-50), at 30 °C. Drug content was measured via HPLC. Modified from<sup>131</sup>.

### In vitro evaluation

The effectivity of the formulation was shown in vitro in a culture of *P. falciparum* NF54 in human erythrocytes. Drug-free SEMDDS-20 and 10 mg/g ART in SMEDDS-20 were compared to an ART solution in DMSO (all diluted in culture medium). An ED<sub>50</sub> of 1-2 ng/ml was found for ART in SMEEDS-20 and in DMSO, suggesting that the drug was readily available from the ME. Hence, poor performance due to an overly high affinity of the drug to the carrier and resulting partitioning effects are unlikely. Activity of the drug-free formulation in vitro was ruled out, and no hemolysis was observed for the SMEDDS.

### In vivo studies

For animal treatment, SMEDDS-50 was chosen as the carrier for intranasal administration. The high percentage of SMEEDS-100 ensures good solubility of ART in small volumes of the ME and the considerable viscosity of SMEDDS-50 a prolonged time of residency on the nasal mucosa<sup>173</sup>.

Oral, transdermal, and i.p. administration was performed with ART in SMEDDS-20. This ME still possesses a considerable amount of lipid excipients, but the comparatively low viscosity also allows for the use as a spray and oral administration in mice through fine needles as gavage.

Two animal models for murine cerebral malaria and murine schistosomiasis were used in the in vivo experiments (**Figure 14**).

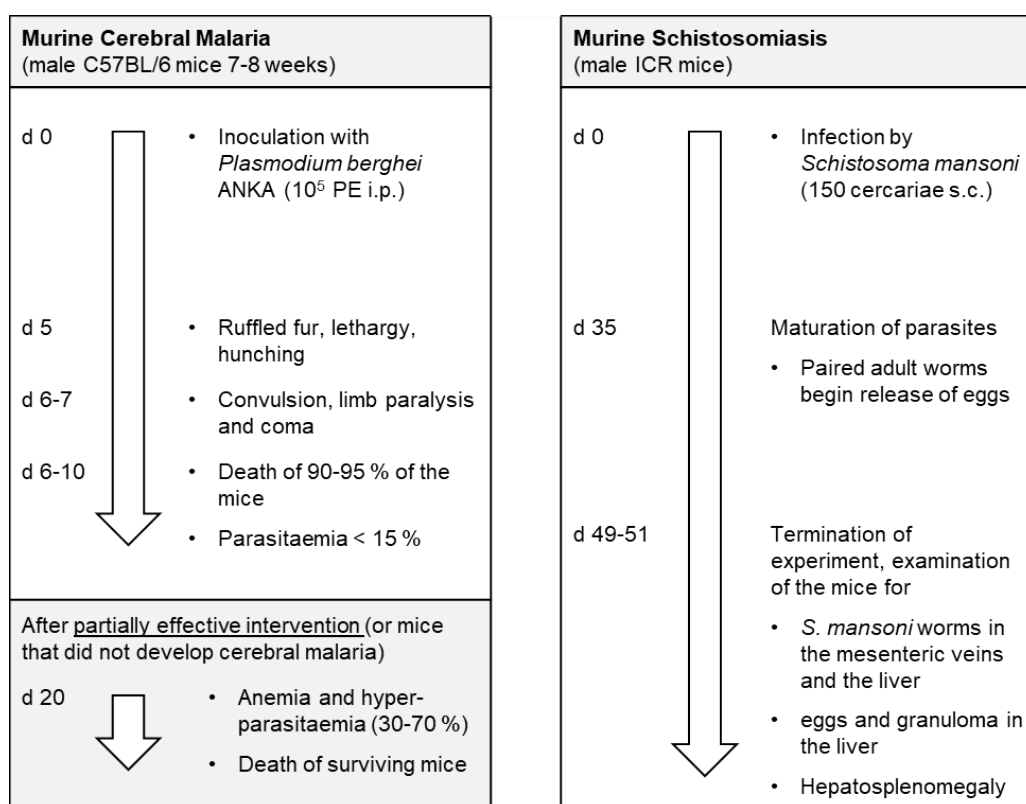


**Figure 14.** Animal models used in the in vivo testing. [PE] Parasitized erythrocytes.

### Schistosomiasis

The pathology of infection with *Schistosoma mansoni* in mice is not identical but similar to that in humans. Murine infections are therefore routinely examined in the testing of therapies against bilharzia<sup>174–176</sup>.

The successful ART delivery from the self-microemulsifying DDS was demonstrated for the oral treatment in *Schistosoma* infected mice (**Table 9**).

**Table 9.** Oral treatment of murine schistosomiasis. 40 mg/kg bodyweight artemisone in 300  $\mu$ l SMEDDS or the same volume drug-free SMEDDS-20 were administered via gavage twice per day on days 23-25 and 29-31 post infection. Recovered worms in the liver and mesenteric veins, eggs, and granuloma were counted from hematoxylin-eosin stained cuts of liver sections.

	Worms per mouse*	Eggs / cm <sup>2</sup>	Granuloma / cm <sup>2</sup>
<b>40 mg/kg ART [n=6]</b>	1.8 $\pm$ 1.5	0	0
<b>Placebo [n =9]</b>	49.1 $\pm$ 16.2	85 $\pm$ 50	51 $\pm$ 22

\*No worms were found in 2/6 of the treated animals. All worms found in the treated mice were degenerate. An average of 42.6  $\pm$  13.2 worms was counted in the untreated infected control group [n=9].

Treatment of *S. mansoni* infections produced a 96 % reduction of worms compared to placebo-treated mice. No eggs and resulting granuloma were present in the liver sections of the treated animals (**Figure 15**). These findings are especially remarkable compared to the 400-450 mg/kg ART (all drug doses given as mg/kg bodyweight) needed to achieve similar outcomes when the same mouse model is treated orally with an aqueous drug suspension<sup>113</sup>. Similarly, for other artemisinin derivatives, between 100 and 400 mg/kg were mostly used in successful oral treatment<sup>115</sup>. Admittedly, the dosing regime in these experiments is not identical with this work which somewhat restricts direct comparison. However, the equivalent efficacy of only 10 % of administered drug distinctly points at a highly increased ART uptake from SMEDDS-20 due to enhanced drug solubility in the lipid formulation.

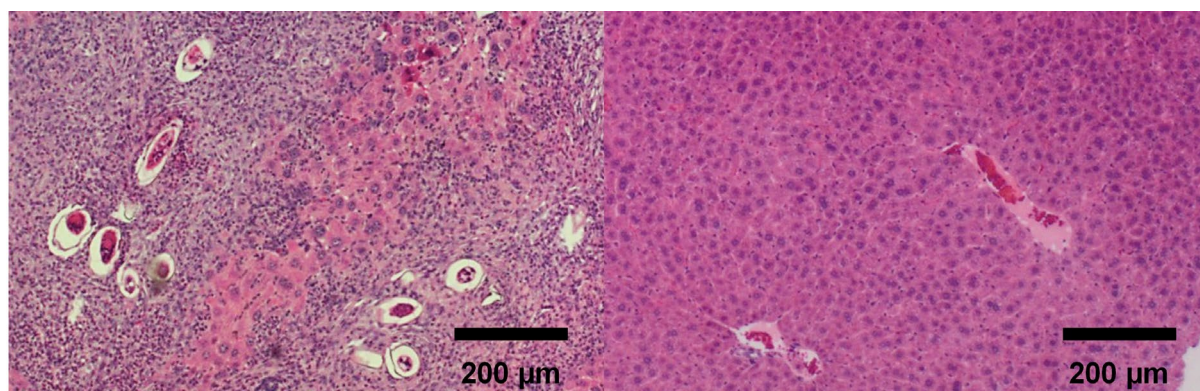


**Figure 15.** Hematoxylin-eosin stained cuts of liver sections of *S. mansoni* infected mice. Placebo-treated animal: many eggs and granulomas (**left**); Artemisone-treated mouse: no granulomas, the larger structures represent blood vessels (**right**).

### Cerebral Malaria

A more comprehensive understanding of ART delivery and absorption kinetics from the developed carrier system was obtained in a murine model of cerebral malaria (**Figure 14**). In this in vivo model, the course of the infection can be easily followed quantitatively over time in each individual animal, and results are gained within a few weeks.

*Plasmodium falciparum*, the main cause for severe and cerebral malaria [CM] in humans, cannot be cultivated in mice due to the parasite's host specificity<sup>177</sup>. The infection of mice with the rodent parasite *Plasmodium berghei* has therefore long been established as a reliable model of CM<sup>178–180</sup>. Successful intervention ideally eradicates all parasites but may also lead to a shift from CM to the development of anemic malaria [AM]. This shift can already be considered a beneficial outcome: the delayed mortality due to anemia - compared to an early death because of CM - offers a time window for proper diagnosis and treatment. This can result in an increased chance of survival in the analogous treatment of *P. falciparum* in human patients.

To establish the required dose for the in vivo treatment of *P. berghei* infections, 10, 20, or 40 mg/kg ART in SMEDDS-20 were administered to mice via gavage. Clear dose dependence was found for the delay in parasite detection and survival of the mice, mainly due to the shift from CM to AM in the 20 and 40 mg/kg groups (**Figure 16**). However, a 10 mg/kg dose was not sufficient to achieve the same effect. 20 mg/kg/day, therefore, proved to be the most suitable dose for further experiments.

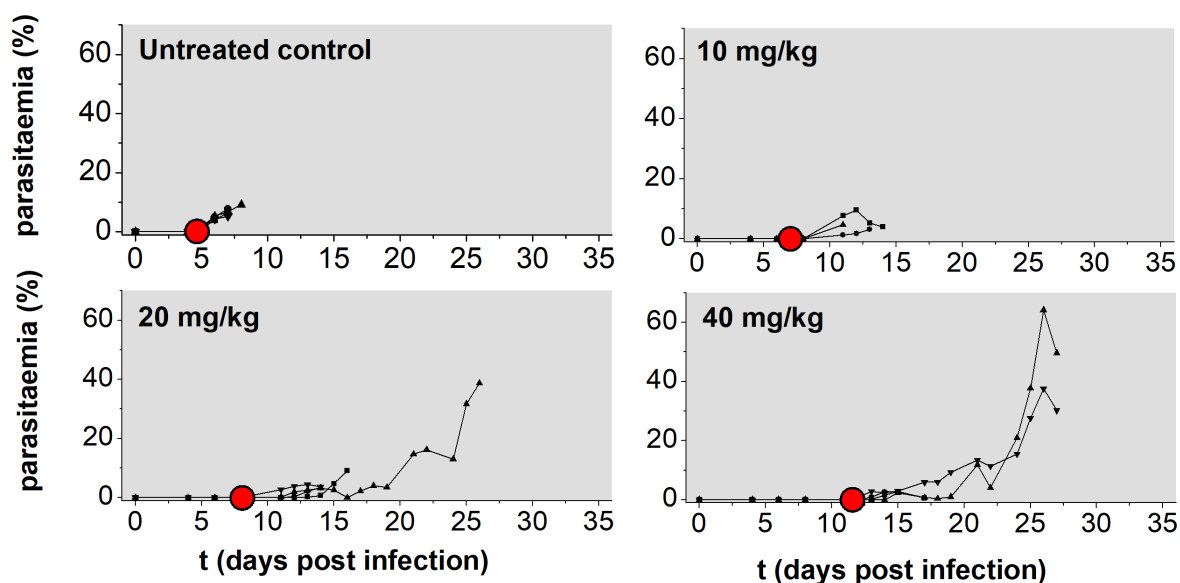


**Figure 16.** Parasitaemia in *P. berghei* infected mice treated with 10/20/40 mg/kg ART via gavage every 24 h on days 3-5 post infection. Each line represents one animal; the end of a line indicates the death of the mouse. The red circles mark the earliest detection of parasites in the bloodstream: note the dose-dependent shift from day 5 (untreated control) to day 12 (40 mg/kg). Modified from<sup>132</sup>.

Drug delivery from oral microemulsions is usually rapid, with  $c_{max}$  being reached within 1-4 hours<sup>19,28,181,182</sup>. Similar absorption kinetics were also found for the developed system (**Table 10**). Serum concentrations between 900 and 2,300 ng/ml, about ten times the maximum concentration of ART in the first human tolerability studies (140 ng/ml)<sup>121</sup>, and a thousand times higher than the  $ED_{50}$  of 1 to 2 ng/ml against *P. falciparum* growth in culture, were reached after 2 hours.

The much lower drug serum concentrations at 8 h imply that drug uptake has mostly been completed after a few hours, and ART is then rapidly cleared from the bloodstream.

These assumptions are supported by a series of prophylactic treatment experiments in mice which were reported in<sup>132</sup> and served as an in vivo bioassay to gain additional information on the pharmacokinetics of the formulation. Taken together, serum concentrations and prophylactic treatment indicate fast absorption of high amounts of ART from the DDS.

**Table 10.** ART serum concentrations found in ICR mice (n= 3 per time point) 2 and 8 hours after treatment with either drug-free formulation or 40 mg/kg body weight ART in SMEDDS-20 via gavage, measured via HPLC-MS.

Time post administration	Administered formulation	ART serum ( $\mu\text{g/ml}$ )
2 h	Placebo	0   0   0
	40 mg/kg ART	0.9   2.3   1.3
8 h	40 mg/kg ART	0.6   <LLQ   <LLQ*

\*[LLQ] lower limit of quantification = 0.18  $\mu\text{g/ml}$ . Vertical lines separate results of individual mice.

The increase in bioavailability through the complete dissolution of ART in the formulation is also underlined by comparison to serum concentrations recently reported by Gibhard et al. for a simple aqueous suspension of ART in 0.5 % hydroxypropylmethylcellulose with 0.2 % Tween 80<sup>126</sup>. Here, oral administration of 50 mg/kg ART suspended in the carrier resulted in an AUC of 1.1  $\mu\text{mol}\cdot\text{h/L}$ . This is less than half of the 2.4  $\mu\text{mol}\cdot\text{h/L}$  found after intravenous injections of one-tenth of the dose (5 mg/kg), proving very poor bioavailability from the suspension. Additionally, only about 120 ng/ml and 6 ng/ml ART were found in the serum 1 and 3 hours after gavage of 50 mg/kg drug in the suspension, respectively - compared to the 900-2,300 ng/ml measured 2 hours after 40 mg/kg were administered in SMEDDS-20. This is in good accordance with the much lower drug dose needed to treat murine schistosomiasis when using the author's self-emulsifying formulation instead of a suspension.

Obviously, direct comparison with the pharmacokinetic results from the suspension discussed above<sup>126</sup> must be seen with some caution (two separate experiments in different laboratories, different strains of mice, and a difficult to explain  $t_{max}$  for the suspension of only 5 minutes). But the roughly 50 to 100-fold increase in the ART serum concentrations if given in SMEDDS-20 definitively demonstrates that a suitable enabling formulation can greatly enhance oral ART bioavailability.

However, serum concentrations and prophylactic treatment results also revealed a possible weakness of a self-emulsifying system for ART delivery in malaria. It has been argued that a longer cumulative duration of time over which the plasmodia are exposed to concentrations above the minimum parasiticidal concentration <sup>f</sup> [MPC] is crucial for their successful eradication <sup>183,184</sup>. For the artemisinins with their short half-lives (2.79 h for ART in humans <sup>121</sup>, 0.39 h in mice <sup>126</sup>), serum concentrations above the MPC might not be retained over a sufficient time <sup>183,184</sup>, depending on the dosing interval and route of application. This issue could be exacerbated by the rapid uptake of the drug from the SMEDDS, as the author discussed extensively in <sup>132</sup>. It was, therefore, examined whether a change in dose frequency and a different route of application could further enhance the efficacy of the SMEDDS formulation beyond the already increased oral absorption.

Changing the dosing interval by splitting the delivered daily dose of ART drastically improved the outcome of the treatment of murine cerebral malaria: All animals that received the full daily dose of 20 mg/kg every 24 hours died from the infection. In contrast, the mice that were given 20 mg/kg as a split dose of 10 mg/kg ART twice per day cleared all parasites and showed no recrudescence of the infection (**Figure 17A**). This observation is supported by pharmacological modeling of artemisinin monotherapy of *P. falciparum* infections in humans <sup>184,185</sup>, as discussed in detail in <sup>132</sup>. Briefly, according to Kay et al. <sup>184</sup>, parasite-killing saturates at high drug concentrations. Therefore, in a split-dose regimen, the increase in cumulative killing time correlates with the subsequent increase in parasite eradication. Thus, a simple change in the dosing scheme lent the ART-SMEDDS a dramatically increased effectiveness while also reducing the risk of treatment failure and dose-related toxicity.

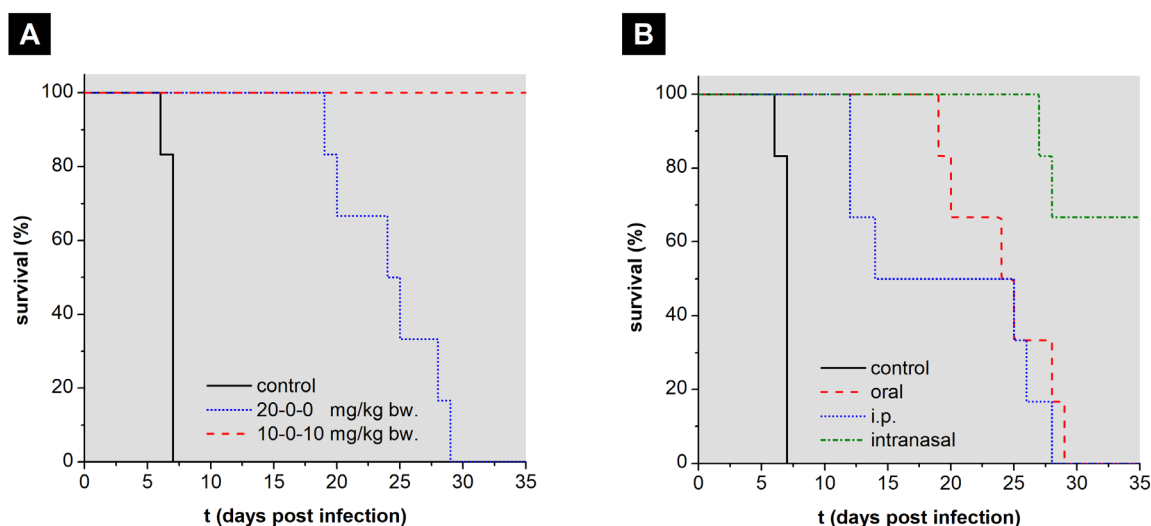


**Figure 17. (A)** Effect of different dosing intervals on survival of *P. berghei* infected mice treated by gavage on days 3-5 post infection with 20 mg/kg ART in 200  $\mu$ l SMEDDS-20 every 24 h (n= 6) or 10 mg/kg ART in 100 ml SMEDDS-20 every 12 h (n= 5); Untreated control mice n= 8. **(B)** Effect of the route of application on mouse survival. Mice were treated with 20 mg/kg ART on days 3-5 post infection with *P. berghei* every 24 h by gavage (n= 6, ART in 200  $\mu$ l SMEDDS-20), i.p. injection (n= 6, ART in 100  $\mu$ l SMEDDS-20), and intranasal administration (n= 6, ART in 25  $\mu$ l SMEDDS-50); Untreated control mice n= 8. From <sup>132</sup>.

<sup>f</sup> The minimum parasiticidal concentration is defined by White as “the lowest blood, plasma, or free plasma concentration which produces the maximum parasiticidal effect” <sup>183</sup>.



Similarly, the kinetics of drug uptake are greatly influenced by the route of administration and proved to be decisive in the outcome of malaria treatment with the developed formulation. SMEDDS/ME systems are safe for use via different routes, allowing to compare i.p. injections (parenteral route), oral administration, and intranasal treatment and also try transdermal delivery. I.p. injections were less effective than oral administration, which was surpassed by intranasal delivery of ART, leading to the complete parasite-free survival of 50 % of the animals (**Figure 17B**). Similar to the split-dose oral treatment, a prolonged MPC through the retention in the nose of the highly viscous SMEDDS-50 might be the decisive factor for the benefit of the intranasal administration. In contrast, the immediate uptake of the complete drug dose after i.p. injections would lead to a shorter circulation of concentrations of ART above the MPC in the bloodstream. To support this hypothesis, measurements of serum concentrations after drug delivery via the different routes in future experiments will be necessary. However, a difference in bioavailability and brain targeting also need to be considered as contributing to the increased effectiveness of intranasal delivery <sup>132</sup>.

SMEDDS-20 was also tested for transdermal ART delivery and proved highly effective. Administered as a spray on the shaven back of the animals, twice daily on days 2-5 post infection, 40 mg/kg ART in 150  $\mu$ l SMEDDS-20 reliably eradicated all parasites from *P. berghei* infected mice. Even a late treatment with only 4.4 mg/kg shifted the course of the disease to anemic malaria in all animals and prolonged survival by seven days (**Figure 18**). Serum concentrations of ART measured in a bioassay clearly demonstrated transdermal passage of ART to the blood. These were highest one hour after treatment, and 900 ng/ml ART was still present 5 hours after spraying mice with 80 mg/kg ART in SMEDDS-20.

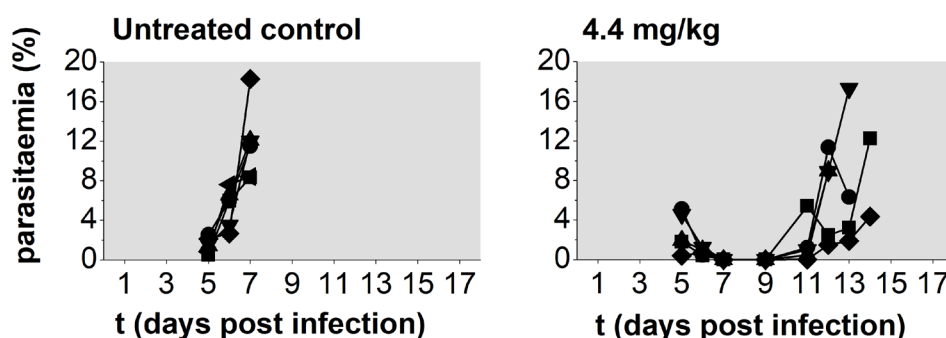


**Figure 18.** Transdermal treatment with 4.4 mg ART/kg bodyweight in 150  $\mu$ l SMEDDS-20 sprayed on the shaven back of the animals every 24 h on days 5 and 6 post infection with *P. berghei*. Each line represents one mouse; the end of a line indicates the death of the animal (n=5 in the treatment group, n=6 for untreated mice). Modified from <sup>156</sup>.

Using the optimal route of application and dosing frequency induces a complete cure of experimental cerebral malaria. Direct comparison between the transdermal ART delivery and the oral, i.p., and intranasal ART administration experiments is difficult due to the different treatment schemes. However, it can be concluded, according to the current results, that the self-emulsifying formulation successfully delivers ART via the oral, intranasal, and transdermal route of administration, proving to be a very versatile and easily adaptable, lipid-based solubility enhancing carrier for artemisone.

## 4.2 Electrospun polymer fibers

This part of the work investigates different electrospun polymer fiber carriers as drug delivery systems for small molecule drugs, mainly for local application. In particular, possible parameters controlling drug loading and resulting release mechanisms and kinetics were investigated in detail for two different types of fiber scaffolds (**Table 11**).

Publication IV <sup>75</sup> presents the development of a fiber mat with the active compound, BCS class II drug nimodipine, incorporated within the individual fibers.

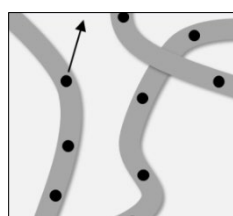
A three-dimensional polymer fiber sponge that could be loaded with drug through (a) encapsulation within the fibers during the spinning process, as well as through (b) immobilization of drug solutions in the pores of the sponge post-processing, is studied in publication V <sup>157</sup>.

Both systems could allow the local delivery of sufficient concentrations of poorly soluble substances through an increase in dissolution rate and solubility but should preferably also control burst release.

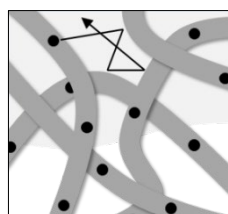
**Table 11.** Possible parameters controlling drug delivery mechanisms from the electrospun polymer fiber systems studied in publication IV <sup>75</sup> and V <sup>157</sup>.

### Polymer fiber mat

### Polymer fiber sponge

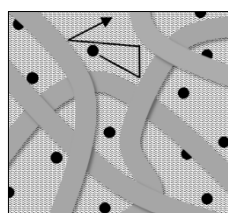


- Drug-loaded fibers*
- Fiber diameter
  - Drug incorporation (amorphous/ crystalline)
  - $T_g$  fiber matrix
  - Release medium
  - Loss of geometry



- (a) Drug-loaded scaffold*
- Scaffold fluid penetration
  - Fiber fluid penetration
  - Air escape
  - Changes in fiber micro-environment

- drug molecule
- aqueous fluid (water, buffer, bodily fluid)
- ▒ lipophilic fluid (oily drug solvent)



- (b) Drug-solution filled scaffold*
- Scaffold oil penetration
  - Air escape
  - Oil retention
  - Restriction of diffusion
  - Interaction drug/scaffold



### 4.2.1 Electrospun nimodipine-loaded polymer fiber mats

#### Formulation development

An electrospun polymer fiber fleece was developed as a potential intracranial DDS for NIMO for the treatment of secondary ischemia after aneurismal subarachnoid hemorrhage, vestibular schwannoma, and maxillofacial surgery.

The requirements for local delivery systems in the brain are particularly stringent due to the delicate brain tissue<sup>186</sup>. Injury through mechanical strain and any toxicity to the very sensitive brain cells must be ruled out. Electrospun polymer fibers are particularly well suited to meet these requirements. They allow the fabrication of soft, flexible materials that adapt to the respective site of application. Electrospinning also offers a broad choice of possible polymers and sufficient drug loading in a reasonably small-sized DDS.

To avoid further irritation at the site of trauma, the system must be biodegradable based on a mechanism applicable to the brain with its limited routes of metabolism, without breaking down into harmful compounds or causing unacceptable shifts in pH or osmolarity. The aliphatic polyester PLGA was thus selected as the matrix polymer for the fiber mats. PLGA is biodegradable and has already been approved for various parenteral DDS<sup>187</sup>. Simple ester hydrolysis makes the degradability of PLGA independent of the presence of specific enzymatic mechanisms. A local acidic pH, common in larger monolithic PLGA carriers undergoing bulk erosion, is not expected for electrospun fiber mats. Rather, EPF undergo surface erosion due to their smaller individual structures and large surface area<sup>188,189</sup>.

Poly(D,L-lactide-co-glycolide) 50:50 with a  $M_w$  of 24,000–38,000 and a glass transition temperature [ $T_g$ ] of 44–48 °C was successfully formulated into NIMO-loaded EPF through blend electrospinning of a solution of polymer and drug. Electrospinning parameters were adjusted systematically to establish a stable and reliable spinning process and are laid out in detail in<sup>75</sup>.

1 % [NIMO 1 %] and 10 % [NIMO 10 %] (wt.%) NIMO were incorporated into the fiber matrix of round fleece mats of around 40  $\mu\text{m}$  thickness. The individual fibers had an average diameter of 1–3  $\mu\text{m}$  and a smooth surface (**Figure 19**). <sup>1</sup>H NMR confirmed that the drug was not affected on a molecular level by the electrospinning process, and HPLC revealed an encapsulation efficiency of 97–105 % (results > 100 % are due to variability of sample preparation and analytics).

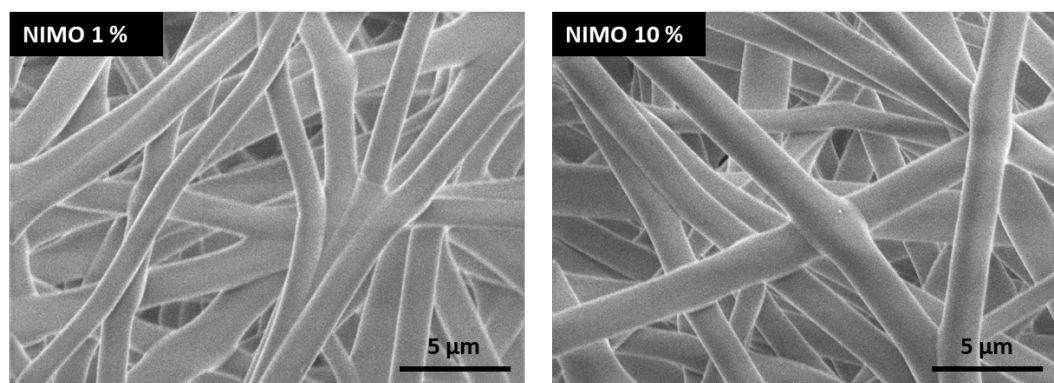


**Figure 19:** SEM images of NIMO 1 % and NIMO 10 % fiber mats. Note that no pore formation or crystallization is visible on the smooth fiber surface. From<sup>75</sup>.

The state of the drug – crystalline or amorphous - and where it is deposited within the fiber is mainly responsible for resulting release profiles of EPF <sup>71,72</sup>. Incompatibility between drug and polymer (lipophilic/hydrophilic) or drug and solvent favors crystallization of the drug, occurring mostly on the fiber surface <sup>71,72</sup>. This often results in an intense burst release even for poorly soluble compounds <sup>71,72</sup>. Similar effects can be observed when amounts of drug above its solubility in the polymer are used <sup>68,69</sup>. With the right choice of process variables and excipients the formation of an amorphous solid dispersion of the drug within the fiber matrix can be achieved via blend electrospinning. For the BCS class II compound NIMO this can be employed as a dissolution rate and solubility enhancing formulation approach. The state of NIMO in the EPF was thus of great interest and analyzed via x-ray scattering and DSC.

For the NIMO-loaded fibers, x-ray powder diffractograms only gave the broad signal of amorphous material. However, in a physical mixture of drug and polymer the sharp and narrow signals for the crystalline drug were still observed (**Figure 20C**).

DSC was performed to verify the x-ray scattering results. Samples were subjected to two heating cycles.

No melt peaks of crystalline NIMO were found during the first heating cycle, supporting the assumption that NIMO was incorporated in the fibers in the amorphous state (**Figure 20A**).

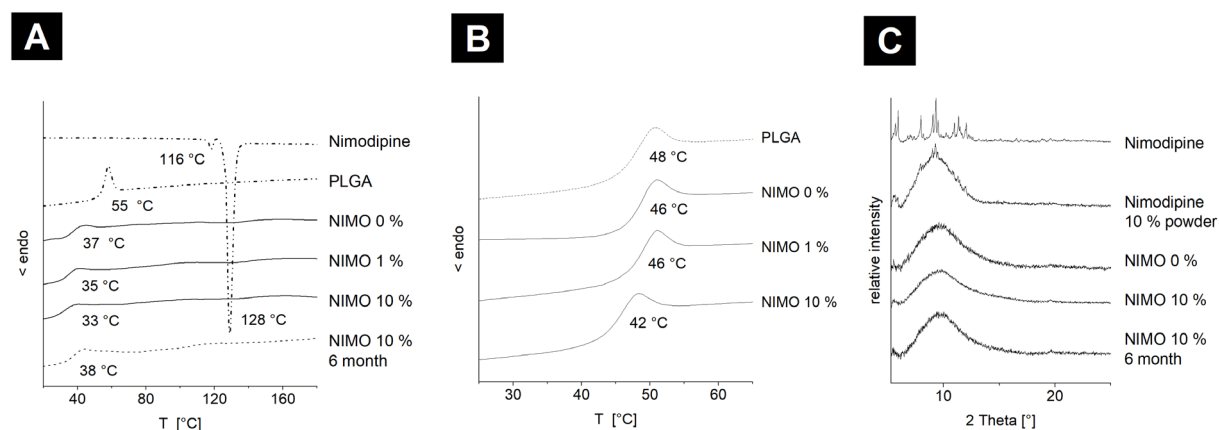


**Figure 20.** (A) DSC curves (first heating cycle) of nimodipine powder, unprocessed PLGA as received, electrospun fiber mats immediately after drying, and NIMO 10 % stored for 6 months. Numbers indicate the melt peaks (Nimodipine) and  $T_g$  of samples. (B) DSC curves (second heating cycle) of unprocessed PLGA and electrospun fiber mats. Numbers indicate the  $T_g$  of samples. (C) X-ray powder diffractometry patterns of nimodipine powder, a cryo-milled mixture of 10 % nimodipine in PLGA (Nimodipine 10 % powder), electrospun fiber mats immediately after drying, and NIMO 10 % stored for 6 months. From <sup>75</sup>.

DSC measurements demonstrated that the electrospinning process considerably decreased the  $T_g$  of the polymer forming the fiber matrix. A  $T_g$  of 37 °C for drug-free fibers was found during the first heating cycle, compared to the 55 °C of bulk PLGA. As the fleece samples fused into beads during the first heating, results obtained during the second heating cycle were independent of the influence of fiber geometry and the electrospinning process. The  $T_g$  for drug-free fibers and bulk PLGA was found to be almost identical again for the second heating (**Figure 20B**). Several explanations for this are given in <sup>75</sup>, the most common being that the stretched long-range polymer network caused by whipping and bending of the fiber

during the electrospinning process is preserved through rapid drying, leading to less polymer chain entanglement<sup>190</sup>. With the additional plasticizing effect of NIMO, the  $T_g$  of NIMO 1 % and NIMO 10 % (35 °C and 33 °C respectively) is below the 37 °C body temperature. The EPF will thus be in the rubbery state, which might increase release rates through higher polymer chain mobility<sup>191</sup> but can also affect the stability and integrity of the fiber network.

### In vitro nimodipine release

The release of NIMO from the EPF was studied in two different media, in a pharmacopeia-based surfactant solution and in cell-free culture medium under the conditions applied in the cell culture experiments. The very different release rates decidedly demonstrate the significant influence the release media have, a fact that is often overlooked when evaluating the release kinetics of DDS.

For the therapy of aneurysmal subarachnoid hemorrhage and the preservation and regeneration of nerve functions after neurosurgery, a local release of NIMO at the site of trauma over around 14-21 days would be ideal<sup>192-194</sup>. Sufficient therapeutic NIMO concentrations in the targeted tissue should be accomplished while also preventing a strong burst release.

As laid out in the introduction, to obtain the desired drug delivery profile, the interplay of (a) increased dissolution rate from the electrospun non-wovens due to small diameters and large surface area, (b) drug-polymer compatibility and amorphous/crystalline state, and the drug's inherent poor aqueous solubility needs to be carefully balanced<sup>75</sup>. The aim was to achieve this through the amorphous incorporation of the poorly soluble NIMO in a PLGA matrix.

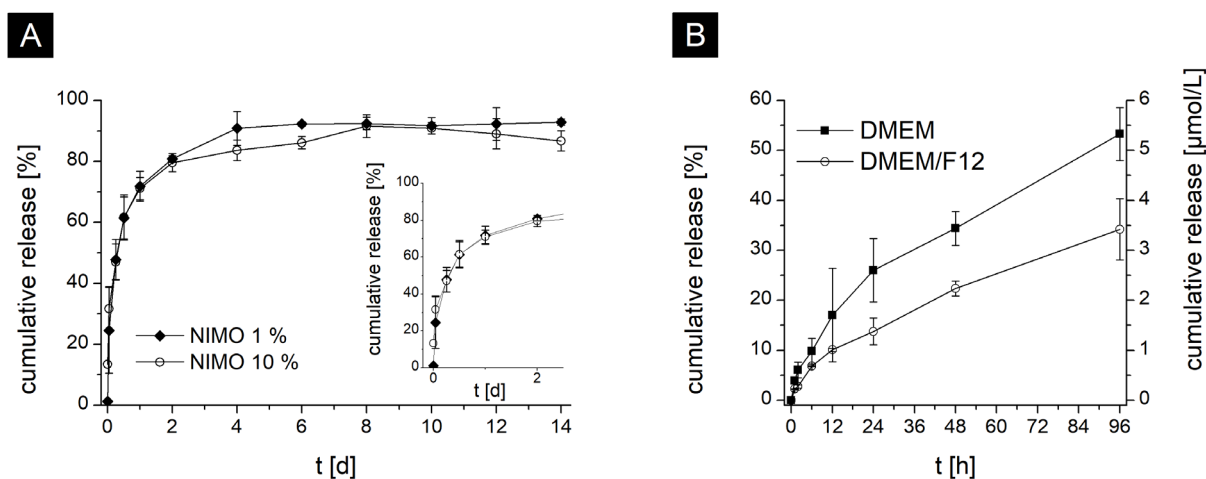


**Figure 21.** (A) Nimodipine release from NIMO 1 % and NIMO 10 % in PBS pH 7.4 with 1 % Tween 80, over 14 days. (B) Nimodipine release from NIMO 1 % in cell-free culture media over 4 days. Experiments in DMEM were performed at 37 °C, CO<sub>2</sub> 5 %, samples in DMEM-F12 were incubated at 33 °C, CO<sub>2</sub> 5 %. The release experiments were carried out under light exclusion. Drug release was calculated from the residual amount of nimodipine in the fiber mats measured via HPLC. From<sup>75</sup>.

The NIMO release from the EPF was studied in PBS pH 7.4 with 1 % Tween 80 rather than just an aqueous buffer, to ensure sink conditions in a reasonable volume. A relatively fast nimodipine release was observed with 48 % and 47 % for NIMO 1 % and NIMO 10 % within the first 6 hours, respectively (Figure 21A). The release profiles are almost identical for both

drug loads. NIMO release was complete after 6 days for NIMO 1 % and 8 days for NIMO 10 %, about half the period initially attempted to cover.

This relatively fast drug liberation can mainly be attributed to the fiber geometry and the rubbery state of the polymer. The electrospinning process and drug incorporation already reduced the  $T_g$  of the dry EPF to several degrees below the 37 °C used in the release experiments. Increased mobility of the polymer chains above the  $T_g$  favors a more rapid drug release due to fast water penetration and diffusion of the drug molecules out of the fiber<sup>191,195</sup>. This was further intensified by the plasticizing effect of the incubation medium. Blasi et al. found that exposition to water depressed the  $T_g$  of PLGA by about 15 °C<sup>196</sup>, while a plasticizing effect on polymers was also seen for surfactants<sup>197</sup>. The decisive influence of the surfactant is made even more evident when looking at the NIMO release in the culture medium. Here an almost linear release was achieved from 24 h to 96 h. There was no significant burst, and only 53 % (DMEM) and 34 % (DMEM-F12, 33 °C) were released after 4 days (**Figure 21B**).

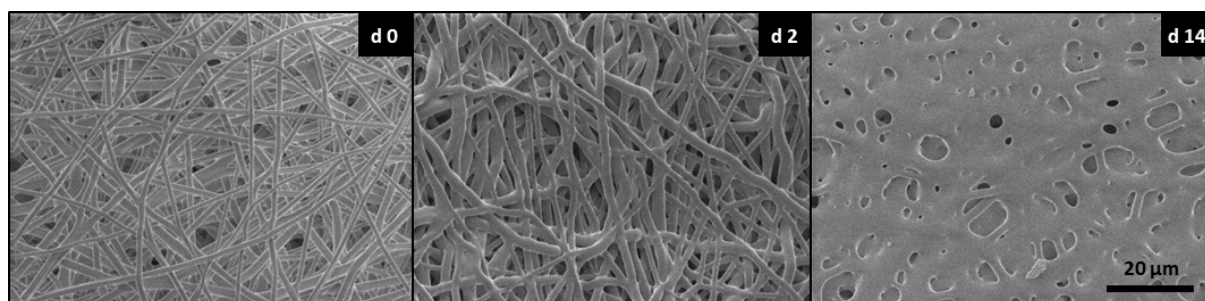


**Figure 22.** Changes in fiber morphology during release experiment of fiber mats in PBS and 1 % Tween 80. SEM images were taken of dry fiber mats (d 0) and samples removed from the experiment after 2 or 14 days.

Over the course of the release experiments, the softening of the PLGA matrix resulted in the fiber mats fusing into porous films after several days (**Figure 22**). This complete loss of the fiber geometry fundamentally alters release-governing mechanisms and kinetics and partially eliminates the unique advantages of the electrospun non-wovens.

The influence of not only the inherent fiber properties but also external factors on drug liberation, therefore, have to be carefully considered when designing an EPF-based DDS, also and especially when using *in vitro* data to predict *in vivo* release.

#### **Activity in relevant brain cell line cultures**

The NIMO EPF exhibited no cell toxicity towards a number of different brain cell lines. A 42-81 % reduction in NIMO concentration in the culture media after the cell stress experiments, compared to release in cell-free media, suggests significant drug uptake by the cells (though NIMO breakdown cannot be completely ruled out as a possible explanation). Further, the fiber mats significantly reduced cell death of oxidative, osmotic, and heat-induced cell stress in *in vitro* cell models of Schwann cells, neuronal cells, immortalized and primary astrocytes. EPF could thus be a suitable DDS to make intracranial, local NIMO delivery available for the treatment of secondary ischemia after aneurismal subarachnoid hemorrhage, vestibular schwannoma, and maxillofacial surgery.

#### 4.2.2 Polymer fiber sponges

Three-dimensional polymer fiber sponges fabricated from electrospun nonwovens were first described by Duan et al. in 2015<sup>82</sup>. The PFS are formed via self-assembly from short EPF through freeze-drying of suspensions of cut fibers. Contrary to other systems with nano- and microscale structures, the monolithic sponges are easy to handle and do not require any attention paid to successful dispersion.

Cylindrical poly(D,L-lactide) [PLA] scaffolds (**Figure 24A**) as potential implantable DDS were prepared as detailed in<sup>198</sup> and coated with poly(p-xylylene) [PPX] to increase mechanical stability (**Figure 23**)<sup>199</sup>. As a pharmaceutical excipient the biodegradable PLA is well established and approved by the regulatory agencies for use in parenteral DDS<sup>187</sup>.

PPX cannot be degraded in the body and must therefore only be seen as a model compound that will need to be replaced by a more suitable alternative in the future.

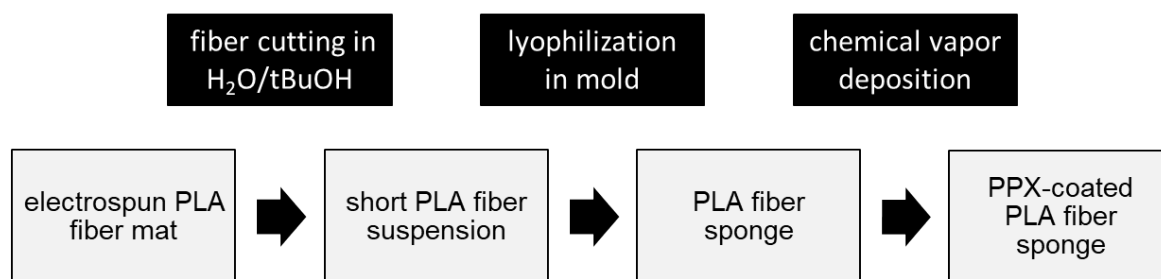


**Figure 23.** Preparation of PLA-PPX polymer fiber sponges.

PFS combine the large surface area and small diameters of EPF with a low density, high porosity, all-directional open-porous fiber scaffold (**Figure 24B**). The fabrication process allows to freely adjust scaffold diameters and control density and porosity as needed<sup>199</sup>. After PPX-coating, the sponges possessed a density of 28 mg/cm<sup>3</sup> and 98 % porosity. Due to their uniform scaffold material, PFS can provide a more well-defined, easily adjustable delivery platform than sponges formed through lyophilization that are currently used as DDS, e.g., GENTA-COLL® resorb 200.

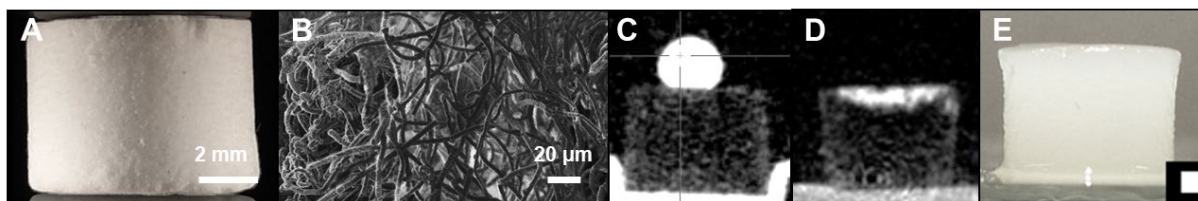


**Figure 24.** Characteristics of the PFS used in this study. **(A)** Dry PLA-PPX sponge. **(B)** SEM image of PLA-PPX fiber scaffold. **(C)**  $\mu$ CT scan of PFS after placing of water or **(D)** MCT on the surface. **(E)** MCT-filled PFS retaining its shape after oil loading. Modified from<sup>157,200</sup>.

The PLA-PPX PFS were highly hydrophobic, with a water contact angle of 144 ° but rapid MCT absorption (**Figure 24C and D**). As characteristic for these systems<sup>201</sup>, the PFS can hold high volumes of fluid. 34 g MCT per g sponge – 99 % of the theoretically available

specific pore volume - could be loaded in the PLA-PPX PFS without losing their form or integrity (**Figure 24E**).

Besides incorporation of drug within the individual fibers of the scaffold, loading of the PFS pore-system with drug solutions could allow the use of PFS DDS that provide user-adjustable doses and drug combinations at the point-of-care<sup>202,203</sup>.

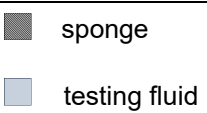
PFS-specific release controlling parameters were therefore tested for two scenarios: (a) drug encapsulation within the fiber scaffold and (b) liquid loading of the pores with a lipophilic drug solution.

#### (a) Drug-loaded scaffold

For a drug incorporated within the individual fibers, the duration of the penetration of the sponge pores with bodily fluids upon implantation will greatly determine the release rate. The high hydrophobicity and poor wetting of the PFS could thus potentially be used to control the drug liberation, similar to what was proposed by Yohe et al. for EPF fiber mats<sup>204</sup>.

Infiltration of the PFS with PBS or a 5 % solution of bovine serum albumin [BSA], a model liquid for the more surface-active bodily fluids, was followed via  $\mu$ CT and spectral-spatial EPR imaging. To assess the impact of air replacement in the scaffold, samples were incubated in both closed-bottom and open-bottom sample holders (**Table 12**).

**Table 12.** Sample holders used for sponge incubation and liquid-loading results from EPR and  $\mu$ CT imaging. Duration of the uptake of different fluids in the nanofiber derived PPX-coated PLA sponges, given in days unless stated otherwise. Vertical lines separate the results of individual sponges. From<sup>157</sup>.

	Close-bottom sample holder		Open-bottom sample holder		
	EPR	$\mu$ CT	EPR	$\mu$ CT	
<b>PBS</b>	168 245 315	131 131 204	28 28 28	-	
<b>5 % BSA</b>	77  77  77	63 70 70	-	-	
<b>MCT</b>	-	28 42 42	-	< 5 < 5 min	

Results show that, due to the high hydrophobicity of the sponges, PBS penetration (in closed-bottom sample holders) is slow, taking between 19 and 45 weeks. Reduced surface tension/increased wetting of the sponges through incubation in 5 % BSA reduced that time considerably to about 10 weeks. Similar to the release experiments with the NIMO fiber mats, results again demonstrate that attention has to be paid to the actual physiological conditions present in a potential in vivo setting to realistically model release behavior in vitro.

The escape of air from within the scaffold also greatly influenced the rate of liquid uptake. A slowly shrinking air pocket was encased by the proceeding liquid front inside the PFS in the closed-bottom holders (**Figure 25**). If an escape for air was provided via the open bottom,



PBS uptake was complete after only 4 weeks. Surprisingly, air entrapment was also observed when sponges were incubated in the lipophilic MCT. Oil uptake was thus prolonged from a few seconds to 6 weeks in the closed-bottom holders, showing that this process can occur independently from poor wetting.

Hydrophobicity and gradual air replacement thus both contribute to a slowed uptake of aqueous fluids in the PFS and can induce extended release. But these mechanisms can only be exploited if the sponges are placed in a cavity that provides protection from mechanical pressure, e.g., within a bone or as an intracranial implant. Otherwise, compression of the PFS could affect the liquid absorption and consequent release rates. Prolonged delivery of nimodipine after brain surgery from the fibers of a PFS implant rather than an EPF mat could be one possible application for this unique 3D DDS.

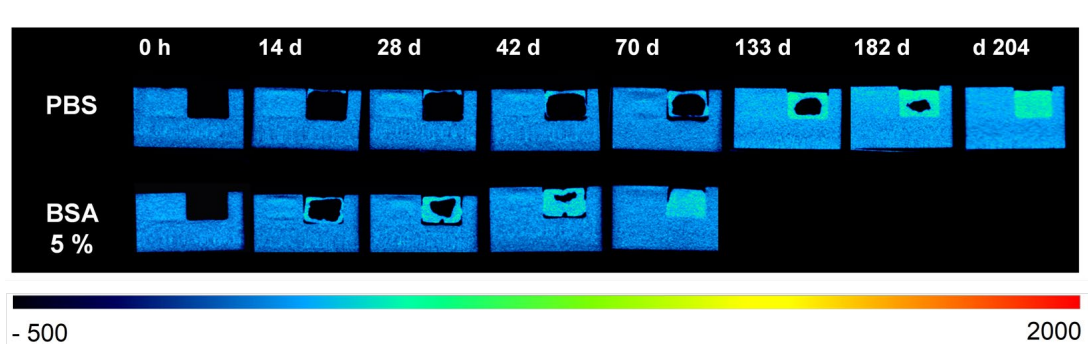


**Figure 25.**  $\mu$ CT scans of the liquid-uptake of PFS incubated in closed-bottom sample holders. Dry areas of the PFS are not visible due to the low density of the material. Modified from <sup>157</sup>.

#### (b) Drug-solution filled scaffold

As carrier scaffolds for oily drug solutions - here represented by MCT - PFS can hold liquid lipids in a predetermined shape. This is especially important when aiming for controlled release. By controlling surface area and diffusion length, the oil-loaded PFS implants could make release kinetics far more predictable than injections of lipophilic drug solutions that usually result in oily depots of varying shapes and sizes. Considering the ultra-low density of the sponges, the characteristics of a lipid-based formulation - namely solubility enhancing properties and good tolerability - would dominate in this hybrid DDS.

Compression experiments were performed to test mechanical stability and oil retention in the PFS, both prerequisites for this form of application. Only a minor loss in maximum compression was observed for dry and oil-loaded scaffolds after 500 compression cycles, indicating good mechanical stability. However, compression of fully MCT-loaded PFS resulted in oil release that was not completely reversible, i.e., 3-12 % of the MCT was not reabsorbed. As this would lead to varying release profiles, partly oil-loaded PFS were also investigated as an alternative. If loading left a void equal to the maximum compression (e.g., 80 % oil loading and 20 % maximum compression), oil release was still observed, but complete MCT reabsorption could be attained. These findings thus again underline the susceptibility to mechanical strain inherent to the PFS and the severe implications this can have on their suitability as carrier platforms for drug delivery.

To better understand the possible interaction between oil and the fiber scaffold, transverse magnetization relaxation [ $T_2$ ] distributions and the diffusion coefficients  $D$  for free MCT and oil immobilized in the PFS were acquired using  $^1\text{H}$  NMR.

A large fraction of the oil in the PFS undergoes bulk relaxation. This MCT exists as free liquid in the PFS pores. However, different populations of  $T_2$  relaxation times also indicate a considerable number of oil molecules immobilized at the surface of the PPX-coated fibers undergoing surface relaxation (**Figure 26A**)<sup>205</sup>. These spin-spin interactions between the oil and the PFS material could be due to MCT-PPX van-der-Waals interactions.

The diffusion coefficient  $D$  was slightly lower for the MCT-loaded PFS than free MCT ( $2.8 \times 10^{-10} \text{ m}^2/\text{s}$  and  $4.6 \times 10^{-10} \text{ m}^2/\text{s}$  at  $37^\circ\text{C}$ , respectively), suggesting that diffusion of the oil molecules was slightly restricted by the fiber scaffold<sup>206,207</sup>.

To further evaluate whether the sponge scaffold itself can alter the drug delivery from oily drug solutions through oil-fiber interactions and limiting diffusion, the release of the small molecule EPR spin-probe 4-Hydroxy-Tempo-d17 [dTempol] from the PFS was studied. The release profiles of this model compound were almost identical for both free and immobilized MCT, and the influence of the scaffold must thus be seen as negligible (**Figure 26B**).

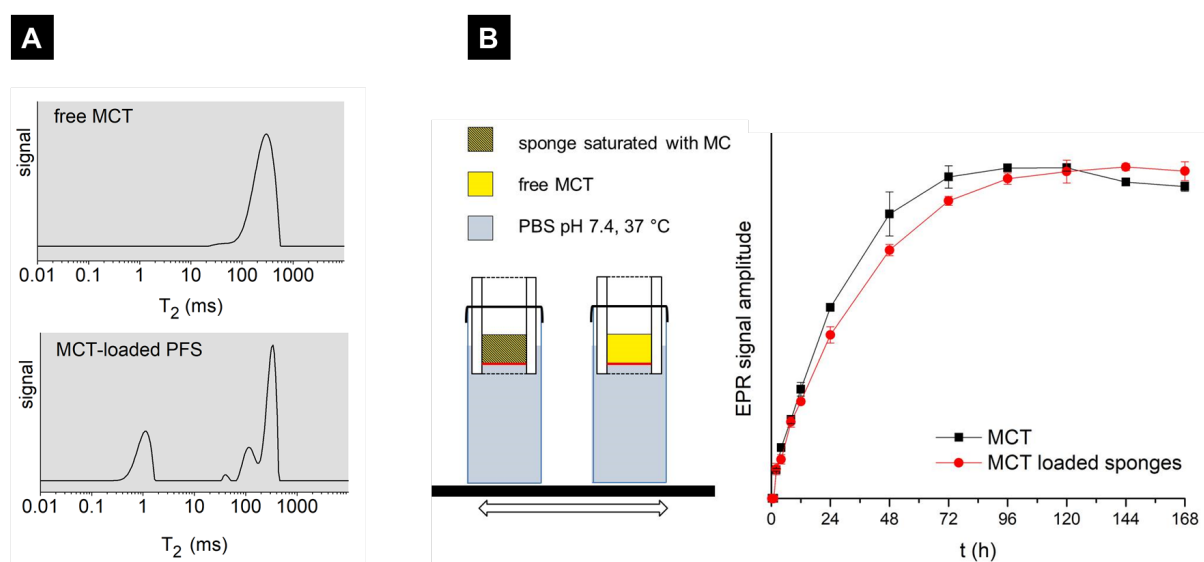


**Figure 26. (A)**  $^1\text{H}$  NMR spectroscopy: exemplary  $T_2$  distribution of free MCT (top) and MCT-loaded PFS (bottom) at  $37^\circ\text{C}$ . **(B) Left:** Setup for release study of dTempol from MCT. The red lines indicate the interface between oil and PBS, identical for both free MCT and oil immobilized in the scaffolds. **Right:** Release of dTempol from free MCT and MCT-loaded PFS, given as signal amplitude of x-band EPR spectroscopy measurements. MCT was spiked with 10 mM dTempol; release was assayed in PBS pH 7.4 at  $37^\circ\text{C}$ . Modified from<sup>157</sup>.



## 5. SUMMARY AND FUTURE PERSPECTIVES

Drug delivery systems can be defined as “*engineered technologies for the targeted delivery and/or controlled release of therapeutic agents*”<sup>208</sup>. A particular need for such effective DDS has long been identified for the BCS class II drugs. Their translation into clinical use is primarily impeded by poor aqueous solubility and consequent low oral bioavailability<sup>89</sup>, but sufficient solubility is also indispensable for many non-oral routes of application. This challenge has been addressed by the implementation of the Developability Classification System<sup>2</sup>, which places special emphasis on the advantage of solubility enhancing formulations for solubility limited compounds. Such customized DDS that cater to the properties of the particular molecule can permit successful therapy that is otherwise unobtainable.

Subject of this work was the development of two very different DDS – a SMEDDS and electrospun polymer fibers – as solubility enhancing formulations for the delivery of small-molecule BCS class II drugs, and to explore their potential to improve the delivery of these compounds. A concluding summary of the formulation development and the in vitro and in vivo performance of these DDS are outlined in the following section. Based on the encouraging results, suggestions are made on how to continue this work on a path to possible clinical application.

### 5.1 Artemisone self-microemulsifying drug delivery system

The first three publications examine a self-microemulsifying formulation as a solubility enhancing DDS for the delivery of artemisone, addressing the drug’s development-restricting low aqueous solubility and poor stability.

A suitable DDS for ART is of particular interest because the antimalarial proved superior to the currently commercially available artemisinin derivatives<sup>119,120</sup>. In addition, ART also showed promising results when tested against schistosomiasis and a broad range of other diseases, clearly indicating the benefit to large numbers of patients if suitable ART formulations are made available<sup>106–109,112–115</sup>.

As a first step, the systematic characterization of ART solubility and aqueous stability increased the understanding of these main properties, making a more rational formulation design approach possible than what had hitherto been attempted in previous works<sup>132</sup>.

Experiments also confirmed the excellent capability of lipid-based excipients to increase the solubility of the drug. Based on these findings, a SMEDDS system was developed as DDS for ART. It is comprised of mainly safe and routinely used excipients, the only exception being the inclusion of the isosorbide diester Polysorb ID 46 as a novel pharmaceutical ingredient. Besides good stability and rapid self-emulsification, the water-free SMEDDS (SMEDDS-100) promises a low cost of production due to the fairly affordable ingredients and easy scale-up of the manufacturing process, a simple single mixing step.

Extensive physicochemical characterization of the carrier and its behavior provided a comprehensive understanding of the system and the microstructures formed upon self-emulsification. Experiments also identified two SMEDDS-100-based microemulsions, SMEDDS-50 and SMEDDS-20 (50 % water with a bicontinuous structure and 80 % water

resulting in clustered micelles, respectively), as additional suitable ART DDS for in vivo testing.

Due to the meticulous formulation design, SMEDDS-100 proved to be an effective solvent for ART, increasing solubility 660 fold compared to PBS (to 59 mg ART/g SMEDDS) and preventing precipitation during self-emulsification, even at high water volume fractions. ART exhibited good storage stability when dissolved in the water-free SMEDDS-100. Contrary to its poor aqueous stability, the drug also only showed negligible degradation in SMEDDS-50. This could be attributed this to the protection of the drug within the lipid domains of the bicontinuous microemulsion<sup>34–36</sup>, possibly also protecting ART from the acidic aqueous environment in the upper GIT after oral administration.

In a first in vitro experiment, ART-loaded SMEDDS proved successful against *P. falciparum*, the human malaria parasite mainly responsible for severe and cerebral malaria.

The formulation's ability to deliver ART and the consequent efficacy were then tested in in vivo models of murine cerebral malaria and schistosomiasis.

A dose of 40 mg/kg bodyweight ART dissolved in SMEDDS-20 was very efficacious against *Schistosoma mansoni* in mice. While the placebo had no effect, treatment with the drug-loaded formulation showed similar activity to a suspension of 400-450 mg/kg ART<sup>113</sup>. The 90 % reduction in the required dose strongly points to a greatly increased oral bioavailability from SMEDDS-20.

In murine cerebral malaria, clear dose-dependence was established with 20 mg/kg bodyweight ART as the optimal daily dose for oral treatment. ART serum concentrations measured via HPLC-MS show that the self-microemulsifying system dramatically increased oral ART delivery around 50 to 100-fold compared to a suspension of the crystalline drug described by Gibhard et al.<sup>126</sup>. The results illustrate that good oral bioavailability of the poorly soluble BCS class II drug ART can be made possible with a carefully tailored enabling formulation.

Further pre-clinical testing in mice provided answers to questions related to the choice of dosing regimen, route of application, pharmacokinetics, and resulting therapeutic efficacy of the DDS. When treatment frequency and delivery route are chosen correctly, a complete cure of murine cerebral malaria is achieved with the SMEDDS formulation.

Comparative experiments showed a decisive advantage in delivering a split dose given twice per day, over once-daily administration of the entire amount of drug. Consequently, only a reduced individual dose is needed if an optimized treatment scheme is applied, reducing the risk of dose-related toxicity.

Besides oral administration, the formulation also allows successful ART delivery via the intranasal and transdermal routes as well as intraperitoneally. Intranasal administration is more effective than oral delivery, while i.p. injections of drug loaded SMEDDS-20 were least successful. Transdermal application of ART led to high drug serum concentrations and could eradicate the malaria parasites in mice at drug doses similar to what was administered orally. The good penetration behavior suggests that delivery into specific areas of the skin might also be possible with the carrier for indications requiring local treatment.

Taken together, the results demonstrate that the excellent performance of the developed self-microemulsifying formulation is reached through the combination of high drug solubility,

stability, and consequent good bioavailability, strongly underlining the importance of the right DDS for further clinical success of artemisone.

To the author's knowledge, there are currently no other as-comprehensively studied, efficient DDS for the delivery of ART. However, further development and additional exhaustive preclinical testing of the formulation will be necessary to safely promote the system's possible translation into clinical practice.

Two important aspects that were not studied in detail in this work but will need close attention are the effect of food on the oral ART uptake from the carrier and the toxicity of the formulation on a cellular level. Though a pronounced food effect is commonly not expected for LFCS Type III formulations, *in vitro* and *in vivo* studies to confirm this assumption are vital to guarantee reliable, reproducible bioavailability for a safe and effective therapy. Considering the rapid degradation of ART under acidic conditions, filling in capsules with an enteric coating could be tried to obtain additional protection of the drug from the acidic stomach contents.

No apparent toxicity was observed for the formulation in the animal experiments. But mucosal damage on the nasal epithelium and irritation of the lining of the GIT cannot be entirely ruled out due to the high percentage of surfactant and should be examined more closely in histological studies.

More pre-clinical *in vivo* testing will complete the understanding of the pharmacokinetics of ART in the DDS. With respect to ethical considerations, only limited data on drug serum concentrations were obtained. But given the favorable results, a more comprehensive examination with an increased number of time points is justified.

Possible further studies should compare drug uptake and efficacy of treatment for the ART-loaded SMEDDS and crystalline drug within the same experiment to better quantify the absorption-enhancing effect of the formulation. Detailed serum concentration time curves for oral, *i.p.*, intranasal, and transcutaneous delivery should be obtained to more thoroughly understand the mechanisms that cause different treatment outcomes. In the case of intranasal application, drug concentrations in the brain should also be quantified. An even more exact prediction of the absorption kinetics can then be used to adapt this versatile formulation for the use against other identified ART targets and provide additional options to test for the treatment of these diseases.

Considering ART's good transcutaneous bioavailability, the development of a transdermal therapeutic system based on the SMEDDS might be attempted. Prolonged constant serum concentrations may thus be accessible, effectively counterbalancing the drug's relatively short half-life.

Drug delivery could also be directed locally into the affected tissue in skin diseases such as cutaneous tuberculosis<sup>209</sup> and melanoma<sup>106</sup>. SMEDDS-20 applied as a topical ART spray has already been tested to treat cutaneous leishmaniasis. Following the treatment, there was a significant inhibition of the development of lesions caused by *Leishmania major* in BLAB/c mice (data is currently being prepared for publication).

Finally, SMEDDS formulations for ART should ideally be suited to the prerequisites for use in malaria- and schistosomiasis-endemic areas and allow safe treatment, even in the absence of professional medical care. Patient safety could be increased if single-dose units such as

SMEDDS-filled capsules are made available, ruling out incorrect dosing of liquid DDS, a common cause for medication dosing errors. A suitable option should be designed for vomiting or comatose patients and young children, using either the intranasal or transdermal route offered by the SMEDDS. Additional stability testing should be performed according to the requirements for the appropriate ICH climatic stability zones <sup>210</sup>. Only if the formulation meets all the requirements of the real-life situation can it improve the therapy and contribute to the critical fight against malaria, schistosomiasis, and other diseases.

## 5.2 Electrospun polymer fibers

Publication IV and V investigate different aspects of drug release from two electrospun polymer fiber systems. Electrospun non-wovens have been shown to hold great potential in drug delivery but have not yet entered the market as commercial drug delivery platforms. Electrospinning allows the incorporation of drugs in a micro- to nanosize polymer matrix as amorphous solid dispersions, improving dissolution rate and solubility. As solubility enhancing formulation technique, it is thus of especial interest for the delivery of poorly soluble compounds. The correct choice of process parameters and combination of drug and polymer also allows uniting an increase in bioavailability with a sustained release over several days to weeks.

The introduction of three-dimensional EPF-based scaffolds can further broaden the range of available electrospun materials as DDS. Their compact 3D scaffold provides an alternative to the sheet-like fiber mats usually obtained through electrospinning, and their unique properties offer additional mechanisms to modify and control drug release from polymer fibers.

The intracranial site-specific delivery of the BCS class II calcium antagonist nimodipine to improve the outcome of aneurismal subarachnoid hemorrhage, vestibular schwannoma and maxillofacial surgery has been attempted with several DDS <sup>153–155,211–214</sup>. However, no such formulation is currently available. Publication IV explores a NIMO-releasing electrospun fiber mat as an easily manufactured, stable DDS for local therapy in the brain. The work focuses mainly on drug incorporation and the resulting release profile.

A successful blend electrospinning process reliably produced PLGA NIMO fiber mates with excellent encapsulation efficiency and a narrow fiber diameter distribution for 1 % and 10 % drug load. The drug was incorporated in the fiber matrix in the amorphous state, and the amorphous solid dispersion remained stable over at least 6 months. DSC analysis revealed the influence of both the electrospinning process and the drug incorporation on polymer chain mobility and thus the  $T_g$  of the EPF.

The influence of release conditions on the EPF is still only rarely included in the studies of fiber-based DDS and was therefore particularly closely examined in this work. Incubation in a standardized surfactant solution release medium led to a complete loss of the fiber geometry. The specific advantages of EPF, their micron sized structures and large surface area, were thus undone. The results emphasize the importance of looking beyond the often practiced use of just one buffer solution as standard medium for in vitro release studies. While

incubation in the surfactant solution resulted in a strong burst release, linear release over several days was achieved when fiber mats were incubated in cell culture media.

It could be demonstrated that the NIMO EPF possess excellent compatibility with different brain cell lines in vitro and provided the therapeutically desired cytoprotective effect. Cell death in stressed cells was significantly reduced when incubated with the drug-releasing fiber mats, suggesting a beneficial therapeutic outcome for local NIMO therapy with electrospun nonwovens.

Thus, EPF appeared to be a well-suited DDS for intracranial local NIMO delivery due to easy manufacturing, good drug stability, and excellent compatibility with the relevant brain cell types.

However, the delivery rate of NIMO still needs to be better understood and adjusted to provide the desirable prolonged, steady release reliably. The choice of a higher molecular weight PLGA, a blend with a different polymer, crosslinking or a coating of the fiber matrix could be tested to enhance the form-stability of the EPF during release. Ultimately, to retain individual fibers and guarantee a more strictly controlled release, a  $T_g$  of the fiber mat well above 37 °C after water uptake upon incubation should be obtained while also preserving compatibility between drug and matrix polymer.

Considering the effect of the release medium on release kinetics, drug delivery should then be studied in artificial cerebrospinal fluid to allow a more realistic assessment.

The compatibility between the fiber mats and brain tissue in vivo rather than individual cell lines will need to be ascertained to further confirm the excellent suitability of EPF for site-specific intracranial delivery. As such, electrospun nonwovens as a widely adaptable, solubility enhancing DDS could close a pivotal gap in patient care in neurosurgery where local delivery to specific brain areas is still only available for very few of the possible indications.

The specific characteristics of release from PLA-PPX-coated PFS are examined in publication V. The performance of the short electrospun fiber based sponges has been tested in a variety of different fields such as insulation<sup>215</sup>, as catalysts<sup>216</sup>, emulsion separators<sup>217</sup>, and in tissue engineering<sup>198</sup>. But their potential as DDS has not yet been methodically evaluated. Publication V thus presents a first systematic assessment of factors governing the drug release inherent to the PFS with their extreme porosity and strong lipophilicity.

Drug loading in PFS can potentially be achieved by incorporation within the fiber matrix. But the high porosity of the sponge also allows loading with drug solutions after scaffold preparation. Both methods were considered in this study. Implantation was seen as the main route of application.

The extremely slow uptake of aqueous fluids into the pores of the PFS was identified as a potential mechanism to prolong drug release from these systems. Depending on experimental conditions, complete water saturation, a prerequisite for successful drug delivery from drug-loaded fiber scaffolds, can take 4-45 weeks. Noninvasive  $\mu$ CT and EPR imaging revealed that liquid penetration was mainly controlled by possible air entrapment in the PFS 3D structure and the surface activity of the aqueous incubation medium.

Loading with lipophilic/oily drug solutions could make PFS patient-individual DDS with high flexibility regarding drug, drug combinations, and dose. As an essentially fiber-reinforced lipid-based delivery system, they also offer the benefit of enhanced solubility for a variety of different poorly soluble compounds.

PFS showed good mechanical stability and oil retention after loading with the oil MCT.  $^1\text{H}$  NMR measurements of  $T_2$  distributions and diffusion coefficients revealed an interaction of the oil with the fiber scaffold and a restriction on distribution. Still, no significant effect was observed on the actual release of a small molecule model drug from the PFS.

The results provide a first broad overview of the mechanisms governing release from the PFS as novel DDS. For further studies the PPX-coating should be replaced by a biodegradable material because the more desirable coating with a polymer more suitable for clinical use might considerably change the sponges' characteristics.

Liquid uptake should be tested with a larger number of samples as results varied greatly for some setups. Also, considering the influence of the surface-active protein BSA on the water uptake, liquid penetration should ideally be tested with human serum or a very close substitute to create more realistic experimental conditions. Similar to what has been done for the NIMO nonwovens, the PFS should be examined after incubations via electron microscopy to notice any changes in fiber morphology that could also influence drug release. To test actual drug release from PFS, a small-molecule drug should be electrospun into the fibers of scaffolds.

One such drug that could potentially benefit from the controlled delivery from PFS scaffolds is nimodipine. The sponges appear to be particularly well suited as intracranial implants. The skull provides protection from mechanical pressure and deformation of the PFS. At the same time, the soft scaffold material and the, compared to EPF, more compact geometry of the PFS could be advantageous for implantation in the sensitive brain tissue.

As a whole, carrying on the work already done on the release from polymer fiber sponges is highly expedient. No carrier system similar to these very versatile, easily adjustable scaffolds has been proposed or made available yet. The polymer fiber sponges can thus offer completely novel and unique features, applications, and advantages in drug delivery and patient care.

---

**BIBLIOGRAPHY**

- 1 Amidon GL, Lennernäs H, Shah VP, Crison JR. A Theoretical Basis for a Biopharmaceutic Drug Classification: The Correlation of in Vitro Drug Product Dissolution and in Vivo Bioavailability. *Pharm Res* 1995; **12**: 413–420.
- 2 Butler JM, Dressman JB. The Developability Classification System: Application of Biopharmaceutics Concepts to Formulation Development. *J Pharm Sci* 2010; **99**: 4940–4954.
- 3 Nelemans LC, Gurevich L. Drug delivery with polymeric nanocarriers-cellular uptake mechanisms. *Materials (Basel)* 2020; **13**: 366.
- 4 Augustijns P, Wuyts B, Hens B, Annaert P, Butler J, Brouwers J. A review of drug solubility in human intestinal fluids: Implications for the prediction of oral absorption. *Eur J Pharm Sci* 2014; **57**: 322–332.
- 5 U.S. Food and Drug Administration. Waiver of In Vivo Bioavailability and Bioequivalence Studies for Immediate-Release Solid Oral Dosage Forms Based on a Biopharmaceutics Classification System Guidance for Industry. 2017.<http://www.fda.gov> (accessed 21 Jul2021).
- 6 Dahan A, Miller JM, Gordon L. Amidon. Prediction of Solubility and Permeability Class Membership: Provisional BCS Classification of the World's Top Oral Drugs. *AAPS J*; **11**: 740–746.
- 7 Pires A, Fortuna A, Alves G, Falcão A. Intranasal drug delivery: How, why and what for? *J Pharm Pharm Sci* 2009; **12**: 288–311.
- 8 Ting JM, Porter WW, Mecca JM, Bates FS, Reineke TM. Advances in Polymer Design for Enhancing Oral Drug Solubility and Delivery. *Biocunjugate Chem* 2018; **29**: 939–952.
- 9 Di L, Fish P V., Mano T. Bridging solubility between drug discovery and development. *Drug Discov Today* 2012; **17**: 486–495.
- 10 Landis MS, Bhattachar S, Yazdanian M, Morrison J. Commentary: Why Pharmaceutical Scientists in Early Drug Discovery Are Critical for Influencing the Design and Selection of Optimal Drug Candidates. *AAPS PharmSciTech* 2018; **19**. doi:10.1208/s12249-017-0849-3.
- 11 Pouton CW. Formulation of poorly water-soluble drugs for oral administration: Physicochemical and physiological issues and the lipid formulation classification system. *Eur J Pharm Sci* 2006; **29**: 278–287.
- 12 Buckley ST, Frank KJ, Fricker G, Brandl M. Biopharmaceutical classification of poorly soluble drugs with respect to 'enabling formulations'. *Eur J Pharm Sci* 2013; **50**: 8–16.
- 13 Ditzinger F, Price DJ, Ilie AR, Köhl NJ, Jankovic S, Tsakiridou G *et al*. Lipophilicity and hydrophobicity considerations in bio-enabling oral formulations approaches – a PEARRL review. *J Pharm Pharmacol* 2019; **71**: 464–482.
- 14 Gupta S, Kesarla R, Omri A. Formulation Strategies to Improve the Bioavailability of Poorly Absorbed Drugs with Special Emphasis on Self-Emulsifying Systems. *ISRN Pharm* 2013; **2013**: 1–16.
- 15 Arbor Pharmaceuticals Inc. NYMALIZE® (nimodipine) oral solution Prescribing Information. 2013.[www.fda.gov/medwatch](http://www.fda.gov/medwatch). (accessed 15 Sep2021).
- 16 Bristol-Myers Squibb Company. TAXOL® (paclitaxel) injection Prescribing Information. 2011.<https://www.accessdata.fda.gov> (accessed 15 Sep2021).
- 17 GlaxoSmithKline. AVODART® (dutasteride) soft gelatin capsules Prescribing Information. 2020.[www.fda.gov/medwatch](http://www.fda.gov/medwatch). (accessed 16 Sep2021).

- 18 Fresenius Kabi USA L. DIPRIVAN® (propofol) injectable emulsion Prescribing Information. 2014. <https://www.accessdata.fda.gov> (accessed 16 Sep2021).
- 19 Novartis Pharmaceuticals Corporation. NEORAL® Prescribing Information. 2009. <https://www.accessdata.fda.gov> (accessed 6 May2020).
- 20 European Medicines Agency Evaluation of Medicines for Human Use. CHMP Assessment report for Intelence. *Doc Ref EMEA/CHMP43952/2008* 2008; : 1–52.
- 21 AbbVie Inc. KALETRA® (lopinavir and ritonavir) Prescribing Information. 2016. [www.fda.gov/medwatch](http://www.fda.gov/medwatch) (accessed 15 Sep2021).
- 22 Janssen Pharmaceuticals. SPORANOX® (itraconazole) oral solution Prescribing Information. 2003. <https://www.janssenlabels.com> (accessed 16 Sep2021).
- 23 Murteira S, Ghezaiel Z, Karray S, Lamure M. Drug reformulations and repositioning in pharmaceutical industry and its impact on market access: reassessment of nomenclature. *J Mark Access Heal Policy* 1AD. doi:10.3402/jmahp.v1i0.21131.
- 24 Pouton CW. Lipid formulations for oral administration of drugs: Non-emulsifying, self-emulsifying and 'self-microemulsifying' drug delivery systems. *Eur J Pharm Sci* 2000; **11**: 93–98.
- 25 Pouton CW. Key issues when formulating hydrophobic drugs with lipid. *Bulletin Tech Gattefossé* 1999; **92**: 41–50.
- 26 Savla R, Browne J, Plassat V, Wasan KM, Wasan EK. Review and analysis of FDA approved drugs using lipid-based formulations. *Drug Dev Ind Pharm* 2017; **43**: 1743–1758.
- 27 Hückstädt K. *Entwicklung und Charakterisierung von pharmazeutischen Mikroemulsionen*. [dissertation]. Kiel: Christian Albrecht University, 2005.
- 28 Lawrence MJ, Rees GD. Microemulsion-based media as novel drug delivery systems. *Adv Drug Deliv Rev* 2012; **64**: 175–193.
- 29 Moangella Andrade de Assis K, Maísa da Silva Leite J, Ferreira de Melo D, Cordeiro Borges J, Matheus Barreto Santana L, Maria Lucas dos Reis M *et al*. Bicontinuous microemulsions containing Melaleuca alternifolia essential oil as a therapeutic agent for cutaneous wound healing. *Drug Deliv Transl Res* 2020; **10**: 1748–1763.
- 30 Sacchetti M, Nejati E. Prediction of Drug Solubility in Lipid Mixtures from the Individual Ingredients. *AAPS PharmSciTech* 2012; **13**: 1103–1109.
- 31 Patel S V., Patel S. Prediction of the solubility in lipidic solvent mixture: Investigation of the modeling approach and thermodynamic analysis of solubility. *Eur J Pharm Sci* 2015; **77**: 161–169.
- 32 Holt DW, Johnston A. Cyclosporin microemulsion. A guide to usage and monitoring. *BioDrugs* 1997; **7**: 175–197.
- 33 Coukell A, Plosker GL. Cyclosporin microemulsion (Neoral®): A pharmacoeconomic review of its use compared with standard cyclosporin in renal and hepatic transplantation. *Pharmacoeconomics* 1998; **14**: 691–708.
- 34 Gupta S, Kesarla R, Omri A. Formulation Strategies to Improve the Bioavailability of Poorly Absorbed Drugs with Special Emphasis on Self-Emulsifying Systems. *ISRN Pharm* 2013; **2013**: 16.
- 35 Sarciaux JM, Acar L, Sado PA. Using microemulsion formulations for oral drug delivery of therapeutic peptides. *Int J Pharm* 1995; **120**: 127–136.
- 36 Sun M, Si L, Zhai X, Fan Z, Ma Y, Zhang R *et al*. The influence of co-solvents on the stability and bioavailability of rapamycin formulated in self-microemulsifying drug delivery systems. *Drug Dev Ind Pharm* 2011; **37**: 986–994.



- 37 Kogan A, Garti N. Microemulsions as transdermal drug delivery vehicles. *Adv Colloid Interface Sci* 2006; **123–126**: 369–385.
- 38 Abbott Laboratories. NORVIR® (ritonavir) Soft Gleetine Capules for oral use, Prescribing Information. 2012www.fda.gov/medwatch. (accessed 29 Sep2021).
- 39 Boehringer Ingelheim International GmbH. APTIVUS® (tipranavir) capsules, Prescribing Information. 2011.www.fda.gov/medwatch. (accessed 29 Sep2021).
- 40 Boys C V. On the production, properties, and some suggested uses of the finest threads. *Proc Phys Soc London* 1887; **9**: 8–19.
- 41 Doshi J, Reneker DH. Electrospinning process and applications of electrospun fibers. In: *Conference Record of the 1993 IEEE Industry Applications Conference Twenty-Eighth IAS Annual Meeting Toronto, Ontario, Canada*. 1993, pp 1698–1703.
- 42 Tucker N, Stanger JJ, Staiger MP, Razzaq H, Hofman K. The history of the science and technology of electrospinning from 1600 to 1995. *J Eng Fiber Fabr* 2012; **7**: 63–73.
- 43 Taylor G. Disintegration of water drops in an electric field. *Proc R Soc London A Math Phys Sci* 1964; **280**: 383–397.
- 44 Taylor G. Electrically driven jets. *Proc R Soc London A Math Phys Sci* 1969; **313**: 453–475.
- 45 Zeleny J. The electrical discharge from liquid points, and a hydrostatic method of measuring the electric intensity at their surfaces. *Phys Rev* 1914; **3**: 69–91.
- 46 Shin YM, Hohman MM, Brenner MP, Rutledge GC. Electrospinning: A whipping fluid jet generates submicron polymer fibers. *Appl Phys Lett* 2001; **78**: 1149–1151.
- 47 Reneker DH, Yarin AL, Fong H, Koombhongse S. Bending instability of electrically charged liquid jets of polymer solutions in electrospinning. *J Appl Phys* 2000; **87**: 4531–4547.
- 48 Niu H, Lin T. Fiber generators in needleless electrospinning. *J Nanomater* 2012; **2012**. doi:10.1155/2012/725950.
- 49 Schoolaert E, Cossu L, Becelaere J, Van Guyse JFR, Tigrine A, Vergaelen M *et al*. Nanofibers with a tunable wettability by electrospinning and physical crosslinking of poly(2-n-propyl-2-oxazoline). *Mater Des* 2020; **192**.
- 50 Lv H, Cui S, Zhang H, Pei X, Gao Z, Hu J *et al*. Crosslinked starch nanofibers with high mechanical strength and excellent water resistance for biomedical applications. *Biomed Mater* 2020; **15**: 25007.
- 51 Sayin S, Tufani A, Emanet M, Genchi GG, Sen O, Shemshad S *et al*. Electrospun Nanofibers With pH-Responsive Coatings for Control of Release Kinetics. *Front Bioeng Biotechnol* 2019; **7**.
- 52 Díaz JE, Barrero A, Márquez M, Loscertales IG. Controlled encapsulation of hydrophobic liquids in hydrophilic polymer nanofibers by co-electrospinning. *Adv Funct Mater* 2006; **16**: 2110–2116.
- 53 Klein S, Kuhn J, Avrahami R, Tarre S, Beliavski M, Green M *et al*. Encapsulation of bacterial cells in electrospun microtubes. *Biomacromolecules* 2009; **10**: 1751–1756.
- 54 López-Rubio A, Sanchez E, Sanz Y, Lagaron JM. Encapsulation of living bifidobacteria in ultrathin PVOH electrospun fibers. *Biomacromolecules* 2009; **10**: 2823–2829.
- 55 Letnik I, Avrahami R, Rokem JS, Greiner A, Zussman E, Greenblatt C. Living Composites of Electrospun Yeast Cells for Bioremediation and Ethanol Production. *Biomacromolecules* 2015; **16**: 3322–3328.

- 56 Ang HY, Irvin SA, Avrahami R, Sarig U, Bronshtein T, Zussman E *et al.* Characterization of a bioactive fiber scaffold with entrapped HUVECs in coaxial electrospun core-shell fiber. *Biomatter* 2014; **4**.
- 57 Dror Y, Kuhn J, Avrahami R, Zussman E. Encapsulation of enzymes in biodegradable tubular structures. *Macromolecules* 2008; **41**: 4187–4192.
- 58 Shenoy SL, Bates WD, Frisch HL, Wnek GE. Role of chain entanglements on fiber formation during electrospinning of polymer solutions: Good solvent, non-specific polymer-polymer interaction limit. *Polymer* (2005; **46**: 3372–3384.
- 59 Khanlou HM, Sadollah A, Ang BC, Kim JH, Talebian S, Ghadimi A. Prediction and optimization of electrospinning parameters for polymethyl methacrylate nanofiber fabrication using response surface methodology and artificial neural networks. *Neural Comput Appl* 2014; **25**: 767–777.
- 60 Samadian H, Zakariaee SS, Faridi-Majidi R. Evaluation of effective needleless electrospinning parameters controlling polyacrylonitrile nanofibers diameter via modeling artificial neural networks. *J Text Inst* 2019; **110**: 477–486.
- 61 Ismail N, Maksoud FJ, Ghaddar N, Ghali K, Tehrani-Bagha A. Simplified modeling of the electrospinning process from the stable jet region to the unstable region for predicting the final nanofiber diameter. *J Appl Polym Sci* 2016; **133**: 1–11.
- 62 Khatti T, Naderi-Manesh H, Kalantar SM. Application of ANN and RSM techniques for modeling electrospinning process of polycaprolactone. *Neural Comput Appl* 2019; **31**: 239–248.
- 63 He H, Wang Y, Farkas B, Nagy ZK, Molnar K. Analysis and prediction of the diameter and orientation of AC electrospun nanofibers by response surface methodology. *Mater Des* 2020; **194**: 3–9.
- 64 Fetz AE, Fantaziu CA, Smith RA, Radic MZ, Bowlin GL. Surface Area to Volume Ratio of Electrospun Polydioxanone Templates Regulates the Adsorption of Soluble Proteins from Human Serum. *bioengineering* 2019; **6**: 1–16.
- 65 Zhu L, Zaarour B, Jin X. Direct generation of electrospun interconnected macroporous nanofibers using a water bath as a collector. *Mater Res Express* 2020; **7**.
- 66 Ding Y, Li W, Zhang F, Liu Z, Zanjanizadeh Ezazi N, Liu D *et al.* Electrospun Fibrous Architectures for Drug Delivery, Tissue Engineering and Cancer Therapy. *Adv Funct Mater* 2019; **29**.
- 67 Dott C, Tyagi C, Tomar LK, Choonara YE, Kumar P, Du Toit LC *et al.* A Mucoadhesive Electrospun Nanofibrous Matrix for Rapid Oramucosal Drug Delivery. *J Nanomater* 2013.
- 68 Kenawy E-R, Bowlin GL, Mansfield K, Layman J, Simpson G, Sanders EH *et al.* Release of tetracycline hydrochloride from electrospun poly(ethylene-co-vinylacetate), poly(lactic acid), and a blend. *J Control Release* 2002; **81**: 57–64.
- 69 Natu M V., de Sousa HC, Gil MH. Effects of drug solubility, state and loading on controlled release in bicomponent electrospun fibers. *Int J Pharm* 2010; **397**: 50–58.
- 70 Xie Z, Buschle-Diller G. Electrospun Poly(D,L-lactide) fibers for drug delivery: The influence of cosolvent and the mechanism of drug release. *J Appl Polym Sci* 2010; **115**: 1–8.
- 71 Zeng J, Yang L, Liang Q, Zhang X, Guan H, Xu X *et al.* Influence of the drug compatibility with polymer solution on the release kinetics of electrospun fiber formulation. *J Control Release* 2005; **105**: 43–51.
- 72 Seif S, Franzen L, Windbergs M. Overcoming drug crystallization in electrospun fibers - Elucidating key parameters and developing strategies for drug delivery. *Int J Pharm*

- 2015; **478**: 390–397.
- 73 Szabo E, Zahonyi P, Brecka D, Galata DL, Meszaros LA, Madarasz L *et al.* Comparison of Amorphous Solid Dispersions of Spironolactone Prepared by Spray Drying and Electrospinning: The Influence of the Preparation Method on the Dissolution Properties. *Mol Pharm* 2021; **18**: 317–327.
- 74 Sagiv A, Parker N, Parkhi V, Nelson KD. Initial Burst Measures of Release Kinetics from Fiber Matrices. *Ann Biomed Eng* 2003; **31**: 1132–1140.
- 75 Zech J, Leisz S, Göttel B, Syrowatka F, Greiner A, Strauss C *et al.* Electrospun Nimodipine-loaded fibers for nerve regeneration: Development and in vitro performance. *Eur J Pharm Biopharm* 2020; **151**: 116–126.
- 76 Xue J, He M, Liu H, Niu Y, Crawford A, Coates P *et al.* Drug loaded homogeneous electrospun PCL/ gelatin hybrid nanofiber structures for anti-infective tissue regeneration membranes. *Biomaterials* 2014; **35**: 9395–9405.
- 77 Roman JA, Reucroft I, Martin RA, Hurtado A, Mao HQ. Local Release of Paclitaxel from Aligned, Electrospun Microfibers Promotes Axonal Extension. *Adv Healthc Mater* 2016; **5**: 2628–2635.
- 78 Suzuki K, Tanaka H, Ebara M, Uto K, Matsuoka H, Nishimoto S *et al.* Electrospun nanofiber sheets incorporating methylcobalamin promote nerve regeneration and functional recovery in a rat sciatic nerve crush injury model. *Acta Biomater* 2017; **53**: 250–259.
- 79 Zhang C, Wang X, Zhang E, Yang L, Yuan H, Tu W *et al.* An Epigenetic Bioactive Composite Scaffold with Well-aligned Nanofibers for Functional Tendon Tissue Engineering. *Acta Biomater* 2017; **66**: 141–156.
- 80 Keirouz A, Chung M, Kwon J, Fortunato G, Radacsi N. 2D and 3D electrospinning technologies for the fabrication of nanofibrous scaffolds for skin tissue engineering: A review. *WIREs Interdiscip Rev Nanomedicine Nanobiotechnology* 2020; **12**.
- 81 Duan G, Bagheri AR, Jiang S, Golenser J, Agarwal S, Greiner A. Exploration of Macroporous Polymeric Sponges As Drug Carriers. *Biomacromolecules* 2017; **18**: 3215–3221.
- 82 Duan G, Jiang S, Jérôme V, Wendorff JH, Fathi A, Uhm J *et al.* Ultralight, soft polymer sponges by self-assembly of short electrospun fibers in colloidal dispersions. *Adv Funct Mater* 2015; **25**: 2850–2856.
- 83 Persano L, Camposeo A, Tekmen C, Pisignano D. Industrial upscaling of electrospinning and applications of polymer nanofibers: A review. *Macromol Mater Eng* 2013; **298**: 504–520.
- 84 Vass P, Szabó E, Domokos A, Hirsch E, Galata D, Farkas B *et al.* Scale-up of electrospinning technology: Applications in the pharmaceutical industry. *Wiley Interdiscip Rev Nanomedicine Nanobiotechnology* 2020; **12**: 1–24.
- 85 Kumar S, Singh AP, Senapati S, Maiti P. Controlling Drug Delivery Using Nanosheet-Embedded Electrospun Fibers for Efficient Tumor Treatment. *ACS Appl Bio Mater* 2019; **2**: 884–894.
- 86 Li J, Xu W, Li D, Liu T, Zhang YS, Ding J *et al.* Locally Deployable Nanofiber Patch for Sequential Drug Delivery in Treatment of Primary and Advanced Orthotopic Hepatomas. *ACS Nano* 2018; **12**: 6685–6699.
- 87 Ramachandran R, Reddy Junnuthula V, Siddaramana Gowd G, Ashokan A, Thomas J, Peethambaran R *et al.* Theranostic 3-Dimensional nano brain-implant for prolonged and localized treatment of recurrent glioma. *Sci Rep* 2017; **7**. doi:10.1038/srep43271.
- 88 Hsu Y, Chen DW, Ta C-D, Chou Y, Liu S-J, Ueng SW-N *et al.* Biodegradable drug-

- eluting nanofiber-enveloped implants for sustained release of high bactericidal concentrations of vancomycin and ceftazidime: in vitro and in vivo studies. *Int J Nanomedicine* 2014; **9**: 4347–4355.
- 89 Sharma A, Gupta A, Rath G, Goyal A, Mathur RB, Dhakate SR. Electrospun composite nanofiber-based transmucosal patch for anti-diabetic drug delivery. *J Mater Chem B* 2013; **1**: 3410–3418.
- 90 Lancina MG, Singh S, Kompella UB, Husain S, Yang H. Fast Dissolving Dendrimer Nanofiber Mats as Alternative to Eye Drops for More Efficient Antiglaucoma Drug Delivery. *ACS Biomater Biomater* 2017; **3**: 1861–1868.
- 91 Elmarco. Product profile Nanospider Production Line Ns 8S1600U. 2019.
- 92 Inovenso Technology. Industrial Electrospinning/Spraying nanofiber machine | Inovenso, innovative engineering solutions. <https://www.inovenso.com/portfolio-view/nanospinner416/> (accessed 9 Dec2020).
- 93 The Electrospinning Company. Company | The Electrospinning Company. <https://www.electrospinning.co.uk/about-us/company/> (accessed 9 Dec2020).
- 94 Technical Fine Co. nanofiber e-spin Technical Fine Co., Ltd. coating nanotechnology | Contract-production of Nano-fiber products. [https://www.technicalfine.com/contract\\_production.html](https://www.technicalfine.com/contract_production.html) (accessed 9 Dec2020).
- 95 DiPole Materials. Electrospinning Services - Dipole Materials. <https://www.dipolematerials.com/electrospinning-services/> (accessed 9 Dec2020).
- 96 World Health Organization. World Malaria Report 2020. 2021 <https://www.who.int/teams/global-malaria-programme/reports/world-malaria-report-2020> (accessed 4 Jun2021).
- 97 CDC Centers for Disease Control and Prevention. Malaria's Impact Worldwide. 2021. [https://www.cdc.gov/malaria/malaria\\_worldwide/impact.html](https://www.cdc.gov/malaria/malaria_worldwide/impact.html) (accessed 4 Jun2021).
- 98 World Health Organization. WHO Guidelines for malaria. 2021. <https://www.who.int/publications/i/item/WHO-UCN-GMP-2021.01> (accessed 5 Jun2021).
- 99 World Health Organization. World Health Organization Model List of Essential Medicines 21st List 2019. 2019. <https://apps.who.int> (accessed 21 May2021).
- 100 Ashley EA, Dhorda M, Fairhurst RM, Amaratunga C, Lim P, Suon S *et al*. Spread of Artemisinin Resistance in Plasmodium falciparum Malaria. *N Engl J Med* 2014; **371**: 411–434.
- 101 Dondorp AM, Nosten F, Yi P, Das D, Phyo AP, Tarning J *et al*. Artemisinin Resistance in Plasmodium falciparum Malaria. *N Engl J Med* 2009; **361**: 455–467.
- 102 World Health Organization. Artemisinin resistance and artemisinin-based combination therapy efficacy. 2019 <https://apps.who.int> (accessed 5 Jun2021).
- 103 Mithun Rudrapal, Dipak Chetia. Endoperoxide antimalarials: development, structural diversity and pharmacodynamic aspects with reference to 1,2,4-trioxane-based structural scaffold. *Drug Des Devel Ther* 2016; **10**: 3575–3590.
- 104 Hartwig CL, Rosenthal AS, D'Angelo J, Griffin CE, Posner GH, Cooper RA. Accumulation of artemisinin trioxane derivatives within neutral lipids of Plasmodium falciparum malaria parasites is endoperoxide-dependent. *Biochem Pharmacol* 2009; **77**: 322–336.
- 105 Patel OPS, Beteck RM, Legoabe LJ. Exploration of artemisinin derivatives and synthetic peroxides in antimalarial drug discovery research. *Eur J Med Chem* 2021; **213**: 113193.

- 106 Dwivedi A, Mazumder A, du Plessis L, du Preez JL, Haynes RK, du Plessis J. In vitro anti-cancer effects of artemisone nano-vesicular formulations on melanoma cells. *Nanomedicine Nanotechnology, Biol Med* 2015; **11**: 2041–2050.
- 107 Gravett AM, Liu WM, Krishna S, Chan WC, Haynes RK, Wilson NL *et al*. In vitro study of the anti-cancer effects of artemisone alone or in combination with other chemotherapeutic agents. *Cancer Chemother Pharmacol* 2011; **67**: 569–577.
- 108 Lam NS, Long X, Su X zhuan, Lu F. Artemisinin and its derivatives in treating helminthic infections beyond schistosomiasis. *Pharmacol Res* 2018; **133**: 77–100.
- 109 Burger C, Aucamp M, du Preez J, Haynes RK, Ngwane A, du Plessis J *et al*. Formulation of Natural Oil Nano-Emulsions for the Topical Delivery of Clofazimine, Artemisone and Decoquinate. *Pharm Res* 2018; **35**.
- 110 Mazuz ML, Haynes R, Shkap V, Fish L, Wollkomirsky R, Leibovich B *et al*. Neospora caninum: In vivo and in vitro treatment with artemisone. *Vet Parasitol* 2012; **187**: 99–104.
- 111 Mazuz ML, Golenser J, Fish L, Haynes RK, Wollkomirsky R, Leibovich B *et al*. Artemisone inhibits in vitro and in vivo propagation of Babesia bovis and B. bigemina parasites. *Exp Parasitol* 2013; **135**: 690–694.
- 112 Oiknine-Djian E, Weisblum Y, Panet A, Wong HN, Haynes RK, Wolf DG. The Artemisinin Derivative Artemisone Is a Potent Inhibitor of Human Cytomegalovirus Replication. 2018.
- 113 Gold D, Alian M, Domb A, Karawani Y, Jbarien M, Chollet J *et al*. Elimination of Schistosoma mansoni in infected mice by slow release of artemisone. *Int J Parasitol Drugs Drug Resist* 2017; **7**: 241–247.
- 114 Bergquist R, Elmorshedy H. Artemether and praziquantel: Origin, mode of action, impact, and suggested application for effective control of human schistosomiasis. *Trop Med Infect Dis* 2018; **3**.
- 115 Saeed MEM, Krishna S, Greten HJ, Kremsner PG, Efferth T. Antischistosomal activity of artemisinin derivatives in vivo and in patients. *Pharmacol Res* 2016; **110**: 216–226.
- 116 World Health Organization. Schistosomiasis. 2021. <https://www.who.int/news-room/fact-sheets/detail/schistosomiasis> (accessed 6 Jun2021).
- 117 Steinmann P, Keiser J, Bos R, Tanner M, Utzinger J. Schistosomiasis and water resources development: systematic review, meta-analysis, and estimates of people at risk. *Lancet Infect Dis* 2006; **6**: 411–425.
- 118 Utzinger J, Raso G, Brooker S, De Savigny D, Tanner M, Ørnbjerg N *et al*. Schistosomiasis and neglected tropical diseases: towards integrated and sustainable control and a word of caution. *Parasitology* 2009; **136**: 1859–1874.
- 119 Haynes RK, Fugmann B, Stetter J, Rieckmann K, Heilmann HD, Chan HW *et al*. Artemisone - A Highly Active Antimalarial Drug of the Artemisinin Class. *Angew Chemie - Int Ed* 2006; **45**: 2082–2088.
- 120 Vivas L, Rattray L, Stewart LB, Robinson BL, Fugmann B, Haynes RK *et al*. Antimalarial efficacy and drug interactions of the novel semi-synthetic endoperoxide artemisone in vitro and in vivo. *J Antimicrob Chemother* 2007; **59**: 658–665.
- 121 Nagelschmitz J, Voith B, Wensing G, Roemer A, Fugmann B, Haynes RK *et al*. First assessment in humans of the safety, tolerability, pharmacokinetics, and ex vivo pharmacodynamic antimalarial activity of the new artemisinin derivative artemisone. *Antimicrob Agents Chemother* 2008; **52**: 3085–91.
- 122 U.S. Food and Drug Administration. Orphan Drug Designations and Approvals - Artemisone.

- 2017.<https://www.accessdata.fda.gov/scripts/opdlisting/oopd/listResult.cfm> (accessed 15 Jul2021).
- 123 Schmuck G, Keutz E von, Haynes R. Artemifone, a new antimalarial artemisinin derivative: lack of neurotoxicity. In: *Medicin and Health in the Tropics Abstract Book*. Marseille (France), 2005.
- 124 Artemis Therapeutics I. Research & Development – Artemis Therapeutics, Inc. <http://www.artemis-therapeutics.com/research-development/> (accessed 14 Jul2021).
- 125 Artemis Therapeutics I. Artemis Corporate Overview Ticker: ATMS. 2018<http://www.artemis-therapeutics.com/wp-content/uploads> (accessed 26 May2021).
- 126 Gibhard L, Coertzen D, Reader J, Van Der Watt ME, Birkholtz L-M, Wong HN *et al*. The Artemiside-Artemisox-Artemisone-M1 Tetrad: Efficacies against Blood Stage *P. falciparum* Parasites, DMPK Properties, and the Case for Artemiside. *Pharmaceutics* 2021; **13**: 1–19.
- 127 NIH U.S. National Library of Medicine. Artemisone | C19H31NO6S - PubChem. <https://pubchem.ncbi.nlm.nih.gov/compound/Artemisone> (accessed 18 Sep2021).
- 128 Lipinski CA, Lombardo F, Dominy BW, Feeney PJ. Experimental and computational approaches to estimate solubility and permeability in drug discovery and development settings. *Adv Drug Deliv Rev* 1997; **23**: 3–25.
- 129 Ganga Senarathna DK, Page-Sharp M, Crowe A. The Interactions of P-Glycoprotein with Antimalarial Drugs, Including Substrate Affinity, Inhibition and Regulation. *PLoS One* 2016.
- 130 Heyns J, Willers C, Haynes RK, Wong HN, Hamman J, Gouws C. Absorptive and Secretory Transport of Selected Artemisinin Derivatives Across Caco-2 Cell Monolayers. 2018; : 1183–1192.
- 131 Zech J, Gold D, Salaymeh N, Sasson NC, Rabinowitch I, Golenser J *et al*. Oral administration of artemisone for the treatment of schistosomiasis: Formulation challenges and in vivo efficacy. *Pharmaceutics* 2020; **12**.
- 132 Zech J, Salaymeh N, Hunt NH, Mäder K, Golenser J. Efficient treatment of experimental cerebral malaria by an artemisone-SMEDDS system: impact of application route and dosing frequency. *Antimicrob Agents Chemother* 2021; **65**.
- 133 Alskä LC, Porter CJH, Bergströ CAS. Tools for Early Prediction of Drug Loading in Lipid-Based Formulations. *Mol Microbiol* 2015; **13**: 251–261.
- 134 Zech J, Timoracky M, Syrowatka F, Mäder K. Artemisone in Electrosprayed Solid Lipid Microparticles. Paper an poster presented at: *The PBP World Meeting, Granada, Spain*. 2018, pp 1–2.
- 135 Sweetman SC (ed.). *Martindale: The complete drug reference. 36th Edition*. London: *Pharmaceutical Press*. Pharmaceutical Press: London, UK, 2009.
- 136 European Medicines Agency. Public summary of opinion on orphan designation Nimodipine for the treatment of aneurysmal subarachnoid haemorrhage (EU/3/15/1554). 2015.<https://www.ema.europa.eu/contact> (accessed 29 Sep2021).
- 137 Centre for Drug Evaluation and Research - U. S. Food and Drug Administration. CDER Rare Disease and Orphan Drug Designated Approvals (5/10/2013). 2013.<https://fda.report> (accessed 30 Sep2021).
- 138 Scheller C, Wienke A, Tatagiba M, Gharabaghi A, Ramina KF, Ganslandt O *et al*. Prophylactic nimodipine treatment and improvement in hearing outcome after vestibular schwannoma surgery: a combined analysis of a randomized, multicenter, Phase III trial and its pilot study. *J Neurosurg* 2017; **127**: 1376–1383.

- 139 Scheller K, Scheller C. Nimodipine promotes regeneration of peripheral facial nerve function after traumatic injury following maxillofacial surgery: An off label pilot-study. *J Cranio-Maxillofacial Surg* 2012; **40**: 427–434.
- 140 van Lindert E, Hassler W, Della Saletta A. Delayed ischemic optic neuropathy after surgery on skull base meningiomas successfully treated with nimodipine and rheological therapy: Report of two cases. *Skull Base Surg* 2000; **10**: 207–210.
- 141 Woo PYM, See KWM, Chow JKH, Chan Y, Wong HT, Chan KY. Hypertensive-Nimodipine Therapy for Middle Cerebral Artery Vasospasm after Resection of Glioblastoma Multiforme: A Case Report and Literature Review. *Open J Mod Neurosurg* 2015; **05**: 76–83.
- 142 Yu Y, Li Y, Jin Z, Zhao S, Xie X, Chen F. Nimodipine reduces delayed cerebral vasospasm after intracranial tumour surgery: A Retrospective Study. *Clin Exp Pharmacol Physiol* 2021; : 1–8.
- 143 Carlson AP, Hänggi D, Macdonald RL, Shuttleworth CW. Nimodipine Reappraised: An Old Drug with a Future. *Curr Neuropharmacol* 2020; **18**: 65–82.
- 144 Wadworth AN, Mctavish D. DRUG EVALUATION Nimodipine A Review of its Pharmacological Properties, and Therapeutic Efficacy in Cerebral Disorders. *Drugs Aging* 1992; **2**: 262–286.
- 145 Grunenberg A, Keil B, Henck JO. Polymorphism in binary mixtures, as exemplified by nimodipine. *Int J Pharm* 1995; **118**: 11–21.
- 146 Masumoto K, Takeyasu A, Oizumi K, Takashi Kobayashi. Studies of Novel 1,4-Dihydropyridine Ca Antagonist CS-905. I. Measurement of Partition Coefficient (logP) by High Performance Liquid Chromatography (HPLC). *Yakugaku Zasshi* 1995; **115**: 213–220.
- 147 Riekes MK, Pereira RN, Rauber GS, Cuffini SL, Campos CEM de, Silva MAS *et al*. Polymorphism in nimodipine raw materials: Development and validation of a quantitative method through differential scanning calorimetry. *J Pharm Biomed Anal* 2012; **70**: 188–193.
- 148 Zanicco AL, Diaz L, Lopez M, Nunez-Vergara LJ, Squella JA. Polarographic study of the photodecomposition of nimodipine. *J Pharm Sci* 1992; **81**: 920–924.
- 149 Ragno G, Veronico M, Vetuschi C. Analysis of nimodipine and its photodegradation product by derivative spectrophotometry and gas chromatography. *Int J Pharm* 1995; **119**: 115–119.
- 150 Bayer Pharmaceuticals Corporation. NIMOTOP® (nimodipine) capsules for oral use Prescribing Information. 2005. <https://www.accessdata.fda.gov> (accessed 15 Sep2021).
- 151 Bayer New Zealand Limited. NIMOTOP® DATA SHEET. 2017. <https://medsafe.govt.nz> (accessed 7 Feb2019).
- 152 Wyttenbach N, Kuentz M. Glass-forming ability of compounds in marketed amorphous drug products. *Eur J Pharm Biopharm* 2017; **112**: 204–208.
- 153 Carlson AP, Hänggi D, Wong GK, Etminan N, Mayer SA, Aldrich F *et al*. Single-Dose Intraventricular Nimodipine Microparticles Versus Oral Nimodipine for Aneurysmal Subarachnoid Hemorrhage. *Stroke* 2020; : 1142–1149.
- 154 Hänggi D, Etminan N, Macdonald RL, Steiger HJ, Mayer SA, Aldrich F *et al*. NEWTON: Nimodipine Microparticles to Enhance Recovery While Reducing Toxicity After Subarachnoid Hemorrhage. *Neurocrit Care* 2015; **23**: 274–284.
- 155 MacDonald RL, Hänggi D, Strange P, Steiger HJ, Mocco J, Miller M *et al*. Nimodipine pharmacokinetics after intraventricular injection of sustained-release nimodipine for

- subarachnoid hemorrhage. *J Neurosurg* 2019; : 1–7.
- 156 Zech J, Dzikowski R, Simantov K, Golenser J, Mäder K. Transdermal delivery of artemisinins for treatment of pre-clinical cerebral malaria. *Int J Parasitol Drugs Drug Resist* 2021; **16**: 148–154.
- 157 Zech J, Mader M, Gündel D, Metz H, Odparlik A, Agarwal S *et al.* Noninvasive characterization (EPR,  $\mu$ CT, NMR) of 3D PLA electrospun fiber sponges for controlled drug delivery. *Int J Pharm X* 2020; **2**.
- 158 Clarivate Analytics. Journal Impact Factor List 2021. 2021. <https://impactfactorforjournal.com> (accessed 20 Jan2022).
- 159 Parapini S, Olliaro P, Navaratnam V, Taramelli D, Basilico N. Stability of the antimalarial drug dihydroartemisinin under physiologically relevant conditions: Implications for clinical treatment and pharmacokinetic and in vitro assays. *Antimicrob Agents Chemother* 2015; **59**: 4046–4052.
- 160 Flobinus A, Taudon N, Desbordes M, Labrosse B, Simon F, Mazon M-C *et al.* Stability and antiviral activity against human cytomegalovirus of artemisinin derivatives. *J Antimicrob Chemother* 2014; **69**: 34–40.
- 161 Polat Wilairatana, Noppadon Tangpukdee, Srivicha Krudsood. Practical Aspects of Artesunate Administration in Severe Malaria Treatment. *Trop Med Surg* 2013; **1**.
- 162 Zech J, Gold D, Salaymeh N, Sasson NC, Rabinowitch I, Golenser J *et al.* Supplementary Materials: Oral administration of artemisone for the treatment of schistosomiasis: Formulation challenges and in vivo efficacy. *Pharmaceutics* 2020; **12**: 1–5.
- 163 Clause M, Peyrelasse J, Heil J, Boned C, Lagourette B. Bicontinuous structure zones in microemulsions. *Nature* 1981; **293**: 636–638.
- 164 Ni P, Hou W-G. A Novel Surfactant-free Microemulsion System: N,N-Dimethyl Formamide/Furaldehyde/H<sub>2</sub>O. *Chinese J Chem* 2008; **26**: 1335–1338.
- 165 Wang W, Wei H, Du Z, Tai X, Wang G. Formation and characterization of fully dilutable microemulsion with fatty acid methyl esters as oil phase. *ACS Sustain Chem Eng* 2015; **3**: 443–450.
- 166 Łuczak J, Hupka J. Studies on formation and percolation in ionic liquids/TX-100/water microemulsions. *J Mol Liq* 2014; **199**: 552–558.
- 167 Lagourette B, Peyrelasse J, Boned C, Clause M. Percolative conduction in microemulsion type systems. *Nature* 1979; **281**: 60–62.
- 168 Schillén K, Brown W, Johnsen RM. Micellar Sphere-to-Rod Transition in an Aqueous Triblock Copolymer System. A Dynamic Light Scattering Study of Translational and Rotational Diffusion. *Macromolecules* 1994; **27**: 4825–4832.
- 169 Clarke JHR, Nicholson JD, Regan KN. Self-diffusion and polydispersity in water + AOT + p-xylene microemulsions. A dynamic light-scattering study. *J Chem Soc Faraday Trans 1 Phys Chem Condens Phases* 1985; **81**: 1173–1182.
- 170 Fanun M. A study of the properties of mixed nonionic surfactants microemulsions by NMR, SAXS, viscosity and conductivity. *J Mol Liq* 2008; **142**: 103–110.
- 171 Chen CM, Warr GG. Rheology of ternary microemulsions. *J Phys Chem* 1992; **96**: 9492–9497.
- 172 Reza Bagheri A. *Controlled Release of Antimalarial Artemisone by Macromolecular Structures*. [dissertation]. Bayreuth: University Bayreuth, 2020.
- 173 Pennington AK, Ratcliffe JH, Wilson CG, Hardy JG. The influence of solution viscosity on nasal spray deposition and clearance. *Int J Pharm* 1988; **43**: 221–224.



- 174 Abdul-Ghani RA, Hassan AA. Murine schistosomiasis as a model for human schistosomiasis mansoni: similarities and discrepancies. *Parasitol Res* 2010; **107**: 1–8.
- 175 Cheever AW, Lenzi JA, Lenzi HL, Andrade ZA. Experimental models of *Schistosoma mansoni* infection. *Mem Inst Oswaldo Cruz* 2002; **97**: 917–940.
- 176 Cheever AW, Hoffmann KF, Wynn T. Immunopathology of schistosomiasis mansoni. *Immunol Today* 2000; **21**: 465–466.
- 177 Moreno A, Louis J, Rignon P, Morosan S, Mazier D, Benito A. Plasmodium falciparum-infected mice: more than a tour de force. *TRENDS Parasitol* 2007; **23**: 254–259.
- 178 Contreras CE, June CH, Perrin LH, Lambert PH. Immunopathological aspects of Plasmodium berghei infection in five strains of mice. I. Immune complexes and other serological features during the infection. *Clin Exp Immunol* 1980; **42**: 403–11.
- 179 Mackey LJ, Hochmann A, June CH, Contreras CE, Lambert P-H. Immunopathological aspects of Plasmodium berghei infection in five strains of mice. II. Immunopathology of cerebral and other tissue lesions during the infection. *Clin Exp Immunol* 1980; **42**: 412–420.
- 180 Montes De Oca M, Engwerda C, Haque A. *Methods in Molecular Biology Mouse Models of Innate Immunity: Methods and Protocols*. Humana Press: Totowa, NJ, 2013.
- 181 Gibaud S, Attivi D. Microemulsions for oral administration and their therapeutic applications. *Expert Opin Drug Deliv* 2012; **9**: 937–951.
- 182 Zhang P, Liu Y, Feng N, Xu J. Preparation and evaluation of self-microemulsifying drug delivery system of oridonin. *Int J Pharm* 2008; **355**: 269–276.
- 183 White NJ. Pharmacokinetic and Pharmacodynamic Considerations in Antimalarial Dose Optimization. *Antimicrob Agents Chemother* 2013; **57**: 5792–5807.
- 184 Kay K, Hodel EM, Hastings IM. Altering antimalarial drug regimens may dramatically enhance and restore drug effectiveness. *Antimicrob Agents Chemother* 2015; **59**: 6419–6427.
- 185 Hastings IM, Kay K, Hodel EM. How robust are malaria parasite clearance rates as indicators of drug effectiveness and resistance? *Antimicrob Agents Chemother* 2015; **59**: 6428–6436.
- 186 Kaurav H, Kapoor DN. Implantable systems for drug delivery to the brain. *Ther Deliv* 2017; **8**: 1097–1107.
- 187 Yan Wang, Wen Qu, Stepanie H. Choi. FDA's Regulatory Science Program for Generic PLA/ PLGA-Based Drug Products. *Am Pharm Rev* 2016; **20**.
- 188 Behrens AM, Casey BJ, Sikorski MJ, Wu KL, Tutak W, Sandler AD *et al*. In situ deposition of PLGA nanofibers via solution blow spinning. *ACS Macro Lett* 2014; **3**: 249–254.
- 189 Friederike von Burkersroda, Luise Schedl, Achim Gopferich. Why degradable polymers undergo surface erosion or bulk erosion. *Biomaterials* 2002; **23**: 4221–4231.
- 190 Ji Y, Li C, Burman M, Arinstein A, Zussman E, Wang W *et al*. Shifting of the melting point for semi-crystalline polymer nanofibers. *Europhys Lett* 2011; **93**: 46001.
- 191 Lappe S, Mulac D, Langer K. Polymeric nanoparticles - Influence of the glass transition temperature on drug release. *Int J Pharm* 2017; **517**: 338–347.
- 192 Cho S, Bales J, Tran TK, Korab G, Khandelwal N, Joffe AM. Effects of 14 Versus 21 Days of Nimodipine Therapy on Neurological Outcomes in Aneurysmal Subarachnoid Hemorrhage Patients. *Ann Pharmacother* 2016; **50**: 718–724.
- 193 Behrouz R, Sadat-Hosseiny Z. Pharmacological agents in aneurysmal subarachnoid

- hemorrhage: Successes and failures. *Clin Neuropharmacol* 2015; **38**: 104–108.
- 194 Scheller C, Wienke A, Tatagiba M, Gharabaghi A, Ramina KF, Ganslandt O *et al*. Prophylactic nimodipine treatment for cochlear and facial nerve preservation after vestibular schwannoma surgery: A randomized multicenter Phase III trial. *J Neurosurg* 2016; **124**: 657–664.
- 195 Shameem M, Lee H, Deluca PP. A Short-term (Accelerated Release) Approach to Evaluate Peptide Release from PLGA Depot Formulations. *AAPS PharmSci* 1999; **1**.
- 196 Blasi P, D'souza SS, Selmin F, Deluca PP. Plasticizing effect of water on poly(lactide-co-glycolide). *J Control Release* 2005; **108**: 1–9.
- 197 Haq Z, Thompson L. Significance of glass transition temperature to polymer latex stabilisation by nonionic surfactants. *Colloid Polym Sci* 1982; **260**: 212–217.
- 198 Mader M, Jérôme V, Freitag R, Agarwal S, Greiner A. Ultraporous, Compressible, Wetttable Polylactide/Polycaprolactone Sponges for Tissue Engineering. *Biomacromolecules* 2018; **19**: 1663–1673.
- 199 Duan G, Jiang S, Moss T, Agarwal S, Greiner A. Ultralight open cell polymer sponges with advanced properties by PPX CVD coating. *Polym Chem* 2016; **7**: 2759–2764.
- 200 Zech J, Mader M, Gündel D, Metz H, Odparlik A, Agarwal S *et al*. Supplementary Material of Noninvasive characterization (EPR,  $\mu$ CT, NMR) of 3D PLA electrospun fiber sponges for controlled drug delivery. *Int J Pharm X* 2020; **2**.
- 201 Jiang S, Duan G, Kuhn U, Mörl M, Altstädt V, Yarin AL *et al*. Spongy Gels by a Top-Down Approach from Polymer Fibrous Sponges. *Angew Chemie - Int Ed* 2017; **56**: 3285–3288.
- 202 Jennings JA, Beenken KE, Parker AC, Smith JK, Courtney HS, Smeltzer MS *et al*. Polymicrobial Biofilm Inhibition Effects of Acetate-Buffered Chitosan Sponge Delivery Device. *Macromol Biosci* 2016; **16**: 591–598.
- 203 Parker AC, Beenken KE, Jennings JA, Hittle L, Shirliff ME, Bumgardner JD *et al*. Characterization of local delivery with amphotericin B and vancomycin from modified chitosan sponges and functional biofilm prevention evaluation. *J Orthop Res* 2015; **33**: 439–447.
- 204 Yohe ST, Colson YL, Grinstaff MW. Superhydrophobic materials for tunable drug release: Using displacement of air to control delivery rates. *J Am Chem Soc* 2012; **134**: 2016–2019.
- 205 Kleinberg RL, Horsfield MA. Transverse relaxation processes in porous sedimentary rock. *J Magn Reson* 1990; **88**: 9–19.
- 206 Morgan V, Sad C, Constantino A, Azeredo R, Lacerda V, Castro E *et al*. Droplet Size Distribution in Water-Crude Oil Emulsions by Low-Field NMR. *J Braz Chem Soc* 2019; **30**: 1587–1598.
- 207 Broekmann I. *PFG-NMR-Untersuchungen an Monoglycerid-Gelen und Wasser-in-Öl-Emulsionen*. 2002.
- 208 National Institute of Biomedical Imaging and Bioengineering, (National Institutes of Health). Glossary of Terms. <https://www.nibib.nih.gov/science-education/glossar> (accessed 1 Feb2021).
- 209 van Zyl L, Viljoen JM, Haynes RK, Aucamp M, Ngwane AH, du Plessis J. Topical Delivery of Artemisone, Clofazimine and Decoquinone Encapsulated in Vesicles and Their In vitro Efficacy Against Mycobacterium tuberculosis. *AAPS PharmSciTech* 2019; **20**: 1–11.
- 210 International Council for Harmonisation of Technical Requirements for Pharmaceuticals for Human Use. ICH Q1F Guideline Stability Data Package for

- Registration in Climatic Zones III and IV. <https://www.ema.europa.eu> (accessed 12 Dec2021).
- 211 Hänggi D, Etminan N, Steiger HJ, Johnson M, Peet MM, Tice T *et al.* A Site-Specific, Sustained-Release Drug Delivery System for Aneurysmal Subarachnoid Hemorrhage. *Neurotherapeutics* 2016; **13**: 439–449.
- 212 Bege N, Renette T, Endres T, Beck-Broichsitter M, Hänggi D, Kissel T. In situ forming nimodipine depot system based on microparticles for the treatment of posthemorrhagic cerebral vasospasm. *Eur J Pharm Biopharm* 2013; **84**: 99–105.
- 213 Hänggi D, Perrin J, Eicker S, Beseoglu K, Etminan N, Kamp MA *et al.* Local Delivery of Nimodipine by Prolonged-Release Microparticles-Feasibility, Effectiveness and Dose-Finding in Experimental Subarachnoid Hemorrhage. *PLoS One* 2012; **7**: 1–7.
- 214 Koskimäki J, Tarkia M, Ahtola-Sättilä T, Saloranta L, Simola O, Forsback AP *et al.* Intracranial biodegradable silica-based nimodipine drug release implant for treating vasospasm in subarachnoid hemorrhage in an experimental healthy pig and dog model. *Biomed Res Int* 2015.
- 215 Si Y, Wang X, Dou L, Yu J, Ding B. Ultralight and fire-resistant ceramic nanofibrous aerogels with temperature-invariant superelasticity. *Sci Adv* 2018; **4**.
- 216 Duan G, Koehn-Serrano M, Greiner A. Highly Efficient Reusable Sponge-Type Catalyst Carriers Based on Short Electrospun Fibers. *Macromol Rapid Commun* 2017; **38**: 1–6.
- 217 Si Y, Fu Q, Wang X, Zhu J, Yu J, Sun G *et al.* Superelastic and Superhydrophobic Nanofiber-Assembled Cellular Aerogels for Effective Separation of Oil/Water Emulsions. *ACS Nano* 2015; **9**: 3791–3799.

---

## APPENDIX

### Acknowledgements

Bei allen die mich bei der Fertigstellung dieser Dissertation unterstützt und begleitet haben möchte ich mich sehr herzlich bedanken!

An erster Stelle gilt mein besonderer Dank Prof. Karsten Mäder der mir eine so spannende, vielfältige Arbeit ermöglicht hat, für die interessierte und immer zuverlässige Betreuung und große Unterstützung in spezifisch fachlichen sowie auch darüber hinausgehenden Fragen.

Für die schöne Zeit in Halle, die nette Arbeitsatmosphäre im Labor und im Studentenpraktikum bedanke ich mich bei der gesamten Arbeitsgruppe Pharmazeutische Technologie und den Kollegen aus der Biopharmazie.

Ein besonderer Dank dabei geht dabei an Frau Dr. Miriam Klein für die angenehmen Stunden und Gespräche im gemeinsamen Büro und die vielen Runden in der Schwimmhalle nach getaner Arbeit.

Danke an Herrn Benedikt Göttel für die Einführung in das Elektrospinning und seinen Anteil bei der Entwicklung der Nimodipinefasern.

Dr. Hendrik Metz danke ich für die beständige Unterstützung in allen Fragen der EPR und NMR Messungen und seine kontinuierliche Mahnung zum möglichst kritischen wissenschaftlichen Arbeiten allgemein.

Frau Dr. Henrike Lucas sei herzlich gedankt für ihr stets offenes Ohr für jegliche Fragen und Belange eines Doktoranden.

Ich bedanke mich bei Frau Manuela Woigk dafür dass sie mir mit ihrer ausgesprochenen Expertise für HPLC und Massenspektrometrie immer zur Seite stand. Durch ihre vorausschauende Arbeitsweise hat sie mir viel Arbeit abgenommen, mich aber trotzdem immer dabei unterstützt, meine Analytik selbstständig durchzuführen.

Vielen Dank auch an Frau Kerstin Schwarz für die Messungen in der Thermischen Analyse und Frau Bertram für die Hilfe in allen organisatorischen und bürokratischen Dingen.

Für die sehr motivierte, strukturierte und angenehme Zusammenarbeit mit der Universitätsmedizin Halle möchte ich mich bei Frau Dr. Sandra Leisz und Dr. Daniel Gündel herzlich bedanken.

Für zwei interessante Aufenthalte in der Arbeitsgruppe Makromolekulare Chemie II an der Universität Bayreuth danke ich Prof. Andreas Greiner. Dr. Michael Mader sei gedankt für die Bereitstellung und Charakterisierung seiner polymer fiber sponges für unsere weiteren Untersuchungen und seinen großen Einsatz bei der Fertigstellung der Publikation. Außerdem bedanke ich mich bei Frau Dr. Mina Heidari für ihre wunderbare Gastfreundschaft während meiner Zeit in Bayreuth und den exzellenten persischen Tee.

Danken möchte ich auch Herrn Frank Syrowatka und Dr. Gerd Hause für die elektronenmikroskopischen Aufnahmen, Dr. Wolfgang Knolle für die Elektronenstrahlsterilisation sowie

Dr. Christoph Wagner für die Hilfe bei der röntgendiffraktometrischen Untersuchung meiner Formulierungen.

A very special thank you it due to my supervisor in Jerusalem, Dr. Jacob Golenser of the Hebrew University. His constant attention, ceaseless teaching and support in the laboratory and our spirited discussions allowed me to accomplish a lot of research in only a short time and greatly advanced my work. I also thank him and his wife Eti Golenser for their great care, generosity and hospitality. Our many excursions, family Shabbat dinners and adventures made my time in Israel an unforgettable experience of a lifetime: *todah rabah!*

I gratefully acknowledge Prof. Daniel Gold of the Tel Aviv University for the animal experiments on murine schistosomiasis.

Thank you to Nadeen Salaymeh for her support with the malaria experiments, the counting of endless numbers of blood smears and her warm welcome.

Meiner Familie danke ich für die bedingungslose Unterstützung während des Studiums und der Promotionszeit, euren Optimismus und euer fortwährendes Interesse an meiner Arbeit. Insbesondere danke ich meinem Mann für die vielen hilfreichen Diskussionen und Ratschläge und dass er mir neben seiner eigenen Arbeit immer wieder den Rücken freigehalten und mir Zeit zum Schreiben geschaffen hat.

Ohne euch wäre die Fertigstellung dieser Dissertationsschrift nicht denkbar.

## Curriculum Vitae

### Persönliche Daten

---

Name	Johanna Zech
Geburtsdatum	19.01.1989
Geburtsort	Göttingen
Staatsangehörigkeit	Deutsch

### Ausbildung und beruflicher Werdegang

---

seit 09/2019	Angestellte Apothekerin Apotheke Prohlis im Gesundheitszentrum, Dresden
04/2016 – 08/2019	Wissenschaftliche Mitarbeiterin Martin-Luther-Universität Halle-Wittenberg, Halle (Saale) Institut für Pharmazie Pharmazeutische Technologie
03/2015 – 01/2016	Angestellte Apothekerin Kreuz-Apotheke, Flensburg
02/2015	<i>Approbation als Apothekerin / 3. Staatsexamen Pharmazie</i>
07/2014 - 01/2015	Pharmazeutin im Praktikum Hofapotheke, Wiesbaden-Biebrich
01/2014 - 06/2014	Pharmazeutin im Praktikum University of Toronto Leslie Dan Faculty of Pharmacy Department of Molecular Toxicology
11/2013	<i>2. Staatsexamen Pharmazie</i>
08/2011	<i>1. Staatsexamen Pharmazie</i>
10/2009 – 11/2013	Studium der Pharmazie Christian-Albrechts-Universität zu Kiel
06/2008	<i>Allgemeine Hochschulreife</i> Freie Waldorfschule Göttingen

---

 (Ort, Datum)

---

 (Unterschrift)

---

## List of Publications

### Peer-reviewed research articles

Zech J, Leisz S, Göttel B, Syrowatka F, Greiner A, Strauss C, et al. Electrospun Nimodipine-loaded fibers for nerve regeneration: Development and in vitro performance. *Eur J Pharm Biopharm* 2020; **151**:116–26.

Zech J, Gold D, Salaymeh N, Sasson NC, Rabinowitch I, Golenser J, et al. Oral administration of artemisone for the treatment of schistosomiasis: Formulation challenges and in vivo efficacy. *Pharmaceutics* 2020; **12**.

Zech J, Mader M, Gündel D, Metz H, Odparlik A, Agarwal S, et al. Noninvasive characterization (EPR,  $\mu$ CT, NMR) of 3D PLA electrospun fiber sponges for controlled drug delivery. *Int J Pharm X* 2020; **2**.

Zech J, Salaymeh N, Hunt NH, Mäder K, Golenser J. Efficient treatment of experimental cerebral malaria by an artemisone-SMEDDS system: Impact of application route and dosing frequency. *Antimicrob Agents Chemother* 2021; **65**.

Zech J, Dzikowski R, Simantov K, Golenser J, Mäder K. Transdermal delivery of artemisinins for treatment of pre-clinical cerebral malaria. *Int J Parasitol Drugs Drug Resist* 2021; **16**: 148–54.

### Conference contributions

Zech J, Timoracky M, Syrowatka F, Mäder K. Artemisone in Electrospayed Solid Lipid Microparticles. Paper and poster presented at: *The 11th World Meeting on Pharmaceutics, Biopharmaceutics and Pharmaceutical Technology*, 2018; Granada, Spain.

Zech J, Timoracky M, Syrowatka F, Mäder K. Electrospayed solid lipid microparticles as high drug-loading formulation of Artemisone. Poster presented at: *The Controlled Release Society Annual Local Chapter Germany Meeting*, 2019; Leipzig, Germany.



## Eidesstattliche Erklärung

Hiermit erkläre ich gemäß § 5 der Promotionsordnung der Naturwissenschaftlichen Fakultät I (Biowissenschaften) der Martin-Luther-Universität Halle-Wittenberg, dass ich die vorliegende Dissertationsschrift selbständig und ohne fremde Hilfe verfasst habe, keine anderen als die von mir angegebenen Quellen und Hilfsmittel benutzt und die den benutzten Werken wörtlich oder inhaltlich entnommenen Stellen als solche kenntlich gemacht habe.

Mit der vorliegenden Dissertationsarbeit bewerbe ich mich erstmals um die Erlangung eines Doktorgrades.

Die Arbeit wurde ausschließlich an der Mathematisch-Naturwissenschaftlichen-Fakultät I (Biowissenschaften) der Martin-Luther-Universität Halle-Wittenberg vorgelegt.

---

(Ort, Datum)

---

(Unterschrift)



# Publications

## Publication I

Zech J, Gold D, Salaymeh N, Sasson NC, Rabinowitch I, Golenser J, *et al.* Oral administration of artemisone for the treatment of schistosomiasis: Formulation challenges and in vivo efficacy. *Pharmaceutics* 2020; **12**.

<https://doi.org/10.3390/pharmaceutics12060509>

Supplementary material:

<https://www.mdpi.com/1999-4923/12/6/509#supplementary>

**Abstract:** Artemisone is an innovative artemisinin derivative with applications in the treatment of malaria, schistosomiasis and other diseases. However, its low aqueous solubility and tendency to degrade after solubilisation limits the translation of this drug into clinical practice. We developed a self-microemulsifying drug delivery system (SMEDDS), which is easy to produce (simple mixing) with a high drug load. In addition to known pharmaceutical excipients (Capmul MCM, Kolliphor HS15, propylene glycol), we identified Polysorb ID 46 as a beneficial new additional excipient. The physicochemical properties were characterized by dynamic light scattering, conductivity measurements, rheology and electron microscopy. High storage stability, even at 30 °C, was achieved. The orally administrated artemisone SMEDDS formulation was highly active in vivo in *S. mansoni* infected mice. Thorough elimination of the adult worms, their eggs and prevention of the deleterious granuloma formation in the livers of infected mice was observed even at a relatively low dose of the drug. The new formulation has a high potential to accelerate the clinical use of artemisone in schistosomiasis and malaria.

## Publication II

Zech J, Salaymeh N, Hunt NH, Mäder K, Golenser J. Efficient treatment of experimental cerebral malaria by an artemisone-SMEDDS system: Impact of application route and dosing frequency. *Antimicrob Agents Chemother* 2021; **65**.

<https://doi.org/10.1128/AAC.02106-20>

**Abstract:** Artemisone (ART) has been successfully tested in vitro and in animal models against several diseases. However, its poor aqueous solubility and limited chemical stability are serious challenges. We developed a self-microemulsifying drug delivery system (SMEDDS) that overcomes these limitations. Here, we demonstrate the efficacy of this formulation against experimental cerebral malaria in mice and the impact of its administration using different routes (gavage, intranasal delivery, and parenteral injections) and frequency on the efficacy of the treatment. The minimal effective daily oral dose was 20 mg/kg. We found that splitting a dose of 20 mg/kg ART given every 24 h, by administering two doses of 10 mg/kg each every 12 h, was highly effective and gave far superior results compared to 20 mg/kg once daily. We obtained the best results with nasal treatment; oral treatment was ranked second, and the least effective route of administration was intraperitoneal injection. A complete cure of experimental cerebral malaria could be achieved through choosing the optimal route of application, dose, and dosing interval. Altogether, the developed formulation combines easy manufacturing with high stability and could be a successful and very versatile carrier for the delivery of ART in the treatment of human severe malaria.

## Publication III

Zech J, Dzikowski R, Simantov K, Golenser J, Mäder K. Transdermal delivery of artemisinins for treatment of pre-clinical cerebral malaria. *Int J Parasitol Drugs Drug Resist* 2021; **16**: 148–54.

<https://doi.org/10.1016/j.ijpddr.2021.05.008>

**Abstract:** Transdermal drug delivery avoids complications related to oral or parenteral delivery - the need for sterility, contamination, gastrointestinal side effects, patient unconsciousness or nausea and compliance. For malaria treatment, we demonstrate successful novel transdermal delivery of artemisone (ART) and artesunate. The incorporation of ART into a microemulsion (ME) overcomes the limitations of the lipophilic drug and provides high transcutaneous bioavailability. ART delivery to the blood (above 500 ng/ml) was proved by examining the sera from treated mice, using a bioassay in cultured *Plasmodium falciparum*. Skin spraying of ART-ME eliminated *P. berghei* ANKA in an infected mouse model of cerebral malaria (CM) and prevented CM, even after a late treatment with a relatively small amount of ART (13.3 mg/kg). For comparison, the artesunate (the most used commercial artemisinin) formulation was prepared as ART. However, ART-ME was about three times more efficient than artesunate-ME. The solubility and stability of ART in the ME, taken together with the successful transdermal delivery leading to animal recovery, suggest this formulation as a potential candidate for trans- dermal treatment of malaria.

## Publication IV

Zech J, Leisz S, Göttel B, Syrowatka F, Greiner A, Strauss C, et al. Electrospun Nimodipine-loaded fibers for nerve regeneration: Development and in vitro performance. *Eur J Pharm Biopharm* 2020; **151**:116–26.

<https://doi.org/10.1016/j.ejpb.2020.03.021>

**Abstract:** Nimodipine is a 1,4-Dihydropyridine type calcium antagonist routinely used to control blood pressure and reduce the risk of secondary ischemia after aneurismal subarachnoid hemorrhage. Additionally, Nimodipine has unique neuroprotective properties. With respect to brain related applications, the full potential of the desired local effect can often not be realized after systemic administration due to systemic side effects. Therefore, it was our aim to develop a biodegradable drug delivery system for the local controlled release of the drug inside the brain. As a suitable and biodegradable system we successfully electrospun PLGA fibers containing 1 and 10% drug.

The results of DSC and X-Ray diffractometry measurements indicate that Nimodipine was incorporated in the polymer matrix in the amorphous state. No drug recrystallization was detected for up to 6 months. Electron- beam sterilization was tried but reduced the drug content of the fiber mats considerably. A sustained drug release over 4–8 days was observed, highly depended on release conditions. The Nimodipine fiber mats exhibited no cell toxicity. In contrast, the electrospun fibers were able to significantly reduce cell death in in vitro cell models of oxidative, osmotic and heat-induced cell stress in Schwann cells, neuronal cells as well as immortalized and primary astrocytes. Therefore, electrospun Nimodipine loaded PLGA fibers represent a promising drug delivery system to realize the drug's benefits for its intracranial use.

## Publication V

Zech J, Mader M, Gündel D, Metz H, Odparlik A, Agarwal S, et al. Noninvasive characterization (EPR,  $\mu$ CT, NMR) of 3D PLA electrospun fiber sponges for controlled drug delivery. *Int J Pharm X* 2020; **2**.

<https://doi.org/10.1016/j.ijpx.2020.100055>

Supplementary material:

<https://www.sciencedirect.com/science/article/pii/S2590156720300177#s0135>

**Abstract:** Highly porous 3D-scaffolds, made from cut, electrospun PLA fibers, are relatively new and promising systems for controlled drug-delivery applications. Because knowledge concerning fundamental processes of drug delivery from those scaffolds is limited, we noninvasively characterized drug-loading and drug-release mechanisms of these polymer-fiber sponges (PFS). We screened simplified PFS-implantation scenarios with EPR and  $\mu$ CT to quantify and 3D-visualize the absorption of model-biofluids and an oil, a possible drug-loading liquid. Saturation of PFS (6 × 8 mm, h × d) is governed by the high hydrophobicity of the material and air-entrapment. It required up to 45 weeks for phosphate-buffered saline and 11 weeks for a more physiological, surface-active protein- solution, indicating the slow fluid-uptake of PFS as an effective mechanism to substantially prolong the release of a drug incorporated within the scaffold. Medium-chain triglycerides, as a good wetting liquid, saturated PFS within seconds, suggesting PFS potential to serve as carrier-vessels for immobilizing hydrophobic drug-solutions to define a liquid's 3D-interface. Oil-retention under mechanical stress was therefore investigated.  $^1\text{H}$  NMR permitted insights into PFS-oil interaction, confirming surface-relaxation and restricted diffusion; both did not influence drug release from oil-loaded PFS. Results facilitate better understanding of PFS and their potential use in drug delivery.